

The effect of locally produced IFN- $\gamma$  on established tumors

# Dissertation

zur Erlangung des akademischen Grades des

doctor rerum naturalium

(Dr. rer. nat.)

eingereicht im Fachbereich Biologie, Chemie, Pharmazie  
der Freien Universität Berlin

vorgelegt von

Diplom-Biologin Dana Briesemeister

geboren am 12.11.1980 in Oranienburg

angefertigt am Institut für Immunologie, Charité Berlin

Berlin 2011

- 
1. Gutachter: Prof. Dr. Thomas Blankenstein
  2. Gutachter: Prof. Dr. Wolfgang Uckert

Disputation am 10. Juni 2011

# Contents

<b>1</b>	<b>Summary</b>	<b>1</b>
<b>2</b>	<b>Zusammenfassung</b>	<b>2</b>
<b>3</b>	<b>Introduction</b>	<b>3</b>
3.1	Cancer . . . . .	3
3.2	Tumor therapy . . . . .	4
3.3	Tumors and tumor stroma . . . . .	6
3.4	Tumor stroma as a target for immunotherapy . . . . .	8
3.5	Cytokines . . . . .	9
3.5.1	Interferon gamma . . . . .	9
3.6	Tumors and IFN- $\gamma$ . . . . .	10
3.7	The tetracycline system . . . . .	10
<b>4</b>	<b>Aims of this thesis</b>	<b>13</b>
<b>5</b>	<b>Materials and Methods</b>	<b>14</b>
5.1	Mice . . . . .	14
5.2	Tumor cell lines . . . . .	14
5.3	Reagents . . . . .	14
5.4	Kits . . . . .	16
5.5	Media and Buffers . . . . .	17
5.6	Consumable Material . . . . .	18
5.7	Equipment . . . . .	18
5.8	Vector for inducible IFN- $\gamma$ expression . . . . .	20
5.9	Production of virus supernatant . . . . .	21
5.10	Transduction of tumor cells . . . . .	22
5.11	Generation of IFN- $\gamma$ -inducible cells . . . . .	22
5.12	Tumor transplantation experiments . . . . .	22
5.13	Re-isolation of tumor cells . . . . .	23

5.14	Analysis of IFN- $\gamma$ serum levels . . . . .	23
5.15	Determination of liver values . . . . .	23
5.16	Immunohistochemistry . . . . .	24
<b>6</b>	<b>Results</b>	<b>25</b>
6.1	The plasmacytoma J558L model . . . . .	25
6.1.1	Generation and in vitro characterization of J558L-IFN- $\gamma^{\text{IND}}$ cells . . . . .	25
6.1.2	High amounts of IFN- $\gamma$ are detectable in the serum after IFN- $\gamma$ induction . . . . .	27
6.1.3	J558L-IFN- $\gamma^{\text{IND}}$ tumor cells grow after induction of IFN- $\gamma$ in IFN- $\gamma\text{R}$ deficient mice . . . . .	27
6.1.4	IFN- $\gamma$ induction in established tumors can lead to tumor rejection . . . . .	31
6.1.5	High IFN- $\gamma$ concentrations cause toxic side effects . . . . .	33
6.1.6	Interval treatment reduces toxic side effects . . . . .	36
6.1.7	IFN- $\gamma$ induction in established tumors causes growth delay in T cell deficient NOD/SCID mice . . . . .	37
6.1.8	Re-isolated J558L-IFN- $\gamma^{\text{IND}}$ tumor cells from NOD/SCID mice lost the ability to produce IFN- $\gamma$ . . . . .	40
6.1.9	Blood vessel destruction and necrosis after IFN- $\gamma$ induction in established J558L-IFN- $\gamma^{\text{IND}}$ tumors . . . . .	41
6.1.10	IFN- $\gamma$ induction in established J558L-IFN- $\gamma^{\text{IND}}$ tumors leads to macroscopically visible tumor necrosis . . . . .	46
6.1.11	Summary J558L-IFN- $\gamma^{\text{IND}}$ . . . . .	47
6.2	The fibrosarcoma MCA313 model . . . . .	48
6.2.1	Generation and in vitro characterization of MCA313-IFN- $\gamma^{\text{IND}}$ cells . . . . .	48
6.2.2	MCA313-IFN- $\gamma^{\text{IND}}$ tumors express high amounts of IFN- $\gamma$ in vivo . . . . .	49
6.2.3	Induction of IFN- $\gamma$ in established MCA313-IFN- $\gamma^{\text{IND}}$ tumors can lead to tumor cell rejection . . . . .	53
6.2.4	IFN- $\gamma$ induction in IFN- $\gamma^{-/-}$ mice can lead to tumor rejection and has no effect in IFN- $\gamma\text{R}^{-/-}$ mice . . . . .	55
6.2.5	IFN- $\gamma$ induction in MCA313-IFN- $\gamma^{\text{IND}}$ cells leads to weight loss in IFN- $\gamma\text{R}$ -competent mice . . . . .	57
6.2.6	Summary MCA313-IFN- $\gamma^{\text{IND}}$ . . . . .	60

<b>7 Discussion</b>	<b>61</b>
7.1 J558L-IFN- $\gamma^{\text{IND}}$ . . . . .	62
7.2 MCA313-IFN- $\gamma^{\text{IND}}$ . . . . .	63
7.3 Conclusion . . . . .	64
<b>Bibliography</b>	<b>75</b>
<b>Nomenclature</b>	<b>76</b>
<b>A Vectors</b>	<b>78</b>
<b>B Sequence Data</b>	<b>80</b>
B.1 Primer sequences . . . . .	80
B.2 DNA-Sequence of tet-IFN- $\gamma$ . . . . .	80
<b>C Acknowledgements</b>	<b>82</b>

# 1 Summary

It has been shown that injecting a suspension of IFN- $\gamma$ -secreting tumor cells results in their rejection. This effect has been attributed to IFN- $\gamma$  preventing tumor stroma formation but not to a direct effect on the cancer cells. However, it is not known, which influence IFN- $\gamma$  has on tumors with an established stroma.

To address this question, the plasmacytoma cell line J558L and the fibrosarcoma MCA313 were transduced with a vector allowing doxycycline-inducible IFN- $\gamma$  gene expression.

After the subcutaneous injection of the tumor cells into mice, IFN- $\gamma$  was induced at different time points. Tumors did not grow when inducing IFN- $\gamma$  immediately after tumor cell inoculation in both tumor models (J558L and MCA313). Approximately half of the tumors were rejected when IFN- $\gamma$  was induced in established J558L-IFN- $\gamma^{\text{IND}}$  tumors within the first two weeks. IFN- $\gamma$  induction in established MCA313-IFN- $\gamma^{\text{IND}}$  tumors led to tumor rejection in 20 % of the mice. Induction of IFN- $\gamma$  two to three weeks after tumor cell inoculation was less efficient in both models. Moreover, IFN- $\gamma$  induction in established tumors led to toxic side effects such as weight loss and increase in liver transaminases. IFN- $\gamma$  induction in established tumors led to a reduction of CD31<sup>+</sup> or CD146<sup>+</sup> endothelial cells and massive necrosis. We think that IFN- $\gamma$  induced blood vessel destruction is the primary mechanism of tumor rejection in our model.

Together, this work shows that vascularized tumors can be rejected by local IFN- $\gamma$  expression. However, rejection of established tumors was less efficient over time, suggesting that transplanted tumors are less susceptible to local IFN- $\gamma$  treatment the better they are established.

## 2 Zusammenfassung

Es wurde bereits gezeigt, dass IFN- $\gamma$ -sekretierende Tumorzellsuspensionen abgestoßen werden. IFN- $\gamma$  übt in diesem Fall keinen direkten Einfluss auf die Tumorzellen aus, sondern verhindert die Bildung von Tumorstroma. Jedoch ist bisher nicht bekannt, welchen Einfluss IFN- $\gamma$  auf Tumoren mit bereits etabliertem Stroma ausübt.

Um diese Frage zu beantworten, wurden die Plasmozytom Zelllinie J558L und das Fibrosarkom MCA313 mit einem Vektor transduziert, der eine Doxycyclin-induzierbare Expression des IFN- $\gamma$  Gens ermöglicht.

Nach subkutaner Tumorzellinjektion wurde IFN- $\gamma$  zu verschiedenen Zeitpunkten induziert: In beiden Modellen (J558L und MCA313) wuchsen die Tumorzellen nicht, wenn IFN- $\gamma$  zeitgleich zur Injektion exprimiert wurde. Ungefähr die Hälfte der dann bereits etablierten J558L-IFN- $\gamma^{\text{IND}}$  Tumoren wurde abgestoßen, wenn IFN- $\gamma$  in den ersten zwei Wochen nach Tumorzellinjektion exprimiert wurde. IFN- $\gamma$  Induktion in etablierten MCA313-IFN- $\gamma^{\text{IND}}$  Tumoren führte zu einer Tumorabstoßung in 20 % der Mäuse.

Wenn IFN- $\gamma$  zwei bis drei Wochen nach Tumorzellinjektion induziert wurde, war die Abstoßung in beiden Modellen weniger erfolgreich. Außerdem führte die Induktion von IFN- $\gamma$  in etablierten Tumoren zu toxischen Nebeneffekten wie Gewichtsverlust und einen Anstieg der Lebertransaminasen.

Die IFN- $\gamma$  Induktion in etablierten Tumoren führte außerdem zu einer Reduktion von CD31<sup>+</sup> oder CD146<sup>+</sup> Endothelzellen und massiver Nekrose. Diese Ergebnisse deuten darauf hin, dass die IFN- $\gamma$ -induzierte Zerstörung der Blutgefäße der primäre Mechanismus der Tumorabstoßung in unseren Modellen sein könnte.

Diese Arbeit zeigt, dass vaskularisierte Tumore durch lokale IFN- $\gamma$  Expression abgestoßen werden können. Da die Abstoßung von etablierten Tumoren mit zunehmender Zeit weniger erfolgreich verläuft, gehen wir davon aus, dass transplantierte Tumoren weniger anfällig für IFN- $\gamma$  Behandlung sind, je etablierter sie sind.

# 3 Introduction

## 3.1 Cancer

Cancer is after cardiovascular diseases the most frequent cause of death in Germany [1]. The risk for cancer increases with age [2]. Cancer incidence is in most instances affected by lifestyle and environmental factors and only in 5–10 % by genetic predisposition [3]. Common risk factors are tobacco, alcohol consumption, obesity, infections and radiation [4–9].

The term tumor means swelling but is usually associated with solid neoplasia which is the Greek word for new growth. This type of newly growing cells is characterized by uncontrolled and excessive cell proliferation. There are two types of tumors, benign and malignant. Benign tumors are enclosed in a capsule of connective tissue. They do not metastasize and do not invade into surrounding tissue. Malignant tumors are characterized by aggressive, infiltrating proliferation and often spread in the body forming metastases.

Solid malignant tumors are classified by the origin of the tumor. Hence, carcinomas are derived from epithelial cells and sarcomas are derived from connective tissue or mesenchymal cells. In contrast, hematopoietic (non-solid) neoplasias are historically classified by their location: Circulating in the bloodstream, they are called leukemias ("White blood"); accumulating in solid tissues like lymph nodes, they are referred to as lymphomas.

The development of a neoplasia can be divided into three phases. In the first, the initiation phase a new gene mutation occurs spontaneously or is caused by a carcinogen, a virus, radiation or chemical mutagens. Alternatively, a mutation can be encoded in the germline such as retinoblastoma or familial adenomatous polyposis. The mutated cells do not form a tumor unless exposed to tumor-promoting agents or conditions which start the second phase, the promotion phase. In this phase, pre-malignant cells are transformed into neoplastic cells. The third phase is the progression phase in which tumor cells start to infiltrate into adjacent tissue [10, 11]. According to Hanahan and Weinberg, tumor development is a result of



multiple mutations [2]. The introduction of only two oncogenes (myc and ras) is sufficient to induce transformation of normal cells into tumor cells in mice [12]. In contrast, it seems to require at least four to six genetic alterations to transform human cells [13].

Mutations which are crucial for tumor development involve genes responsible for the regulation of the cell cycle, cell proliferation and homeostasis. Mutations lead to gain of function of oncogenes or loss of function of tumor suppressor genes.

## 3.2 Tumor therapy

Currently, successful treatment of solid, malignant tumors can usually only be accomplished via surgery. This is often combined with radio- or chemotherapy in order to eliminate microscopic tumor residue or early metastases that would lead to relapse. With tumor progression, these methods dramatically lose effectiveness and therefore hinge on early disease detection. Moreover, they are more or less harmful to healthy tissue.

Diagnostic methods to identify tumors are sometimes not sensitive enough for early detection, or they are too invasive or expensive to use them as screening procedures. Thus, tumors often are only detected at later stages, when conventional therapy fails. As a result, new additional methods like gene therapy, hormone therapy, therapy using angiogenesis inhibitors and immunotherapy have been developed.

In gene therapy, a vector containing a therapeutical gene is inserted into cells and substitutes for the defective or mutated gene.

Some cancers that show hormone-dependent growth - like breast or prostate cancer - are treated with hormone-analogues or hormone inhibitors which are designed to influence the regulatory feedback loops that sustain their growth and progression.

Angiogenesis inhibitors are another treatment option used in the clinic [14]: As they grow, malignant tumors have to rapidly form new blood vessels to maintain their supply with nutrients. Angiogenesis inhibitors can prevent the formation of new blood vessels, and thus progression of the tumor [15]. Because there are many factors influencing angiogenesis and, additionally, they are all involved in wound healing, clinical testing is still running.

The idea behind immunotherapy against cancer is to eliminate the tumor cells with the help of the immune system. Immunotherapy is divided into active and passive immunotherapy and is used to activate and enhance the immune response to tumor cells.

Passive immunotherapy is based on the application of tumor-reactive antibodies, which are designed to detect epitopes expressed by cancer cells. Breast cancer is currently treated using antibodies blocking the mutated, constitutively active form of the growth factor receptor Her2/neu [16]. Unfortunately, besides the improvement of disease, cardiac toxicity arose as a side effect which is due to the HER2 expression on cardiac muscle cells.

Active immunotherapy includes therapies such as cancer vaccines and adoptive T cell transfer (ATT). Vaccination aims to induce an endogenous, long-lasting tumor antigen-specific immune response. T cells are being activated and stimulated to eliminate cancer cells for instance via injection of irradiated, proliferation-deficient tumor cells [17, 18].

Vaccination against tumors has been investigated for the last 15 years. Because tumor cells in vaccination experiments are too weakly immunogenic to induce a sustained immune response, effector mechanisms of the immune cells against tumor cells have to be activated. Methods like immunization with irradiated tumor cells or transfer of cytokine genes into tumor cells have been tested in animal models [18, 19]. However, cytokine gene-modified vaccines were mostly ineffective in cancer patients [20]. Indeed, vaccination against tumors only seems to be successful for small and not established tumors which is usually not the case in humans [21].

Adoptive T cell transfer is used against virus-associated tumors [22, 23]. For instance, T cells of immunosuppressed patients cannot defend against reactivated viruses such as Epstein-Barr virus (EBV). Therefore, lymphocytes are isolated from donors, virus-specific T cells are expanded and then transferred to the immunosuppressed recipient [24].

ATT in mouse models can result in the rejection of even large, established tumors [25]. In fact, recent findings by Rosenberg et al. suggest that transfer of tumor-reactive T cells is applicable in humans [26].

Numerous clinical studies have been investigating the role of active immunotherapy using adoptive transfer of tumor infiltrating lymphocytes (TIL) with varying success [27, 28]. Tumor infiltrating lymphocytes are isolated from the patient's tumor tissue. Tumor-specific T cell clones are selected, expanded *ex vivo* and then transferred back into the patient [29]. Another method to reduce the *ex vivo* culturing period is to isolate TILs and expand them without selection for tumor-specific clones [28, 30]. To suppress endogenous regulatory T cells and establish an optimal environment for T cell expansion, T cells are adoptively transferred after lymphodepletion [31].

Because it is very difficult to obtain and expand TILs from a patient, alternative methods of generating tumor-specific T cells are now tested in clinical trials. The identification and characterization of potential tumor antigens which are overexpressed in human tumors - such as p53, melanoma antigen recognized by T cells (MART-1) and cancer testis antigen (CTA) - have made it possible to generate specific T cell receptors against these structures. Those are then cloned into the patients peripheral blood lymphocytes (PBLs), allowing to gain many T cells with the desired antigen specificity in a short time period. The transfer of genetically engineered lymphocytes bearing MART-1 specific receptors led to tumor regression in some patients, but the treatment has yet to be improved [24].

Other studies focus on cytotoxic T cells which recognize tumor antigens via Major Histocompatibility Class I (MHC I) presentation of tumor-associated peptides and thus destroy tumor cells and cross-presenting stroma cells. To activate CD8<sup>+</sup> T cells, CD4<sup>+</sup> T cell help and costimulatory signals are required. In addition to the activation of cytotoxic CD8<sup>+</sup> T cells, CD4<sup>+</sup> T cells perform cytotoxic effects themselves [32, 33] or - importantly - affect stroma cells via the secretion of cytokines (eg. IFN- $\gamma$ ) [34, 35] and tumor cells via bystander effects. Therefore, in contrast to vaccination, ATT seems to be a more promising approach to cancer treatment.

### 3.3 Tumors and tumor stroma

Whereas injected tumor cell suspensions only consist of tumor cells, solid tumors do not only consist of tumor cells but are embedded in a supportive matrix of stromal cells (Figure 3.1 A and B). Tumor cells influence their microenvironment through growth factors and other molecules, recruit stroma cells and keep them in an activated, tumor-promoting state [34]. The stroma of solid tumors consists of non-hematopoietic cells such as fibroblasts and endothelial cells, of the extracellular matrix (ECM) produced by these cells and of hematopoietic cells such as macrophages, granulocytes and lymphocytes (Figure 3.1 B).

Connective tissue cells belong to a group of mesenchymal cells called fibroblasts, which exercise many tasks. Some generate the extracellular matrix, others are contractile (myofibroblasts) or associated with blood vessels (pericytes). Fibroblasts are an important cell type in tissue repair and wound healing responses. Tumor tissue is continually growing and therefore needs to be remodeled. In this context tumors have been described by Dvorak as wounds that do not heal [36]. In the tumor, fibroblasts are mainly responsible for mechanical support and produce metallopro-

teases and extracellular matrix molecules which serve as means of communication between stroma and tumor. Fibroblasts are also a source of the vascular endothelial growth factor (VEGF) and thereby contribute to angiogenesis.

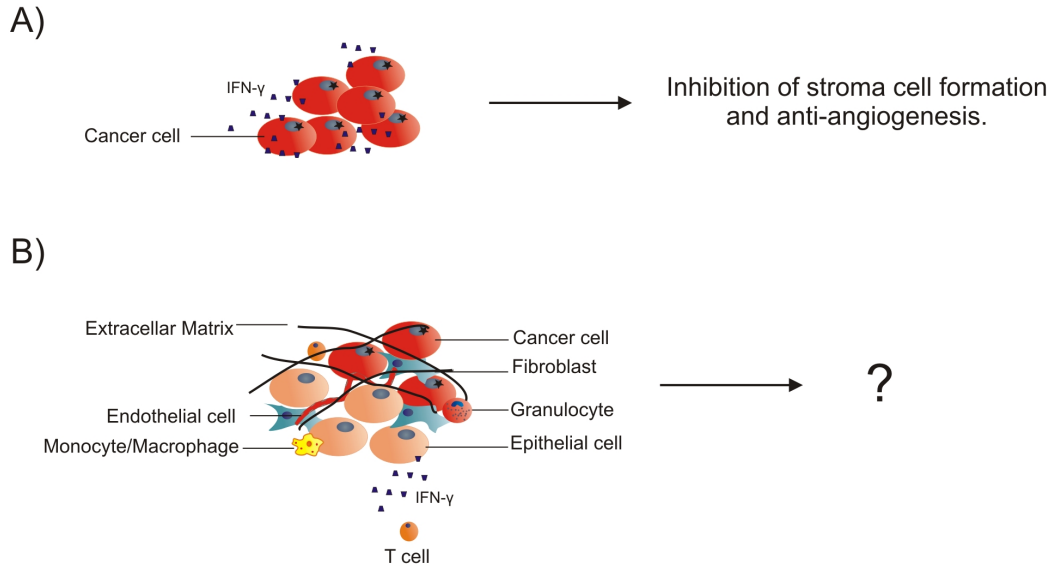


**Figure 3.1. Established tumors differ from tumor cell suspensions.** *In most experimental mouse models tumors are injected as tumor cell suspensions. (A) shows  $IFN-\gamma$  secreting tumor cell suspensions which are rejected in mice because they prevent tumor stroma formation. (B) Established, malignant tumors consist of tumor cells and their supportive matrix which is termed tumor stroma. The stroma of solid tumors consists of non-hematopoietic cells such as fibroblasts and endothelial cells, of the extracellular matrix produced by these cells and of hematopoietic cells such as monocytes/macrophages, granulocytes and T cells. Until now the effect of  $IFN-\gamma$  on established tumors was not investigated.*

Endothelial cells participate in wound healing, as do fibroblasts, forming the scaffold for angiogenesis. Growing tumors need angiogenesis: Up to a diameter of 2 mm a tumor is capable of absorbing nutrients by diffusion. In larger tumors, newly-built blood vessels serve for the supply of nutrients and gas-exchange. The hematopoietic cells usually induce a tumor-promoting inflammatory reaction.

An important aspect in cancer research is the discrimination between spontaneously occurring tumors and transplantable tumors. Spontaneous tumors arise from one transformed cell and develop in humans over a period of several months, years or even decades. In this period the tumor recruits cells which form a tumor-promoting microenvironment, the tumor stroma. To mimic this situation, autochthonous tumor models are developed and analyzed. Due to this time-consuming process, transplantable tumors are often used in experimental research. Tumor cells

require a certain period of time to develop an established stroma consisting of blood vessels, fibroblasts and immune cells.

Experiments in cancer research are often performed by injecting tumor cells into animals. These tumor cell suspensions only contain tumor cells without any supporting matrix or molecules (Figure 3.1 A). Hence, these experiments do not reflect the conditions and environment of human tumors which arise spontaneously and develop over a long period of time. According to Schreiber et al. most tumor cells of a tumor cell suspension die within the first few days after inoculation causing necrosis and an inflammatory reaction. Only a small rim of cancer cells survives adjacent to already existing blood vessels. These tumor cells proliferate, recruit stroma cells and form the tumor (Figure 3.1 B). Schreiber defines an established tumor to be approximately 14 days old and exhibit an average size of 1 cm in diameter. At this stage the transplantable tumor cannot be discriminated from a nontransplanted primary tumor even by a trained pathologist [37]. When tumors are detected in humans they are usually fully established. This suggests that in order to exclude effects of experimental artefacts like inflammation, tumor research should be performed in autochthonous or established tumors.

### 3.4 Tumor stroma as a target for immunotherapy

As discussed, tumor stroma is essential for the growth and maintenance of the tumor. Some publications suggest that cytotoxic T cells do not only target tumor cells but also stromal cells cross-presenting tumor antigens [38, 39]. Spiotto and Schreiber showed that CD8<sup>+</sup> T cells capable of targeting tumor cells and stroma cells led to tumor rejection, whereas antigen-loss variants grew out when only tumor cells were attacked. A more recently published study by Schietinger et al. suggests that not only cytotoxic CD8<sup>+</sup> but also CD4<sup>+</sup> T cells are necessary for bystander killing of cancer cells when antigen cross-presenting stromal cells are targeted [40]. Further studies showed that specific cytokines such as IL-2, IL-4, IL-7, IL-10, IFN- $\gamma$  and TNF [19, 41–43] can lead to tumor rejection. For IL-4 and IFN- $\gamma$  it was shown that they exert an inhibitory effect on non-hematopoietic stroma cells such as fibroblasts [44, 45]. Additionally, Singh et al. observed that inoculation of tumor cells embedded in stroma had higher chances of tumor formation compared to tumor cell inoculation alone [46, 47].

## 3.5 Cytokines

Cytokines are a family of relatively small, soluble proteins which mediate communication between cells [48]. This family of proteins includes mediators like interleukins, chemokines and interferons. Cytokines are responsible for the induction and regulation of the immune response. They are unstable proteins with a short half-life and have usually a more local than systemic effect.

With respect to tumor development and progression, cytokines can have tumor-promoting or tumor-inhibiting potential. Within the tumor tissue, tumor cells as well as stroma cells such as macrophages and T cells can produce cytokines. Cytokines bind specifically to their cognate receptor and trigger cell specific signalling. These small molecules are able to induce a great variety of functions in different cells, but often in redundant fashion. Studies with cytokine gene transduced tumor cells were already performed in the 1980s with marginal therapeutic success [19, 49].

Interferons were discovered in the 1950s as factors interfering with viral replication. This class of cytokines is divided into class I interferons (IFN- $\alpha$  and IFN- $\beta$ ) and class II interferons (IFN- $\gamma$ ). Recently, the U.S. Food and Drug Administration (FDA) approved interferon therapy for treatment of cancer such as hairy cell leukemia, melanoma, follicular non-Hodgkin's lymphoma and AIDS-related Kaposi's sarcoma.

### 3.5.1 Interferon gamma

Interferon gamma (IFN- $\gamma$ ) is a glycoprotein of 34 kDa and is a dimer in its active form [50]. The pro-inflammatory cytokine is mainly produced by stimulated T<sub>H</sub>1-cells, CD8<sup>+</sup> T cells and Natural killer cells (NK cells) [51]. IFN- $\gamma$  acts in many different ways on the cells of the native or adaptive immune system depending on cell type and degree of differentiation. It has already been shown that IFN- $\gamma$  stimulation can regulate more than 200 genes [52]. For instance, it activates neutrophil granulocytes and NK cells and also promotes differentiation of cytotoxic T cells [52]. Another important task of IFN- $\gamma$  is the activation of macrophages, the induction of cell surface expression of MHC I and II and the Fc-receptor. Additionally, it up-regulates other cytokines and chemokines such as the anti-angiogenic factor interferon gamma-induced protein 10 kDa (IP-10) [53].

IFN- $\gamma$  binds to the IFN- $\gamma$  receptor (IFN- $\gamma$ R) which is expressed on all nucleated cells. The IFN- $\gamma$ R consists of two homologous chains: the constitutively expressed IFN- $\gamma$ R 1 or alpha chain is responsible for ligand binding and the IFN- $\gamma$ R 2 or beta

chain for signal transduction [54]. It has been known for some time that IFN- $\gamma$  and IFN- $\gamma$ R are required for tumor rejection [19, 45, 55–58].

### 3.6 Tumors and IFN- $\gamma$

IFN- $\gamma$  is essential for tumor rejection in most models that have been analyzed [34, 59]. For example, IFN- $\gamma$  or IFN- $\gamma$ R deficient mice are impaired in their ability to reject tumors [56]. Similarly, blocking IFN- $\gamma$  by neutralizing antibodies accelerates tumor growth [60] and interferes with rejection of transplanted tumor cells [57]. Additionally, IFN- $\gamma$  secreting tumor cell lines are rejected in mice [19, 55].

The IFN- $\gamma$ R is expressed on almost all cells of the body. Therefore, IFN- $\gamma$  can act on many different cells during tumor rejection. However, because cytokines like IFN- $\gamma$  mostly act locally, the tumor microenvironment is believed to be a target of IFN- $\gamma$  during tumor rejection.

The assumption that the tumor stroma is an important target for IFN- $\gamma$  has been supported by a number of studies using transplantable tumor models [25, 38, 43, 45, 61, 62]. Experiments in bone marrow chimeras showed that hematopoietic [25] as well as non-hematopoietic stromal cells [25, 45] are essential targets of IFN- $\gamma$  during T cell mediated tumor rejection. For example, IFN- $\gamma$  secreted from CD4<sup>+</sup> and CD8<sup>+</sup> T cells interferes with tumor induced angiogenesis by inhibiting the recruitment of CD31<sup>+</sup> endothelial cells into the tumors [45, 63]. The inhibition of blood vessel formation by IFN- $\gamma$  secreted by tumor-specific T cells has been reported for a number of different transplantable tumor models [43, 45]. However, it is not clear whether this results from a direct effect on endothelial cells [64], or whether it is mediated by anti-angiogenic chemokines [65] such as IP-10 [66] or monokine induced by gamma interferon (MIG) [67], which can be induced by IFN- $\gamma$ . In most studies, the anti-angiogenic effect of IFN- $\gamma$  was examined shortly after tumor cell inoculation and prior to the establishment of an intact stroma. This experimental situation poorly resembles the clinical situation, in which tumors usually have grown already to a minimum diameter of 1 cm before they are diagnosed.

### 3.7 The tetracycline system

The transfection of tumors cells with cytokine genes is a widely-used technique [19, 41–43]. However, after transfection tumor cells continuously produce these cytokines. To investigate the effect of IFN- $\gamma$  on the stroma of established tumors

we used an inducible gene expression system. The most frequently used technique in mammalian cells and animals is the tetracycline (tet) system [68–70]. Through the application of the antibiotic tetracycline, a promoter and the following expression of the down–stream gene of interest can be either turned on or off.

The tet system is composed of a tet–controlled transactivator (tTA) which consists of a tetracycline repressor (TetR) derived from *Escherichia coli* fused to an enhancer domain (VP16) derived from Herpes simplex virus. Both are controlled by a cytomegalovirus promoter ( $P_{CMV}$ ). Additionally, there is the tet responsive element (TRE) to which the transactivator can bind. Downstream of this element there is a strong promoter followed by the gene of interest. Gene expression is activated if the transactivator protein binds on the DNA to the TRE element. Using the tet off system, the gene of interest is expressed until tetracycline is applied: Then, the tet molecule binds to the transactivator, which in turn cannot bind to the TRE element and the gene of interest is not transcribed.

The tet–on system acts in a similar way. Because of the exchange of four amino acids in the transrepressor, the transrepressor has to form a complex with tetracycline to be able to bind to the TRE element and start expression of the gene of interest [71]. The expression of the gene of interest is turned on, if tetracycline (or for instance the tetracycline–derivative doxycycline; Dox) is applied. An advantage of the tet system is that it is reversible. By either applying Dox (tet–off) or stopping Dox application (tet–on), gene expression is halted.



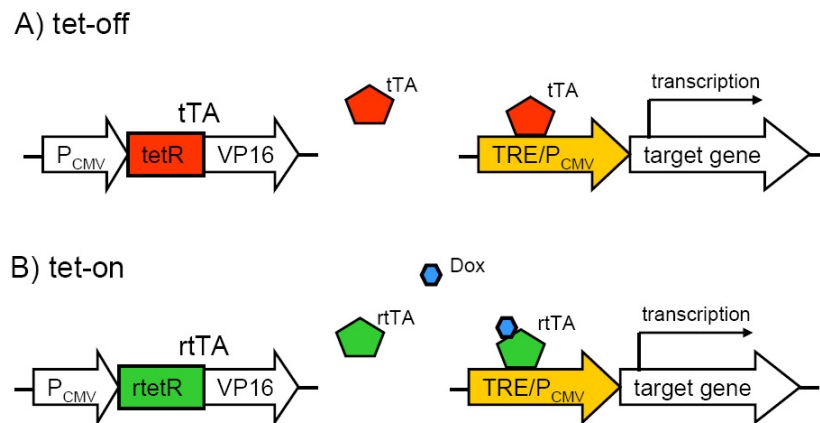


**Figure 3.2. Inducible gene expression in the tet system.** The tetracycline-inducible transactivator (*tTA*) is a fusionprotein consisting of the *tet*-repressor protein (*tetR*) and a viral activation domain (*VP16*) derived from *Herpes simplex virus*. Protein expression is regulated by a viral promoter ( $P_{CMV}$ ). (A) In the *tet-off* system the transactivator (*tTA*) binds to the *tet*-responsive element (*TRE*) only in the absence of *Dox*. Binding induces transcription of the target gene which is regulated by a minimal viral promoter ( $P_{CMV}$ ). (B) The *tet-on* system functions similarly. A change of four aminoacids of the *tTA* protein leads to a reverse transactivator protein (*rtTA*). The *rtTA* protein can only bind to *TRE* and start gene expression if it forms a complex with *Dox*.

## 4 Aims of this thesis

Effector T cells usually express a variety of effector molecules in addition to IFN- $\gamma$ , such as tumor necrosis factor (TNF), perforin or Fas-ligand. Therefore, it was not clear whether tumor rejection is dependent on other T cell-derived effector molecules, rather than on IFN- $\gamma$  alone. To be able to analyze the sole effect of IFN- $\gamma$  and exclude other effector molecules and cytokines on tumor cells, tumor cells were transduced to produce IFN- $\gamma$  themselves.

The contribution of ectopically expressed IFN- $\gamma$  to tumor rejection tumor cell suspensions transplanted under the skin of mice was analyzed in a number of studies in the 1990ies [18, 19, 38, 55]. However, these experiments were done very early in tumor development (day 0–5), with very small tumors [18, 72] or tumor cell suspensions. In these experiments the stroma was not established and inoculation of tumor cell suspensions led to artifacts like massive necrosis and inflammation which do not reflect spontaneously arising human tumors. Generally, tumors in humans are detected when they have a minimum size of 1 cm in diameter and have a well established stroma.

Therefore, we wanted to address the question whether in a more clinically relevant model using tumors with established stroma, IFN- $\gamma$  can mediate rejection of established tumors.

Furthermore, we aimed to clarify whether IFN- $\gamma$  needs to act primarily on the cancer cells or on tumor stroma cells to reach this goal and importantly, which stroma cells are targets of IFN- $\gamma$ .

# 5 Materials and Methods

## 5.1 Mice

BALB/c, C57BL/6 and NOD/SCID mouse strains were purchased from Charles River. BALB/c IFN- $\gamma$ <sup>-/-</sup> (strain no. 002286), C57BL/6 IFN- $\gamma$ <sup>-/-</sup> (strain no. 002287), C57BL/6 IFN- $\gamma$ R<sup>-/-</sup> (strain no. 003288) and RAG1<sup>-/-</sup> mice (strain no. 002216) were obtained from the Jackson laboratories and bred at the FEM, Charité. RAG1<sup>-/-</sup> x IFN- $\gamma$ R<sup>-/-</sup> mice were bred in the FEM. Six to twelve weeks old female and male mice were used for experiments.

## 5.2 Tumor cell lines

The plasmacytoma cell line J558L is derived from a BALB/c mouse. It is a heavy chain loss variant of the plasmacytoma J558 [73]. The IFN- $\gamma$ R deficient fibrosarcoma MCA313 is a methylcholanthrene induced tumor cell line. The tumor was induced by subcutaneous injection of 25  $\mu$ g methylcholanthrene dissolved in sesame-oil in an IFN- $\gamma$ R deficient mouse on the C57BL/6 background. At a size of 15 x 20 x 14 mm the tumor was re-isolated and established as a tumor cell line. Platinum-E cells (Plat-E) are effective retrovirus packaging cells derived from 293T cells and were used for virus production [74].

## 5.3 Reagents

*Table 5.1. List of reagents*

Name	Abbr.	Manufacturer
Acetone		VWR, Darmstadt; GER
Agarose		VWR, Darmstadt; GER
Alexa 594 goat anti-rat		Invitrogen, Karlsruhe, GER

*List of reagents, cont'*

Name	Abbr.	Manufacturer
Antibiotic/Antimycotic		Invitrogen, Karlsruhe, GER
Aquamount		Merck, Darmstadt, GER
Bovine serum albumine	BSA	
CD31, purified rat anti-mouse monoclonal antibody		BD Biosciences, Heidelberg, GER
D-(+)-Glucose	Glc	Sigma, Taufkirchen, GER
Collagenase II		Invitrogen, Karlsruhe, GER
Dimethylsulfoxid	DMSO	Pan, Aidenbach, GER
DNA-Markers (Easyladder I, Hyperladder I)		Bioline, Luckenwalde, GER
Doxycycline	Dox	Sigma, Taufkirchen, GER
Dulbecco modified Eagle Medium	DMEM	Invitrogen, Karlsruhe, GER
Dulbeccos phosphate buffered saline (1x)	PBS	Invitrogen, Karlsruhe, GER
Eosin-Y-alcoholic solution		VWR, Darmstadt; GER
Ethanol	EtOH	VWR, Darmstadt; GER
Ethidiumbromide	EtBr	Sigma, Taufkirchen, GER
FastDigest NcoI	NcoI	Fermentas GmbH, St. Leon-Rot, GER
FastDigest NotI	NotI	Fermentas GmbH, St. Leon-Rot, GER
FastDigest XhoI	XhoI	Fermentas GmbH, St. Leon-Rot, GER
Fetal calf serum	FCS	Invitrogen, Karlsruhe, GER
Forene (isoflurane)		Wiesbaden-Delkenheim, GER
Glycerol		Sigma, Taufkirchen, GER
Goat serum		Linaris, Wertheim-Bettingen, GER
Hematoxyline II Gill		VWR, Darmstadt; GER
Histoclear		Sigma, Taufkirchen, GER
Histomount <sup>TM</sup>		Thermo Shandon; Pittsburgh; PA, USA

*List of reagents, cont'*

Name	Abbr.	Manufacturer
10% Isopropanol	IPA	Sigma, Taufkirchen, GER
Loading buffer 5x		Bioline, Luckenwalde, GER
Methanol		VWR, Darmstadt, GER
Nitrogen (liquid)	N <sub>2</sub> (l)	Air Liquide
Non-essential aminoacid solution	NEAA	Pan, Aidenbach, GER
O.C.T. Compound	OCT	Tissue Tek
Paraffin		Sigma, Taufkirchen, GER
Paraformaldehyde 4 %		Sigma, Taufkirchen, GER
PCR-Buffer 10x		Roche Diagnostics GmbH, Mannheim, GER
Penicillin/Streptomycin	P/S	Invitrogen, Karlsruhe, GER
Protamine sulfate		Sigma, Taufkirchen, GER
RetroNectin		Takara, Apen, GER
RPMI 1640-Medium	RPMI	Invitrogen, Karlsruhe, GER
Sodium chloride solution	NaCl	Roth, Karlsruhe, GER
Sodium pyruvate		Pan, Aidenbach, GER
Tris-Hydrochloride		Roth, Karlsruhe, GER
Trypsin [10 mg/ml]		Invitrogen, Karlsruhe, GER
Trypan blue		Sigma, Taufkirchen, GER
Tween 20		Sigma, Taufkirchen, GER
Vectashield mounting media for fluorescence		Linaris, Wertheim-Bettingen, GER

## 5.4 Kits

*Table 5.2. List of Kits*

Name	Manufacturer
BD OptEIA™ Reagent Set B	BD OptEIA™, Heidelberg, GER
Mouse Th1/Th2 10plex	Bender Medsystems, Vienna, Austria
Mouse Basic Kit	Bender Medsystems, Vienna, Austria
Mouse IFN- $\gamma$ Simplex	Bender Medsystems, Vienna, Austria

*List of Kits, cont'*

Name	Manufacturer
Mouse TNF alpha Simplex	Bender Medsystems, Vienna, Austria
Mouse IL-10 Simplex	Bender Medsystems, Vienna, Austria
Mouse IFN- $\gamma$ ELISA Kit	BD OptEIA <sup>TM</sup> , Heidelberg, GER

To perform an IFN- $\gamma$  ELISA, the BD IFN- $\gamma$  ELISA kit and BD Reagent Set B (including substrates, stopping solution and washing buffer) were used according to the manufacturers instructions. Cytometric bead arrays were performed according to the Bender Medsystems instructions. To measure 10 cytokines in one assay the mouse Th1/Th2 10plex kit was used. To measure single cytokines such as IFN- $\gamma$ , TNF- $\alpha$  or Interleukin 10 the respective mouse simplex kits were used.

## 5.5 Media and Buffers

*Table 5.3. List of Media and Buffers*

Name	Content
Buffer Immunohistology (cell surface proteins)	PBS + 1% BSA
Buffer Immunohistology (intracellular proteins)	PBS + 0.2% Gelatine or 0.1% Tween
FACS buffer	PBS, 1% BSA, 0.1% NaN <sub>3</sub>
Medium I	RPMI, 10% FCS, 1% NEAA, 1% Sodium pyruvate, 1% P/S, 1-2% Antibiotic-Antimycotic
Medium II (for CaPO <sub>4</sub> transfection)	DMEM without additives
Transfection buffer	1% HEPES, 1.5 mM Na <sub>2</sub> HPO <sub>4</sub> , 270 mM NaCl, 10 mM KCl, pH 6.75
50 x TAE	242 g Tris Base, 57.1 g glacial acetic acid, 37.2 g Na <sub>2</sub> EDTA*H <sub>2</sub> O ad 1 l H <sub>2</sub> O; pH 8

## 5.6 Consumable Material

*Table 5.4. List of Consumable Material*

Name	Manufacturer
Cell-culture-plates (96-, 24, 12, 6 well-plates; flat and round bottom)	Corning Costar, Bodenheim, GER
Cell-culture flasks (T-25, T-75, T-150)	Merck, Darmstadt, GER
Combitips	Eppendorf, Hamburg, GER
Cryo tubes	Nunc, Wiesbaden, GER
Cryo tubes (tissue)	Roth, Karlsruhe, GER
Disposable syringes (1 ml)	Becton Dickinson, Heidelberg, GER
Eppendorf tubes (2 ml, 1.5 ml)	Eppendorf, Hamburg, GER
FACS-tube	Becton Dickinson, Heidelberg, GER
Falcon tubes (15 ml, 50 ml)	BD Falcon, Heidelberg, GER
Injection cannulas	Becton Dickinson, Heidelberg, GER
Neubauer counting chamber	Assistant, GER
Object slides	Dako, Hamburg, GER
Picture frame glass	VWR, Darmstadt, GER
Pipette tips	Merck, Darmstadt, GER
Sterile Pipettes (5, 10, 25 ml)	Corning Costar, Bodenheim, GER
Strainer (0.2; 0.45 $\mu$ m)	Becton Dickinson, Heidelberg, GER

## 5.7 Equipment

*Table 5.5. List of Equipment*

Name	Manufacturer
Analytical balance EW600-2M	Gottl. Kern & Sohn GmbH, Balingen-Frommern, GER
BioDoc Analyze Geldocumentation	Biometra GmbH, Goettingen, GER
BioPhotometer	Eppendorf Vertrieb Deutschland GmbH, Wesseling-Berzdorf, GER

*List of Equipment, cont'*

Name	Manufacturer
Bunsen burner	Usbeck Carl Friedrich KG Labor–Metall–Geraete, Radevormwald, GER
Camera ColorView XS Soft Imaging System	Olympus, Hamburg, GER
Centrifuge Sigma 202 MK	SIGMA Laborzentrifugen GmbH, Osterode am Harz, GER
Centrifuge 5415D	Eppendorf, Hamburg, GER
Cleanbench Heraeus	Thermo Fisher Scientific, Karlsruhe, GER
CO <sub>2</sub> Inkubator MCO 17AIC	Sanyo, Japan
Cooling plate CP 60	Microm Int., Walldorf, GER
Cell counting chamber Neubauer improved	Carl Roth GmbH + Co. KG, Karlsruhe, GER
Centrifuge 5804R	Eppendorf, Hamburg, GER
Digital Graphic Printer UP–D890	Sony Professional Solutions Europe, Berlin, GER
ELISA–Reader Opsys MR	Dynex Technologies, Berlin, GER
FACSCalibur flow cytometer	Becton Dickinson GmbH, Heidelberg, GER
Freezer –86 °C	Forma Scientific, Cotech, Berlin, GER
Gel electrophoresis cell	Bio–Rad Laboratories GmbH, Munich, GER
High precision analytical balance MC1	Sartorius AG, Goettingen, GER
Hot air oven	Memmert, Schwalbach, GER
Incubator	Memmert, Schwalbach, GER
KSeries Cryostage System	Jencons Scientific Inc., USA
Liquid nitrogen tank	Messer Griesheim, Griesheim, GER
Megafuge 1.0R	Thermo Fisher Scientific, Karlsruhe, GER
Microscope DMIL	Leica Microsystems, Wetzlar, GER
Microscope BX51	Olympus, Hamburg, GER
Microtom Cryostat HM560	Microm Int., Walldorf, GER



*List of Equipment, cont'*

Name	Manufacturer
Microwave oven	Siemens–Elektrogeraete GmbH, Munich, GER
Milli Q	Millipore, Schwalbach, GER
Paraffin bath 25900	MEDAX GmbH & Co.KG, Rendsburg, GER
pH–meter 761	Knick Elektronische Messgeraete GmbH & Co. KG, Berlin, GER
Pipettes (single–channel, multichannel, Repeater)	Eppendorf, Hamburg, GER
Refrigerator	Liebherr–Hausgeraete Ochsenhausen GmbH, Ochsenhausen, GER
Refrigerator for Bacteria R22	Revco, Thermo Fisher Scientific, Karlsruhe, GER
Shaker Duomax 1030	Heidolph Instruments GmbH&Co.KG, Schwabach, GER
Sled microtom HM430	Microm Int., Walldorf, GER
Spectrophotometer DU650	Beckman Coulter GmbH, Krefeld, GER
Shaking incubator GFL 3033	GFL Gesellschaft fuer Labortechnik mbH, Burgwedel, GER
T3–Thermocycler	Biometra GmbH, Goettingen, GER
Thermomixer Comfort	Eppendorf, Hamburg, GER
Vortexer Reax 2000	Heidolph Instruments GmbH&Co.KG, Schwabach, GER
Water bath WB10	Memmert, Schwalbach, GER

## 5.8 Vector for inducible IFN– $\gamma$ expression

A retroviral vector construct was used for the inducible expression of the IFN– $\gamma$  gene, in which the transactivator and the tetracycline inducible element are combined in one vector. The retroviral vector was constructed on the basis of the recently published pES.1 backbone [75]. A bidirectional promoter has been integrated into

this vector, consisting of a new regulatory unit (Ptet-T2) and a constitutive promoter (hPGK) (Fig. 5.1). While the human phosphoglycerate kinase (hPGK) promoter drives expression of the reverse tet-dependent M2-transactivator ("tet-on") in sense orientation with respect to viral transcription, the regulatory unit expressing the transgene was inverted. As a consequence, the M2-transcript is terminated at the viral poly A signal at the 3'-LTR, while the transcript of the transgene is terminated at a human growth hormone polyadenylation signal (hghpA) added 3'- to the open reading frame [76] (Figure 5.1).

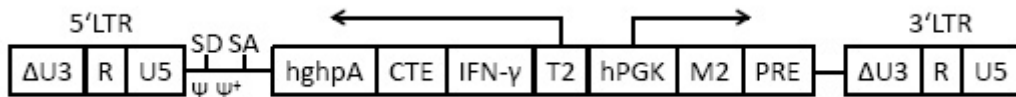


**Figure 5.1. Vector for inducible IFN- $\gamma$  expression.** The retroviral vector consists an extended packing region ( $\psi, \psi^+$ ), splice donor (SD) and acceptor sites (SA). The construct is flanked by self-inactivating long terminal repeats (SIN-LTRs;  $\Delta U3$ ) which minimize the risk of activating the promoter of a gene located adjacent to the integrated vector. The elements for the tet-regulated transgene expression were inserted as a bidirectional expression cassette. In sense direction the reverse tet-responsive transactivator variant M2 is constitutively expressed by the human phosphoglycerate kinase promoter (hPGK), which is followed by the woodchuck hepatitis virus posttranscriptional regulatory element (PRE). In antisense direction the tet-inducible IFN- $\gamma$  is integrated along with the constitutive transport element (CTE), from Mazon Pfizer Monkey Virus and the human growth hormone polyadenylation signal (hghpA). Detailed vector chart is attached in Appendix A.1.

The coding region of the murine IFN- $\gamma$  cDNA was amplified via PCR using primers (Appendix B.1) with NcoI and NotI restriction sites, respectively. The PCR product could not be cloned directly in to the pMOV1.1-T2 (Figure A.1) because of additional NcoI restriction sites in this plasmid. Therefore, the PCR product was first integrated into the plasmid SK-T2IFN- $\gamma$  (Figure A.2) replacing the EGFP gene via NcoI and NotI restriction sites. From the resulting plasmid a fragment including the IFN- $\gamma$  cDNA and the T2 region was excised and integrated into the final pMOV1.1-T2-IFN- $\gamma$  vector using XhoI and NotI restriction sites.

## 5.9 Production of virus supernatant

Plat-E cells are capable of transient production of retroviral particles.  $8 \times 10^5$  Plat-E cells were seeded into 6-well-plates in 3ml medium. After 24 h the transfection mixture was prepared in a falcon tube. 18  $\mu\text{g}$  of the pMOV1.1-T2-IFN- $\gamma$  DNA

were added to a final volume of 135  $\mu\text{l}$   $\text{H}_2\text{O}$  and 15  $\mu\text{l}$   $\text{CaCl}_2$ . While vortexing the tube 150  $\mu\text{l}$  transfection buffer were added drop by drop to the mixture. After 15 min of incubation at room temperature the resulting mixture was added drop by drop to the seeded cells. After 6 h medium was changed. Virus supernatant was used after filtration through a 0.45  $\mu\text{m}$  filter to dispose of cells and cell debris.

## 5.10 Transduction of tumor cells

$2 \times 10^5$  J558L tumor cells were seeded into 24-well-plates coated with RetroNectin (3.5  $\mu\text{g}/\text{well}$ ). 1 ml retrovirus supernatant supplemented with protamine sulfate (final concentration: 4  $\mu\text{g}/\text{ml}$ ) was added and plates were spinoculated with 800 g for 1.5 h at 32 °C.  $5 \times 10^4$  MCA313 cells were seeded into 24-well-plates. 24 h later, 1 ml retrovirus supernatant supplemented with protamine sulfate was added. Cells transduced with the retroviral vector pMOV.1-T2-IFN- $\gamma$  were cultured for one week and cloned by limiting dilution.

## 5.11 Generation of IFN- $\gamma$ -inducible cells

In order to identify IFN- $\gamma$  producing clones of both cell lines, cells were seeded by limiting dilution and growing clones were cultured in the presence of 1  $\mu\text{g}/\text{ml}$  Dox. 48 h after adding Dox, supernatants were taken for analysis and stored at -20 °C. To determine IFN- $\gamma$  levels in the culture supernatant a standard IFN- $\gamma$  Enzyme-linked immunosorbent assay (ELISA) was performed. The clone with the highest inducible IFN- $\gamma$  expression was chosen for the experiments and designated as J558L-IFN- $\gamma^{\text{IND}}$  (clone F11) or MCA313-IFN- $\gamma^{\text{IND}}$  (clone A5), respectively.  $1 \times 10^6$  cells were cultured for 48 h in the presence of increasing amounts of Dox (0, 10, 50, 100 or 1000 ng/ml) and IFN- $\gamma$  levels were determined.

Proliferation of J558L-IFN- $\gamma^{\text{IND}}$  cells was determined via XTT assay, seeding 100 cells in triplicates into 96-well plates in the presence or absence of Dox. XTT was added for 4 hours after 4, 5 or 6 days of culture and absorbance of the metabolized substrate was determined at 450 nm using a spectrophotometer.

## 5.12 Tumor transplantation experiments

$1 \times 10^6$  J558L, J558L-IFN- $\gamma^{\text{IND}}$  or MCA313-IFN- $\gamma^{\text{IND}}$  tumor cells were injected subcutaneously (s.c.) into the right flank of the mice. Tumor size was measured 2–3

times weekly in three dimensions using a caliper. Tumor volume was calculated using the formula:  $\Pi/6 \times (\text{length} \times \text{width} \times \text{height})$ . Volumes indicated in the text are the average of 3–5 mice in one experimental group. Mice were divided into groups with similar tumor sizes and Dox was administered via the drinking water supplemented with 2 mg/ml glucose in concentrations as indicated in the text.

### 5.13 Re-isolation of tumor cells

To analyze whether tumor cells that grew despite Dox-induced IFN- $\gamma$  treatment had lost the ability to produce IFN- $\gamma$  or showed a reduced capacity of IFN- $\gamma$  expression, tumor cells were re-isolated: Tumors were removed, cut into small pieces and after two to four hours of incubation at 37 °C in medium containing 10 % trypsin and 100 mg/ml collagenase II, cells were washed and taken into culture. After two weeks of cell culture  $1 \times 10^6$  re-isolated cells were cultured for 48 h with 1  $\mu\text{g}/\text{ml}$  Dox and IFN- $\gamma$  levels in the supernatant were determined by ELISA.

### 5.14 Analysis of IFN- $\gamma$ serum levels

Blood samples were taken at different time points before and after Dox administration. Blood samples were allowed to coagulate and then centrifuged at 13.000 rpm (Sigma 202 MK centrifuge) for 20 minutes at 4 °C. Serum was aliquoted and stored at -80 °C. All aliquots were used only once for the test. To determine serum IFN- $\gamma$  levels after Dox-mediated induction of IFN- $\gamma$ , 25  $\mu\text{l}$  serum was analyzed using the cytometric bead array from Bender Medsystems according to manufacturer's instructions. Flowcytometric analysis of samples was performed on a BD FACSCalibur and analyzed using the Bender Medsystems software.

### 5.15 Determination of liver values

Blood samples were taken and serum was generated as mentioned above. Serum samples were sent to Laboklin GMBH & Co.KG, Bad Kissingen, Germany for determination of the liver transaminases alanine aminotransferase (ALT) and aspartate aminotransferase (AST).

## 5.16 Immunohistochemistry

Half of the tumor material was embedded in OCT tissue compound, frozen using liquid nitrogen and stored at  $-80\text{ }^{\circ}\text{C}$ .  $4\text{ }\mu\text{m}$  sections were cut using a Microtom Cryostat. The other half of the tumor material was put into 4 % paraformaldehyde, dehydrated and embedded in paraffin.

Immunofluorescent staining was performed using frozen sections: Sections were air-dried for 10 min, fixed with an ice-cold methanol-acetone mixture (1:1) and washed three times with PBS. To block unspecific binding of the antibodies, slides were incubated for 25 min with PBS containing 1 % BSA and 1 % goat serum. Afterwards the primary anti-CD31 antibody was added for two hours. After the washing step sections were incubated for  $\frac{1}{2}$ -1h with the secondary antibody Alexa 594 (goat anti-rat). Slides were washed with PBS containing BSA and briefly with aqua dest. Slides were allowed to dry in the dark, cover-slipped with Vectashield containing DAPI and sealed.

Immunohistochemistry was performed using formalin-fixed, paraffin-embedded material ( $1\text{ }\mu\text{m}$  sections) and endothelial cells were stained with an anti-CD146 antibody (ME-9F1) by Simone Spiekermann [77]. H&E staining was performed according to standard protocols.

## 6 Results

### 6.1 The plasmacytoma J558L model

#### 6.1.1 Generation and in vitro characterization of J558L-IFN- $\gamma$ <sup>IND</sup> cells

In order to establish a model that allows inducible ectopic expression of IFN- $\gamma$  by tumor cells, the IFN- $\gamma$  cDNA was cloned into the bidirectional expression cassette of the retroviral vector pMOV.1-T2. To compare how efficiently IFN- $\gamma$  interferes with stroma recruitment as opposed to destruction of an established stroma, the plasmacytoma cell line J558L was chosen, because constitutively IFN- $\gamma$  producing J558L cells do not grow in mice [19]. J558L cells were transduced with pMOV.1-T2-IFN- $\gamma$ . The cells were subcloned by limiting dilution. Inducible IFN- $\gamma$  expression was tested in vitro by culturing the cells for 48 h with 1  $\mu$ g/ml of Dox. IFN- $\gamma$  concentration in tissue culture supernatant was determined by ELISA. A cell line with inducible IFN- $\gamma$  expression (designated J558L-IFN- $\gamma$ <sup>IND</sup>) was established from a clone. As shown in Figure 6.1 A, IFN- $\gamma$  expression by J558L-IFN- $\gamma$ <sup>IND</sup> cells was inducible and correlated with the amount of Dox used. Importantly, there was no IFN- $\gamma$  expression detectable in the absence of Dox, while the maximum concentration of  $\sim$ 60 ng/ml IFN- $\gamma$  was reached at a Dox concentration of 1000 ng/ml. In order to exclude that IFN- $\gamma$  affected the proliferation of J558L-IFN- $\gamma$ <sup>IND</sup> cells, an XTT proliferation assay was performed. J558L-IFN- $\gamma$ <sup>IND</sup> cells and J558L cells were cultured for four to six days in the presence or absence of Dox and proliferation was determined adding XTT reagent and measuring the metabolic activity by the color change of the substrate XTT via ELISA reader. As shown in Figure 6.1 B and C, the growth kinetics of J558L-IFN- $\gamma$ <sup>IND</sup> and J558L cells did not differ in the presence or absence of Dox. From this result we conclude that IFN- $\gamma$  has no effect on the growth of the tumor cells in vitro.

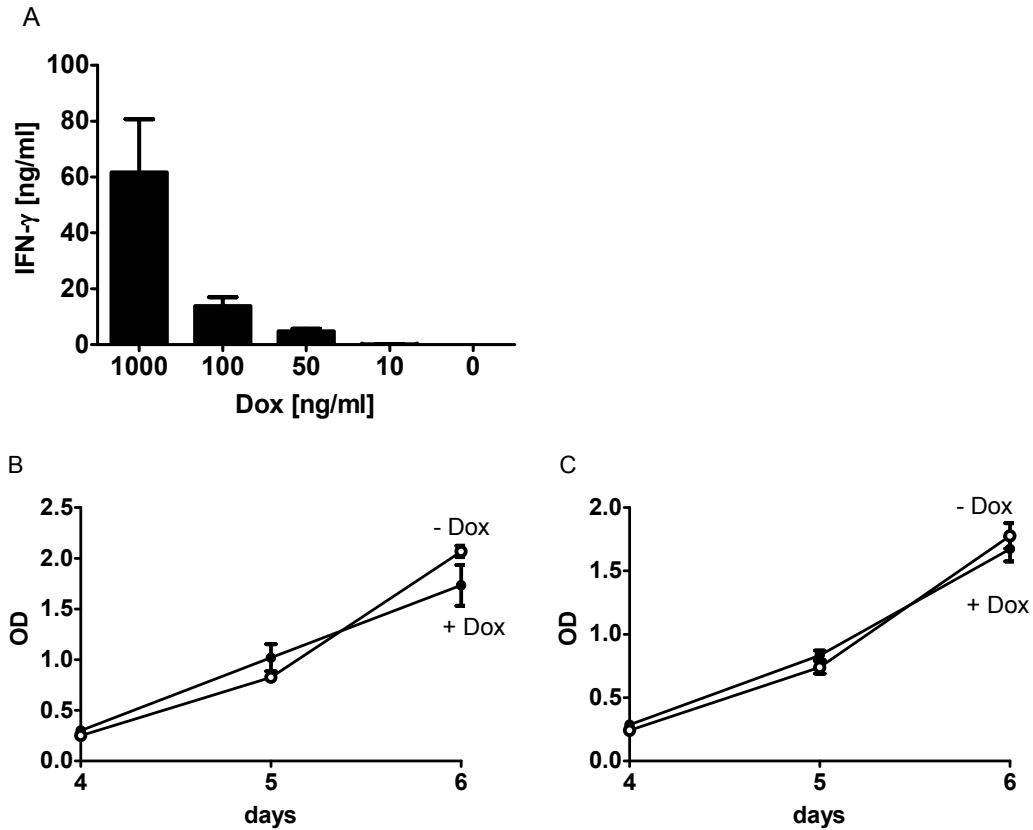


**Figure 6.1.** Characterization of J558L-IFN- $\gamma^{\text{IND}}$  cells. (A) Different concentrations of Dox were added to  $1 \times 10^6$  J558L-IFN- $\gamma^{\text{IND}}$  cells. After 48 h cell culture supernatant was taken and IFN- $\gamma$  concentration was determined by ELISA. Shown are the mean values and SD from 2 experiments. (B) and (C) show XTT proliferation assay with (B) J558L-IFN- $\gamma^{\text{IND}}$  and (C) J558L cells. Hundred cells were cultured for six days either in the presence (closed symbols) or absence (open symbols) of 1  $\mu\text{g/ml}$  Dox. XTT was added to the cultures at days 4, 5 and 6 and metabolization of XTT was determined after 4 h of incubation by measuring light absorbance at a wavelength of 450 nm. Shown are mean values of sextuplicates and SD from one out of two experiments with similar results.

### 6.1.2 High amounts of IFN- $\gamma$ are detectable in the serum after IFN- $\gamma$ induction

To determine the amount of IFN- $\gamma$  produced by the J558L-IFN- $\gamma^{\text{IND}}$  cells in vivo, serum was taken from J558L-IFN- $\gamma^{\text{IND}}$  tumor bearing BALB/c mice at different time points after Dox administration. Cytokine levels were determined using a cytometric bead array (examples shown in Figure 6.3). As shown in Figures 6.2 and 6.3, no IFN- $\gamma$  was detectable without induction, but large amounts of IFN- $\gamma$  were detectable in the serum as early as 48 h after IFN- $\gamma$  induction. IFN- $\gamma$  levels peaked at day four after induction in small tumors and at day twelve after induction in large tumors. Serum levels decreased after these peaks probably due to the rejection process that led to fewer tumor cells producing IFN- $\gamma$ . Similarly, the amounts of IFN- $\gamma$  produced correlated with the size of the tumors (Fig. 6.2). Importantly, there was almost no IFN- $\gamma$  detectable in mice bearing J558L-IFN- $\gamma^{\text{IND}}$  tumors without Dox administration, suggesting a tight system and very low endogenous IFN- $\gamma$  levels.

### 6.1.3 J558L-IFN- $\gamma^{\text{IND}}$ tumor cells grow after induction of IFN- $\gamma$ in IFN- $\gamma\text{R}$ deficient mice

Having excluded an autocrine effect of IFN- $\gamma$  in vitro, we next analyzed tumor growth in the presence or absence of Dox in RAG1 $^{-/-}$  x IFN- $\gamma\text{R}^{-/-}$  and in RAG1 $^{-/-}$  x IFN- $\gamma\text{R}^{+/+}$  mice. We used IFN- $\gamma\text{R}^{-/-}$  mice backcrossed to T cell deficient RAG1 $^{-/-}$  mice, because IFN- $\gamma\text{R}^{-/-}$  mice are on the C57BL/6 genetic background and mice that are sufficiently backcrossed to the BALB/c genetic background were not available. The BALB/c derived J558L cells would have been rejected as an allograft in T cell competent C57BL/6 mice.

No tumors formed after IFN- $\gamma$  induction concomitantly to tumor cell injection in RAG1 $^{-/-}$  x IFN- $\gamma\text{R}^{+/+}$  mice. In contrast, tumors in RAG1 $^{-/-}$  x IFN- $\gamma\text{R}^{-/-}$  mice grew progressively despite IFN- $\gamma$  induction at the day of tumor cell injection (Fig. 6.4 A and C). In addition, established J558L-IFN- $\gamma^{\text{IND}}$  tumors grew despite Dox-mediated induction of IFN- $\gamma$  without delay in RAG1 $^{-/-}$  x IFN- $\gamma\text{R}^{-/-}$  mice, while there was a delay in tumor growth after Dox induction in RAG1 $^{-/-}$  x IFN- $\gamma\text{R}^{+/+}$  mice (Fig. 6.4 B and D) arguing against an autocrine effect of tumor-derived IFN- $\gamma$  in vivo.



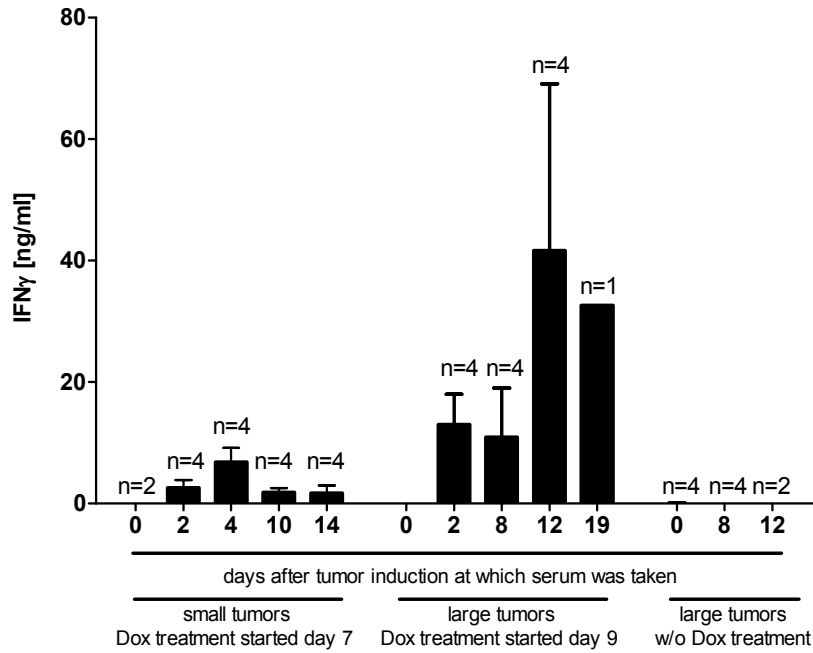


**Figure 6.2. J558L-IFN- $\gamma$ <sup>IND</sup> cells produce high amounts of IFN- $\gamma$  in vivo.**  $1 \times 10^6$  J558L-IFN- $\gamma$ <sup>IND</sup> cells were injected s.c. into BALB/c mice. To determine systemic IFN- $\gamma$  serum levels after Dox-mediated IFN- $\gamma$ -induction in J558L-IFN- $\gamma$ <sup>IND</sup> tumors, serum was taken at different time points after Dox-induction. Using a cytometric bead array, 25  $\mu$ l of the serum was analyzed from BALB/c mice bearing small (Dox from day 7;  $51 \pm 28$  mm<sup>3</sup>) and large tumors (Dox from day 9;  $506 \pm 49$  mm<sup>3</sup>) under Dox treatment and of large tumors without Dox. Shown are the mean values and SD of 2–5 mice (n for each time point indicated above the individual bars).

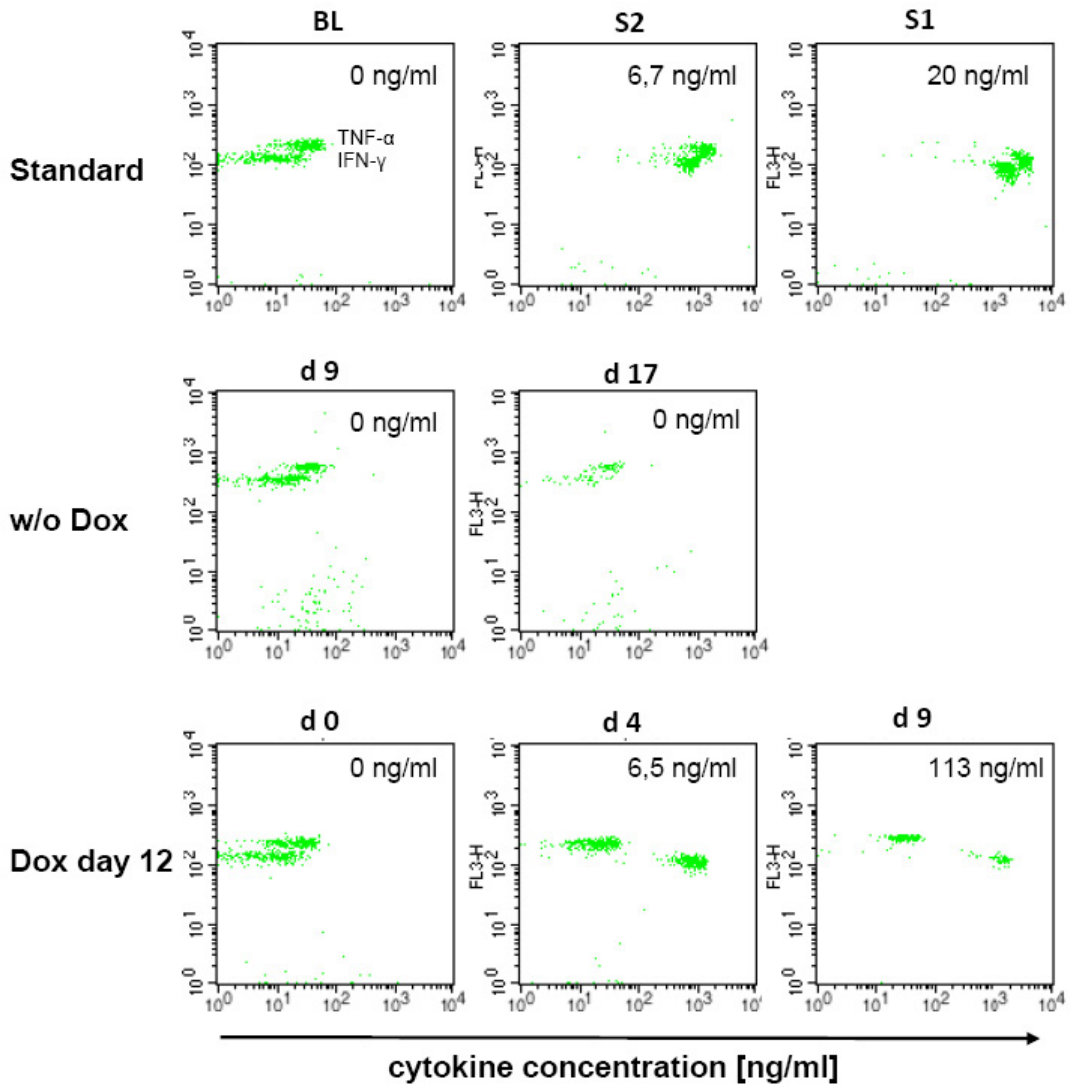


**Figure 6.3.** Cytometric bead array allows the detection of IFN- $\gamma$  produced by J558L-IFN- $\gamma^{IND}$  cells *in vivo*. Serum samples of differently treated groups were taken and measured via cytometric bead array. Shown are individual examples of BALB/c mice bearing J558L-IFN- $\gamma^{IND}$  tumors without IFN- $\gamma$  induction and induced at day 12 after tumor cell injection (mean values shown in Fig. 6.2). The cytokines TNF- $\alpha$  and IFN- $\gamma$  were measured in this bead array. Blank value and two standards are shown in the first row, cytokine levels of an untreated mouse at day 9 and 17 after Dox administration are shown in the second row. The third row shows cytokine levels of a mouse induced at day 12, day 0, 4 and 9 after Dox administration. Corresponding IFN- $\gamma$  concentrations are depicted in the graphs. Third row, Dox administration day 9 equates a 1 in 10 dilution.

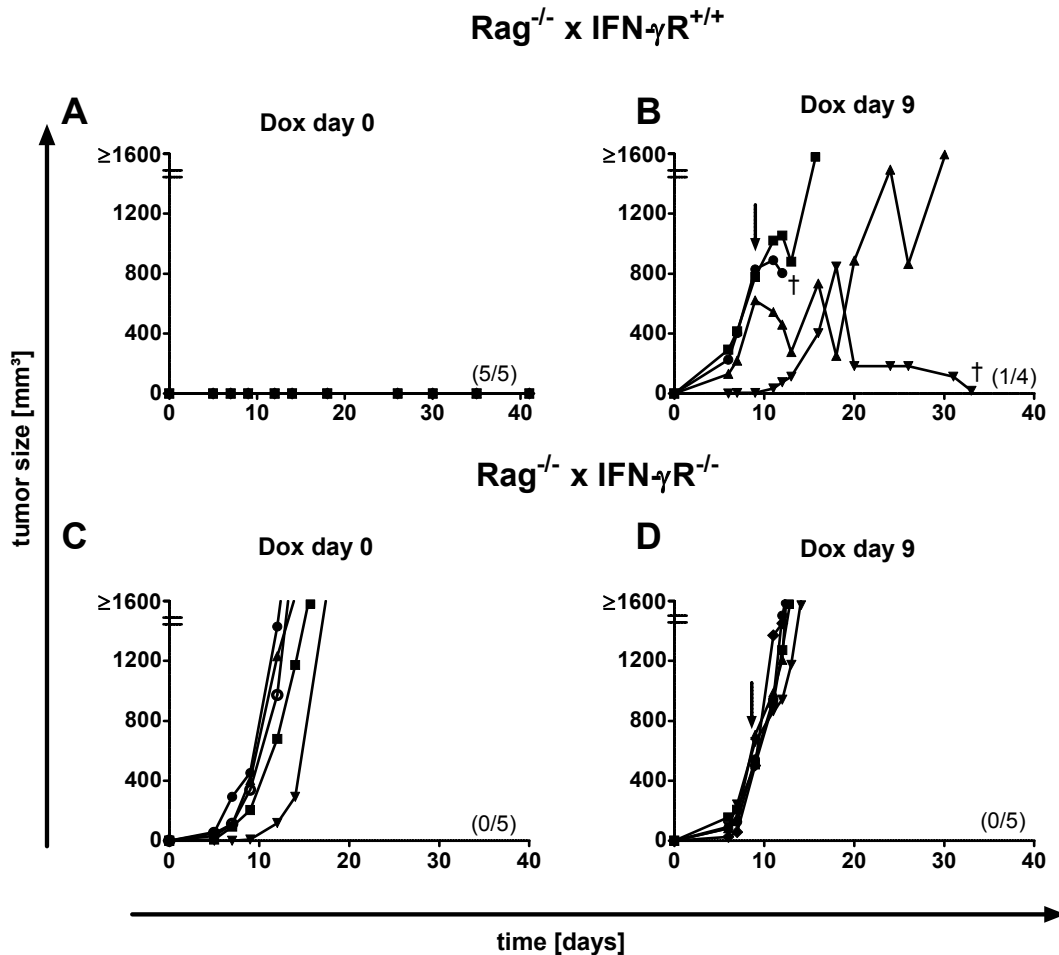


**Figure 6.4.** No growth delay of J558L-IFN- $\gamma$ <sup>IND</sup> tumors after IFN- $\gamma$  induction in hosts lacking IFN- $\gamma$  receptor expression.  $1 \times 10^6$  J558L-IFN- $\gamma$ <sup>IND</sup> cells were injected into (A) and (B) RAG1<sup>-/-</sup> x IFN- $\gamma$ R<sup>+/+</sup> and into (C) and (D) RAG1<sup>-/-</sup> x IFN- $\gamma$ R<sup>-/-</sup> mice. (A) and (C) show mice receiving Dox concomitant to tumor cell injection. In (B) and (D) IFN- $\gamma$  was induced at day 9 by administering Dox (1 mg/ml) via the drinking water and arrows indicate the time point of Dox application. Numbers in parentheses show rejected tumors/total number of mice in the experimental group. A cross indicates that the animal died or had to be sacrificed due systemic toxicity. Each line represents tumor growth in one animal.

### 6.1.4 IFN- $\gamma$ induction in established tumors can lead to tumor rejection

$1 \times 10^6$  J558L or J558L-IFN- $\gamma^{\text{IND}}$  cells were injected into BALB/c mice. J558L cells grew with the same kinetics irrespective of Dox application (Fig. 6.5 B). In the absence of Dox J558L-IFN- $\gamma^{\text{IND}}$  cells grew with the same kinetics as parental J558L cells. J558L-IFN- $\gamma^{\text{IND}}$  cell suspensions did not form tumors when IFN- $\gamma$  expression was started at the point of tumor cell injection (Fig. 6.5 A). To address whether locally produced IFN- $\gamma$  is sufficient to reject established tumors, IFN- $\gamma$  expression was induced at later time points, when tumors were well vascularized. The results in Figures 6.5 C and D show that tumor rejection depended on the size of the tumor. While 50 % (3/6) of tumors with intermediate size (6.5 C, 189 mm<sup>3</sup>, IFN- $\gamma$  induction day 14) were rejected, only 17 % (1/6) of the mice with larger tumors (Fig. 6.5 D, 642 mm<sup>3</sup>) induced on the same day rejected their tumors.

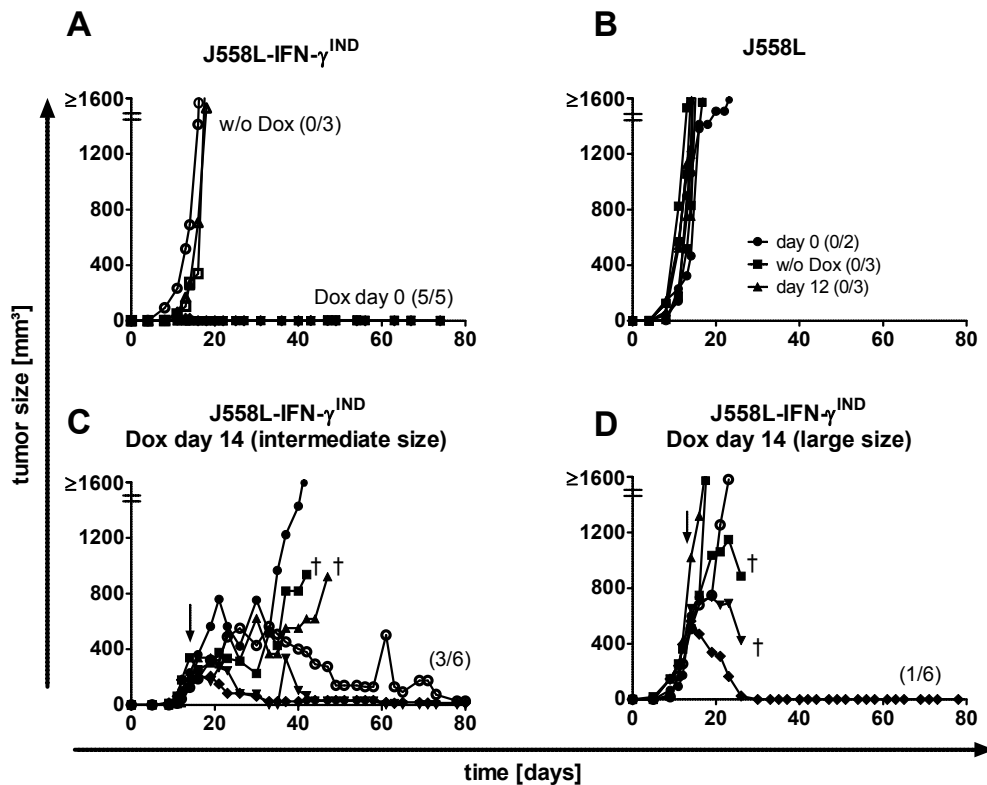
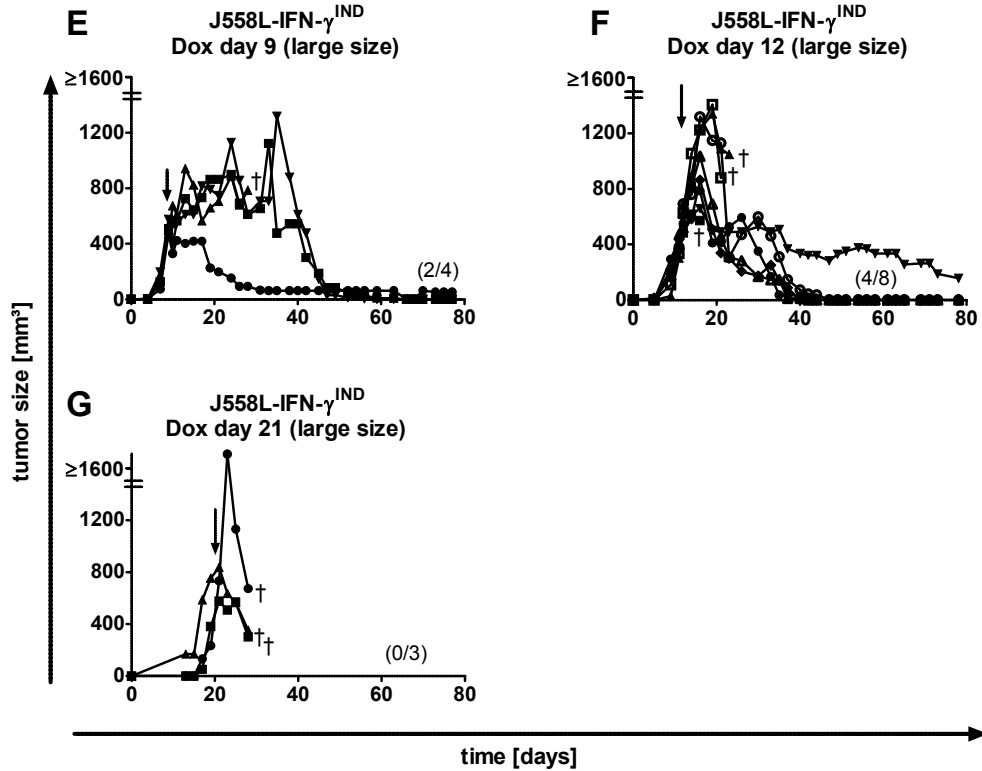


Figure 6.5

A second important factor determining the efficacy of rejection by local IFN- $\gamma$  release was the time point of induction. When comparing the rejection of larger tumors that had grown to reach a size of at least 500 mm<sup>3</sup> after different periods



**Figure 6.5.** (A–G) Efficacy of local IFN- $\gamma$  induction in J558L-IFN- $\gamma$ <sup>IND</sup> cells depends on the size of the tumors and the day of IFN- $\gamma$  induction.  $1 \times 10^6$  J558L-IFN- $\gamma$ <sup>IND</sup> cells were injected into BALB/c mice. Tumor growth kinetics after induction of local IFN- $\gamma$  expression in J558L-IFN- $\gamma$ <sup>IND</sup> and J558L tumors are shown. (A) Tumor bearing mice without administering Dox (open symbols) and mice receiving Dox on the same day as tumor cell injection (closed symbols). (B) Mice injected with parental J558L cells and either left untreated (squares), treated with Dox at day 0 (circles) or treated at day 12 (triangles). (C) J558L-IFN- $\gamma$ <sup>IND</sup> tumors of intermediate size induced at day 14, (D) large tumors induced at day 14. E–G show large J558L-IFN- $\gamma$ <sup>IND</sup> tumors induced at days 9, 12 and 21, respectively. Numbers in parentheses show rejected tumors/total number of mice in the experimental group. A cross indicates that the animal died or had to be sacrificed due systemic toxicity. Each line represents tumor growth in one animal. IFN- $\gamma$  was induced by administering Dox (1 mg/ml) via the drinking water and arrows indicate the time point of Dox application.

of time and that were induced to secrete IFN- $\gamma$ , it became clear that the longer the tumors grew in mice to reach a certain size, the less effective IFN- $\gamma$  mediated rejection was (Fig. 6.5 E-G). For example, half of the mice with large tumors treated on day 9 and 12 rejected their tumors (Fig. 6.5 E and F), while the number of mice that rejected the tumor decreased when IFN- $\gamma$  was induced at day 14 or later (Figures 6.5 D and 6.5 G). These results suggest that two factors influence tumor rejection by IFN- $\gamma$ . The first factor is tumor size and the second is the duration of tumor growth in the mice, independent of tumor size.

### 6.1.5 High IFN- $\gamma$ concentrations cause toxic side effects

Induction of IFN- $\gamma$  in larger tumors was associated with toxic side effects such as massive weight loss of mice in which IFN- $\gamma$  was induced (Fig. 6.6 A-G) and increased serum levels of liver transaminases (Fig. 6.7 H and I).

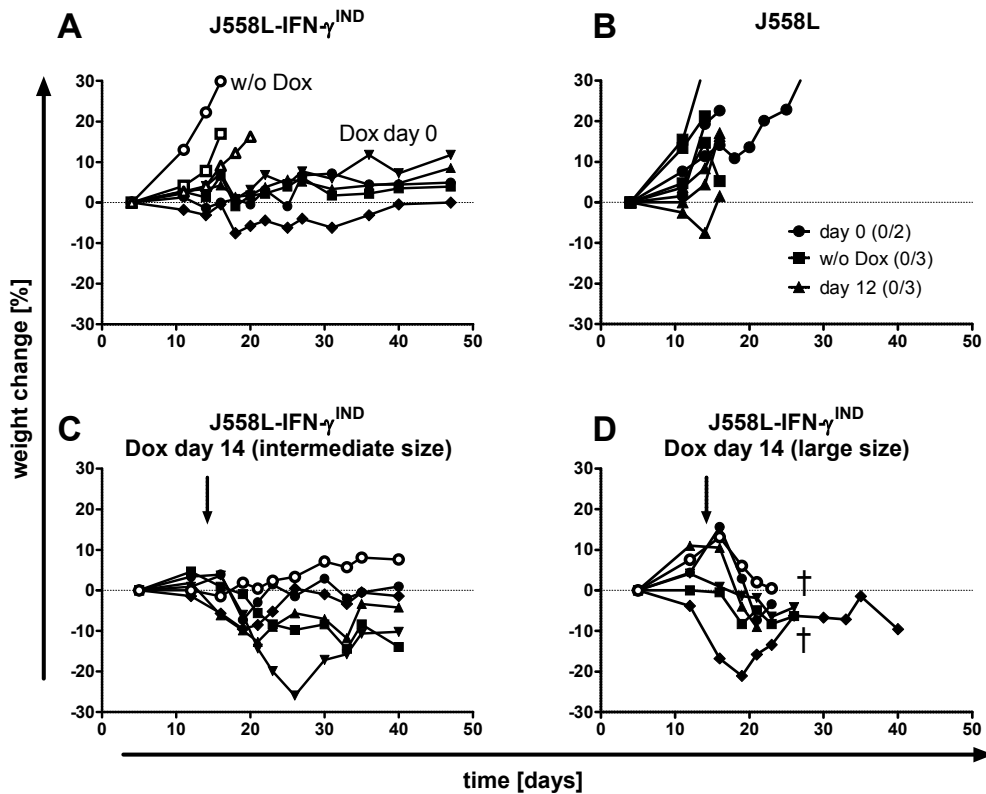
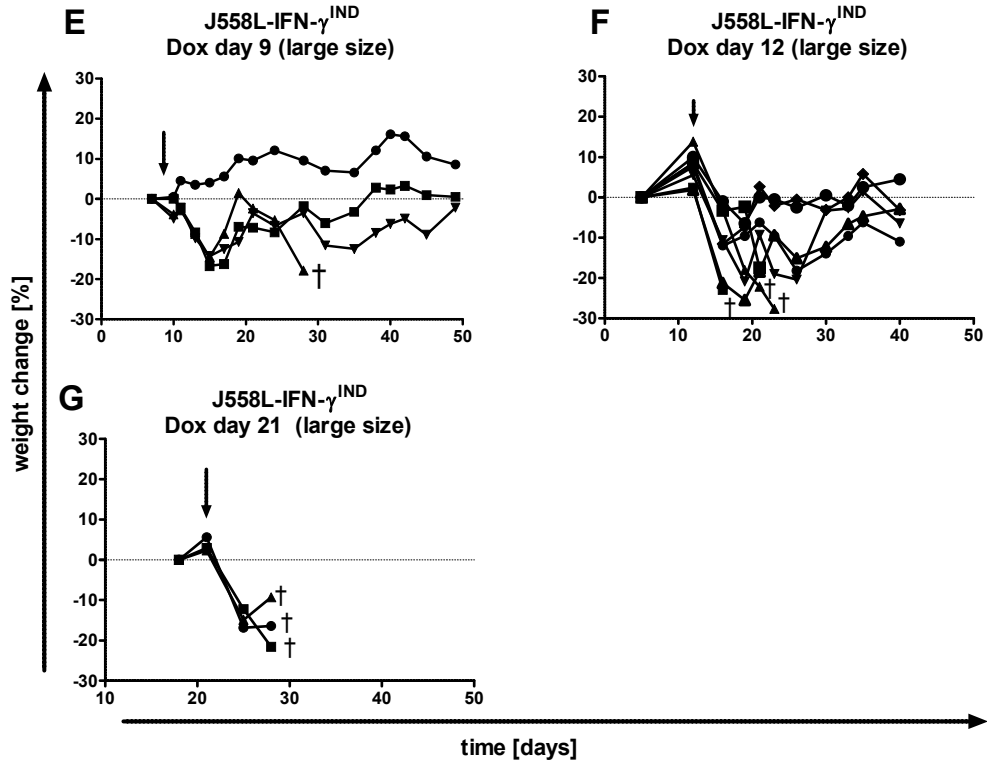
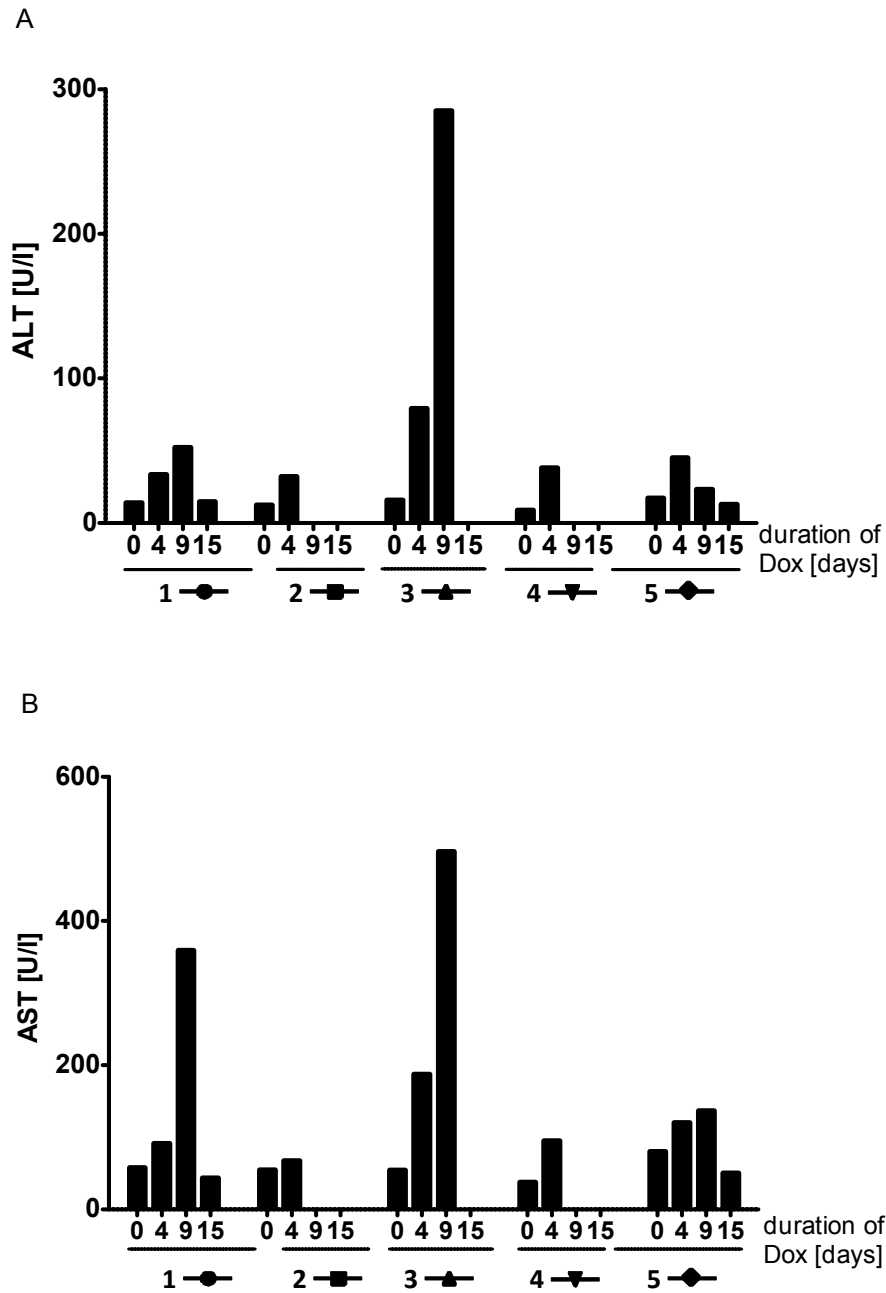


Figure 6.6



**Figure 6.6.** (A–G) Local IFN- $\gamma$  treatment of J558L-IFN- $\gamma^{IND}$  tumors is associated with toxicity as evidenced by severe weight loss.  $1 \times 10^6$  J558L-IFN- $\gamma^{IND}$  or parental J558L cells were injected s.c. into BALB/c mice. (A) Weight changes of mice without administering Dox (open symbols) and receiving Dox from the day of tumor cell injection (closed symbols). (B) Weight changes of mice injected with  $1 \times 10^6$  J558L cells receiving Dox from the day of tumor cell injection (circles), without administering Dox (squares) and receiving Dox at day 12 (triangles). Weight changes after IFN- $\gamma$  induction at day 14 in (C) tumors of intermediate size and (D) large tumors. E–G show weight changes of mice with large tumors after IFN- $\gamma$  induction at days 9, 12 and 21, respectively. A cross indicates that the animal died or had to be sacrificed due to systemic toxicity. Each line represents weight change of one animal. IFN- $\gamma$  was induced by administering Dox (1 mg/ml) via the drinking water and arrows indicate the time point of Dox application. Weight changes for experimental groups for which tumor growth kinetics are depicted in Figure 6.5 and 6.5.



**Figure 6.7.** Local  $\text{IFN-}\gamma$  treatment of  $\text{J558L-IFN-}\gamma^{\text{IND}}$  tumors is leads to increased ALT and AST values.  $1 \times 10^6$   $\text{J558L-IFN-}\gamma^{\text{IND}}$  cells were injected s.c. into BALB/c mice. A and B show that induction of  $\text{IFN-}\gamma$  in  $\text{J558L-IFN-}\gamma^{\text{IND}}$  tumors is associated with toxicity as evidenced by increased ALT and AST values. (A) shows ALT and (B) AST values for the group of large tumors treated day 12 depicted in Fig. 6.5 and Fig. 6.6 F. The symbols below the diagram next to the animal number identify the animal in the graphs Fig. 6.5 and F.



Alanine aminotransferase (ALT) and aspartate aminotransferase (AST) values increased and peaked nine days after IFN- $\gamma$  induction. One mouse showed very high ALT and AST values at day nine after induction and died. Decreasing liver transaminase levels after day 9 were detected in mice which rejected the tumor.

Finally, some of the animals died or had to be sacrificed because of obvious toxicity (Tables 6.1, 6.2 and Figures 6.5 and 6.6).

**Table 6.1.** The efficiency of J558L-IFN- $\gamma$ <sup>IND</sup> tumor rejection by locally produced IFN- $\gamma$  depends on the size of the tumor and the time tumors had grown in the mice.  $1 \times 10^6$  J558L-IFN- $\gamma$ <sup>IND</sup> cells were injected s.c. into BALB/c mice. Mice were divided into groups with similar tumor sizes and Dox was administered from the day indicated in the table. Shown are numbers and percentages of mice which rejected the tumor versus total mice and number of therapy-induced deaths.

Tumor size	Day of IFN- $\gamma$ induction	Tumor vol. (mm <sup>3</sup> )	No. of mice with rejected tumor/injected mice (%)	No. of mice with therapy-induced death
Large	9	530 $\pm$ 59	4/9 (44%)	1
	12	582 $\pm$ 87	4/8 (50 %)	3
	14	642 $\pm$ 193	1/6 (17 %)	2
	21	715 $\pm$ 131	0/3 (0 %)	3
Middle	14	189 $\pm$ 84	3/6 (50 %)	2
Small	7	51 $\pm$ 28	4/5 (80 %)	0
	9	62 $\pm$ 12	2/5 (40 %)	1

### 6.1.6 Interval treatment reduces toxic side effects

To reduce the toxicity and investigate, whether there is a therapeutical window for effective local IFN- $\gamma$  treatment, two strategies were tested. The concentration of Dox was titrated from 1 mg/ml to 0.01 mg/ml or, alternatively, animals were treated with 1 mg/ml Dox in intervals (48–72 h with and 48–72 h without Dox). Using the latter treatment protocol was thought to let the mice recover from the IFN- $\gamma$  burst and the treatment-related systemic toxicity and, on the other hand, to increase the local therapeutic index within the tumor tissue.

Decreasing Dox-concentrations decreased the toxic side effects only at the lowest concentration of 0.01 mg/ml, but at the same time decreased rejection efficiency (Table 6.2). Even IFN- $\gamma$  induction at day 0 did not prevent tumors from growing in mice receiving the lowest Dox concentration (0.01 mg/ml). Higher Dox concentrations (0.05 and 0.1 mg/ml) increased rejection efficiency compared to the lowest concentrations but also increased toxicity (Table 6.2).

**Table 6.2. Local IFN- $\gamma$  induction leads to tumor rejection in a dose dependent fashion but is associated with systemic toxicity.**  $1 \times 10^6$  J558L-IFN- $\gamma^{\text{IND}}$  cells were injected s.c. into BALB/c mice. Mice with similar tumor size were divided into groups and IFN- $\gamma$  was induced at different time points. Dox was administered in different concentrations. The table shows combined data of 2–10 experiments per group. For interval treatment 1 mg/ml Dox was administered in 48–72 h intervals.

Dox conc. (mg/ml)	Induction at day 0 No. of mice with rejected tumor/ injected mice (%)	Induction at day 7–21 No. of mice with rejected tumor/ injected mice (%)	No. of mice with therapy-induced death
0.01	1/4 (25 %)	0/6 (0 %)	0/6
0.05	5/5 (100 %)	1/5 (20 %)	2/5
0.1	4/4 (100 %)	3/19 (16 %)	8/19
1	10/10 (100 %)	15/45 (33 %)	19/45
Interval		18/32 (56 %)	4/32

The second strategy was carried out by applying Dox for 48–72 h and stopping administration for 48 h to provide a recovery period for the mice. Interval treatment of mice reduced systemic toxicity and enhanced efficiency of tumor rejection, indicating a therapeutic window, albeit within a narrow range (Table 6.2).

Next, we wanted to find out whether tumor derived IFN- $\gamma$  alone caused tumor rejection, or whether endogenous IFN- $\gamma$  from the host was involved. Therefore, IFN- $\gamma$  was induced in J558L-IFN- $\gamma^{\text{IND}}$  tumors in IFN- $\gamma$ -deficient animals. As shown in Table 6.3, tumor-derived IFN- $\gamma$  was sufficient to achieve tumor rejection, ruling out the possibility that IFN- $\gamma$  produced by cells of the host contributed to the anti-tumor effect.

### 6.1.7 IFN- $\gamma$ induction in established tumors causes growth delay in T cell deficient NOD/SCID mice

To analyze whether T cells were involved in tumor rejection mediated by local IFN- $\gamma$  induction, experiments were performed in T cell deficient NOD/SCID mice. As shown in Figure 6.8 A, 40 % of the NOD/SCID mice rejected the tumor when inducing IFN- $\gamma$  immediately after inoculation of J558L-IFN- $\gamma^{\text{IND}}$  cells, the other suppressed growth for around 40 days and tumors grew out delayed. In the absence of Dox, J558L-IFN- $\gamma^{\text{IND}}$  cells formed tumors with similar kinetics as parental J558L cells (Fig. 6.8 B, 6.5 B). Even though none of the NOD/SCID mice rejected the tumor once it was established, tumor growth was clearly delayed (Fig. 6.8 C). These

results indicate that T cells were only partially involved in tumor rejection when inducing  $\text{IFN-}\gamma$  concomitantly with tumor cell injection. Because none of the established tumors in NOD/SCID mice were rejected, the local  $\text{IFN-}\gamma$  was comparably ineffective with increasing tumor burden in the absence of T cells.

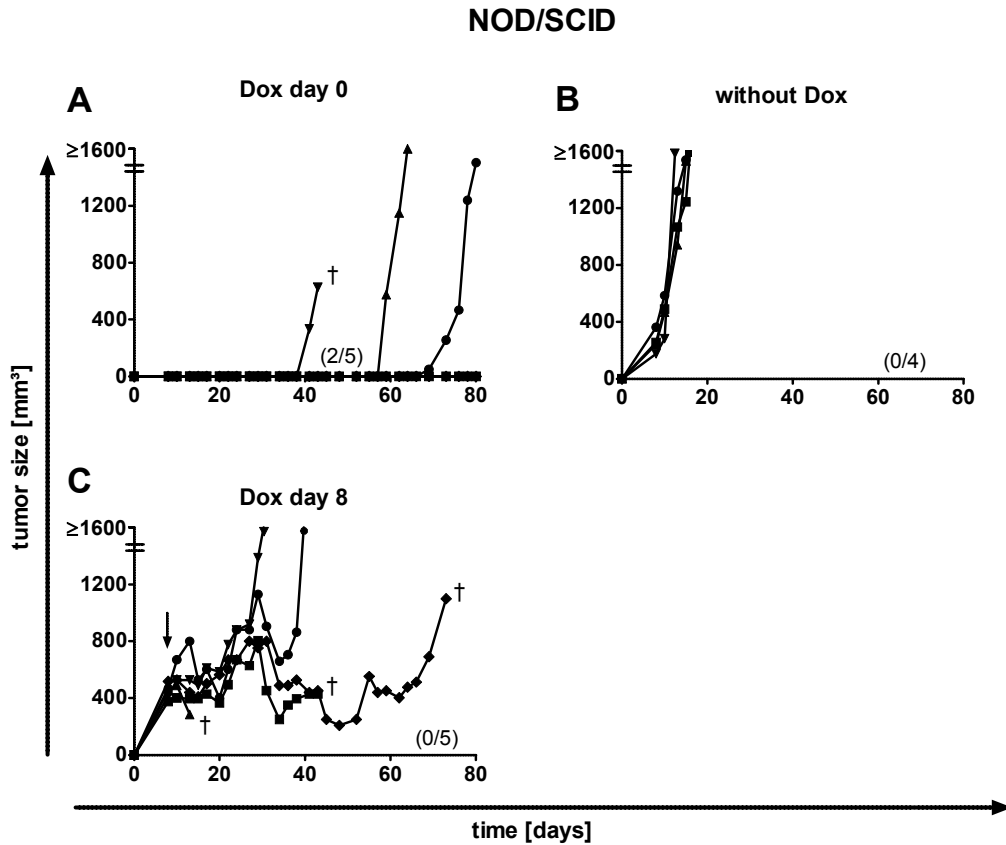


**Figure 6.8.** Local treatment of  $\text{J558L-IFN-}\gamma^{\text{IND}}$  tumors in T cell deficient NOD/SCID mice can lead to tumor rejection of tumor cell suspensions but not of established tumors.  $1 \times 10^6$   $\text{J558L-IFN-}\gamma^{\text{IND}}$  cells were injected into NOD/SCID mice. Tumor growth kinetics after induction of  $\text{IFN-}\gamma$  is shown. (A) Tumors of mice receiving Dox from the day of tumor cell injection (day 0), (B) of mice without Dox-treatment and (C) induced at day 8. Numbers of mice without tumor at the end of the experiment per number of mice in the experiment are indicated in parentheses. A cross indicates that the animal died or had to be sacrificed due systemic toxicity. Each line represents tumor growth in one animal.  $\text{IFN-}\gamma$  was induced by administering Dox (1 mg/ml) via the drinking water and arrows indicate the time point of Dox application.

**Table 6.3. Tumor rejection by locally produced IFN- $\gamma$  is possible in Balb/c, IFN- $\gamma^{-/-}$  and NOD/SCID mice.**  $1 \times 10^6$  J558L-IFN- $\gamma^{IND}$  cells were injected s.c. into BALB/c, IFN- $\gamma^{-/-}$  or NOD/SCID mice. Mice with similar tumor size were divided into groups and IFN- $\gamma$  was induced at different time points. Shown are data of individual experiments.

Mouse strain	Tumor	Day of IFN- $\gamma$ induction	Tumor vol. (mm <sup>3</sup> )	No. of mice with rejected tumor/injected mice (%)	No. of mice with therapy-induced death	
BALB/c	small	0	0	10/10 (100 %)	0	
		7	51 $\pm$ 28	3/5 (60 %)	0	
		9	62 $\pm$ 12	4/5 (60 %)	1	
	middle	12	246 $\pm$ 131	0/2 (0 %)	2	
		12	330	0/1 (0 %)	1	
		14	189 $\pm$ 84	3/6 (50 %)	2	
	large	9	506 $\pm$ 49	2/4 (50 %)	1	
		9	550 $\pm$ 64	2/5 (40 %)	2	
		12	582 $\pm$ 82	4/8 (50 %)	3	
		14	642 $\pm$ 193	1/6 (17 %)	3	
		21	715 $\pm$ 131	0/3 (0 %)	3	
	IFN- $\gamma^{-/-}$	large	w/o		0/9 (0 %)	0
			0	0	2/2 (100 %)	0
			11	435 $\pm$ 179	1/3 (33 %)	0
12			595 $\pm$ 280	0/4 (0 %)	4	
w/o				0/10 (0 %)	0	
NOD/SCID	middle	0	0	5/5 (100 %)	0	
		0	0	2/5 (40 %)	0	
		13	286 $\pm$ 72	0/3 (0 %)	3	
	large	18	201 $\pm$ 89	0/2 (0 %)	1	
		8	446 $\pm$ 54	0/5 (0 %)	2	
		w/o		0/3 (0 %)	0	
		w/o		0/4 (0 %)	0	

### 6.1.8 Re-isolated J558L-IFN- $\gamma$ <sup>IND</sup> tumor cells from NOD/SCID mice lost the ability to produce IFN- $\gamma$

To test whether tumors which grew despite Dox application had lost the ability to produce IFN- $\gamma$ , tumors were re-isolated and cultured for two weeks.

Two tumors that progressively grew despite IFN- $\gamma$  induction concomitant to tumor cell injection were re-isolated from NOD/SCID mice (Figure 6.8). In vitro analysis of re-isolated J558L-IFN- $\gamma$ <sup>IND</sup> cells grown in NOD/SCID mice despite Dox administration from the day of tumor cell injection showed that they had lost the ability to secrete IFN- $\gamma$  (Figure 6.9).

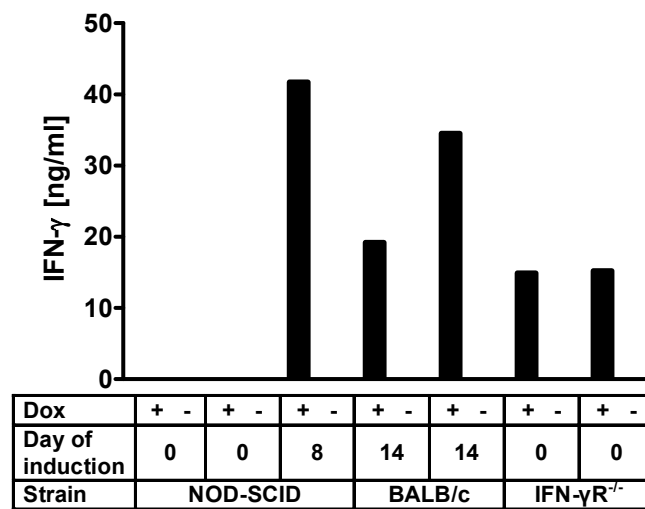


**Figure 6.9.** Only J558L-IFN- $\gamma$ <sup>IND</sup> cells re-isolated from NOD/SCID mice lost the ability to produce IFN- $\gamma$ . J558L-IFN- $\gamma$ <sup>IND</sup> tumors were re-isolated from mice treated with Dox at different time points after tumor cell injection. After 2 weeks of culture,  $1 \times 10^6$  re-isolated J558L-IFN- $\gamma$ <sup>IND</sup> cells were seeded and  $1 \mu\text{g/ml}$  Dox was added for 48 h. IFN- $\gamma$  level of cell culture supernatants were measured by ELISA. Tumors were re-isolated from NOD/SCID (day 43 or 64 after tumor injection, Fig. 6.8), BALB/c (day 42 after tumor injection, Fig. 6.5 C) and RAG1<sup>-/-</sup> x IFN- $\gamma$ R<sup>-/-</sup> mice (day 18 after tumor injection, Fig. 6.4 C). Shown are ELISA values for single measurements.

In contrast, IFN- $\gamma$  induction in large, established tumors did not lead to the loss of IFN- $\gamma$ -inducibility after re-isolation and in vitro analysis, regardless whether tumors were re-isolated from NOD/SCID or BALB/c mice (Figures 6.5, 6.8 and 6.9). Additionally, two tumors that grew in RAG1<sup>-/-</sup> x IFN- $\gamma$ R<sup>-/-</sup> mice treated with Dox from the day of tumor cell injection showed IFN- $\gamma$  production after re-isolation in vitro (Figure 6.4).

These results demonstrate that T cells prevented the selection of IFN- $\gamma$  loss vari-

ants, if there was no systemic toxicity due to the low number of IFN- $\gamma$  producing tumor cells in case of immediate IFN- $\gamma$  induction. In contrast, the continued progression of IFN- $\gamma$  producing tumors, which were induced at a late stage, is probably due to the fact that mice could not be observed for a long enough time because of the systemic toxicity.

### 6.1.9 Blood vessel destruction and necrosis after IFN- $\gamma$ induction in established J558L-IFN- $\gamma^{\text{IND}}$ tumors

To study the local effects of IFN- $\gamma$  release, sections from tumors were analyzed by immunohistology. Immunofluorescent staining for endothelial cells with anti-CD31 antibody was performed with sections of tumors exposed to IFN- $\gamma$  treatment for different time periods.

As shown in Figure 6.10 A, blood vessels were thin and long before IFN- $\gamma$  induction (day 0). One day after induction blood vessels seemed to be shorter and thick and seven days after IFN- $\gamma$  induction there were hardly any blood vessels visible.

To complement the data gained from the CD31 staining, we performed hematoxylin and eosin staining (H&E) and endothelial cell staining with anti-CD-146 antibodies on paraffin sections. We used paraffin sections to improve visibility of the tissue architecture, because paraffin sections of tumor tissue can be cut in thinner slices.

Staining of vascular endothelial cells with an monoclonal anti-CD146 antibody revealed that already at 24 h after IFN- $\gamma$  induction a reduction in the number of endothelial cells was detectable. Blood vessel destruction was even more pronounced 48 h and 72 h after IFN- $\gamma$  induction (Fig. 6.10 B).

To judge the time-dependent effect of IFN- $\gamma$ , a person blinded to the setup evaluated the paraffin sections of J558L-IFN- $\gamma^{\text{IND}}$  tumors derived from BALB/c mice independently. As shown in Table 6.4 blood vessel destruction and tumor necrosis were already visible at 24 h after treatment, but more pronounced after 48 and 72 hours and after interval treatment compared to the untreated tumors.

Importantly, destruction of blood vessels was also observed in NOD/SCID mice after IFN- $\gamma$  induction, although the differences were less pronounced than in T cell competent mice (Fig. 6.10), demonstrating that T cells are not necessary for the induction of vessel destruction. Blood vessel destruction was followed by massive necrosis as evidenced in H&E stained sections (Fig. 6.10 B, first column). At later time points (72 h) the majority of the tumor tissue was necrotic.

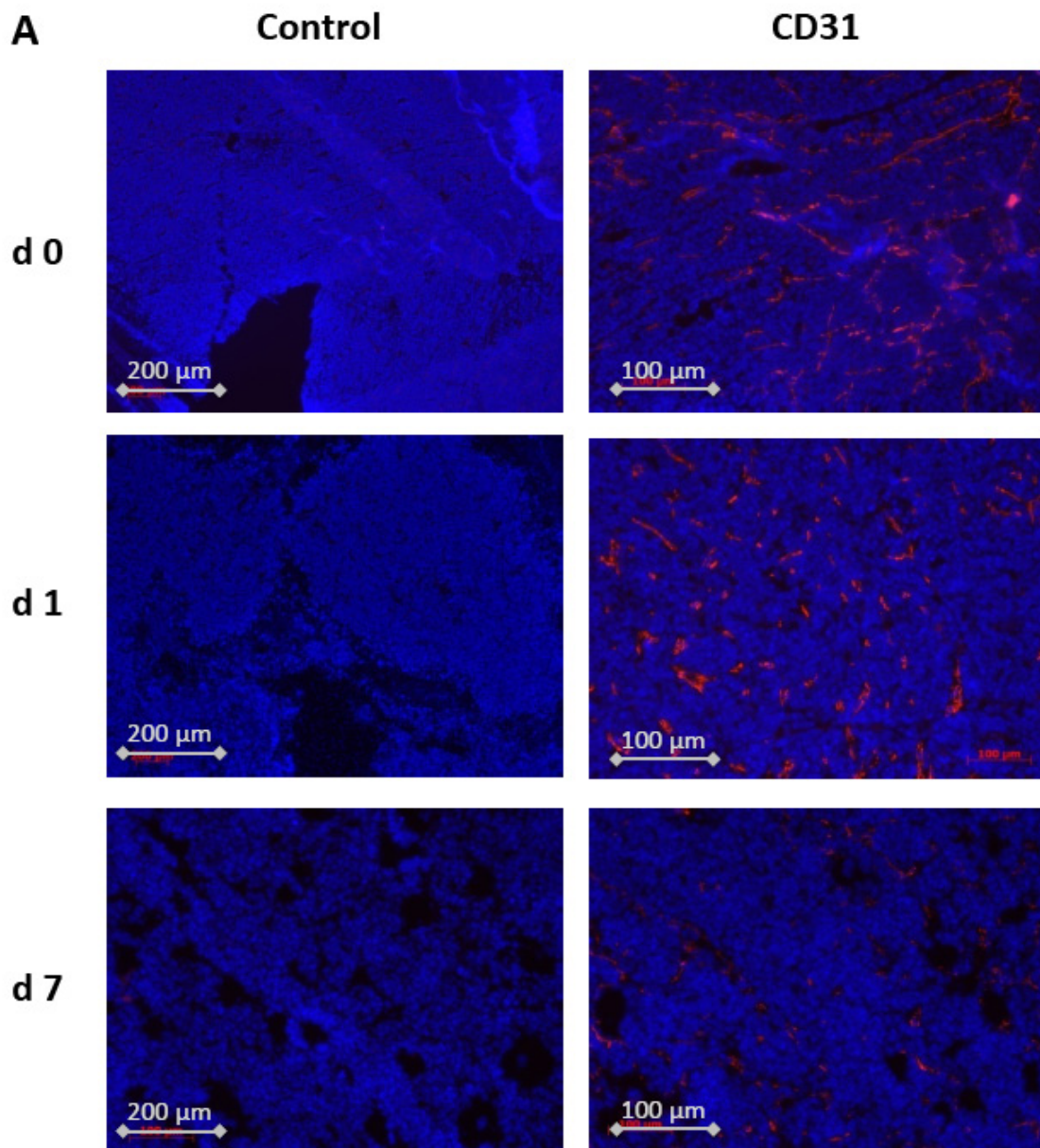


*Figure 6.10*

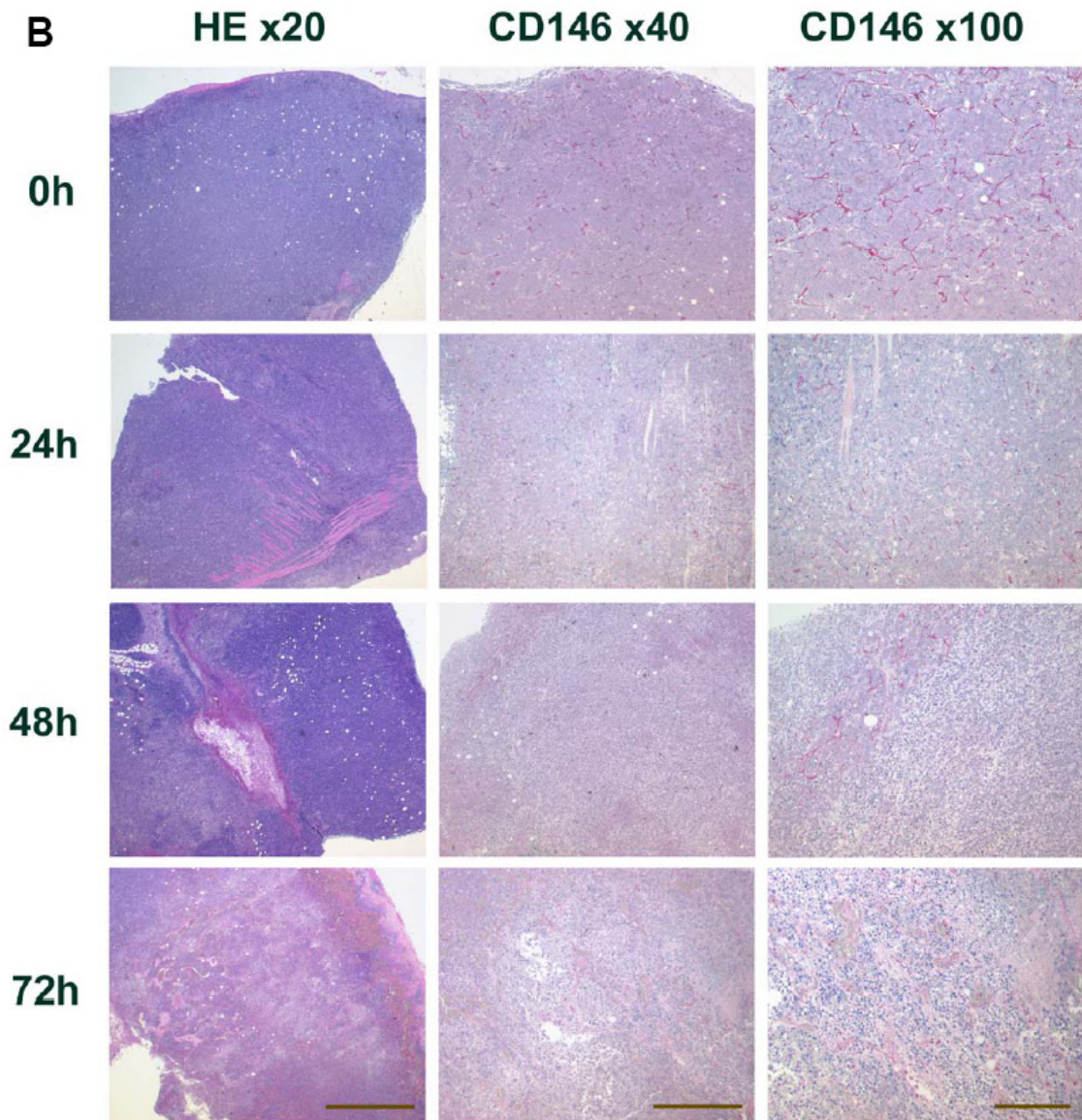


*Figure 6.10*



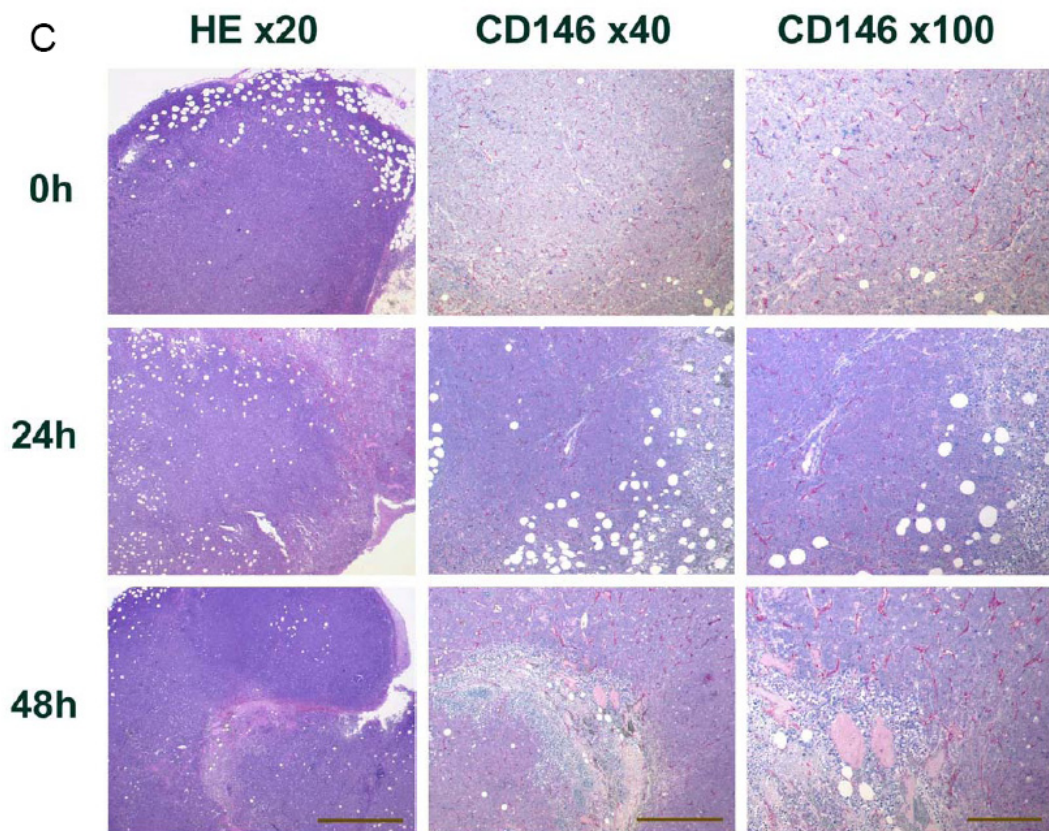


**Figure 6.10. Local IFN- $\gamma$  induction in J558L-IFN- $\gamma^{IND}$  tumors leads to destruction of blood vessels and tumor necrosis.** Immunofluorescence and immunohistological staining of J558L-IFN- $\gamma^{IND}$  tumors taken out and stained at different time points after Dox application. (A) Immunofluorescent staining of J558L-IFN- $\gamma^{IND}$  tumors without IFN- $\gamma$  induction (first row) and one or seven days after IFN- $\gamma$  induction (rows 2 and 3 respectively). Control staining without primary antibody (4 fold magnification, first column, scale bar 200  $\mu\text{m}$ ) and blood vessel destruction is assessed by CD31 staining (40 fold magnification, column 2, scale bar 100  $\mu\text{m}$ , sections 4  $\mu\text{m}$ ). (B) shows histological analysis of tumors without IFN- $\gamma$  induction (first row) and 24, 48 or 72 hours after IFN- $\gamma$  induction (rows 2, 3 and 4 respectively). (C) shows histological analysis of J558L-IFN- $\gamma^{IND}$  tumors injected s.c. into NOD/SCID mice without IFN- $\gamma$  induction (first row) and 24 and 48 hours after IFN- $\gamma$  induction (rows 2 and 3 respectively) Necrosis is assessed by H&E staining (20 fold magnification, first column, scale bar 1000  $\mu\text{m}$ ) and blood vessel destruction is assessed by CD146 staining (40 fold magnification, column 2, scale bar 500  $\mu\text{m}$  and 100 fold magnification, column 3, scale bar 200  $\mu\text{m}$ , sections 1  $\mu\text{m}$ ).

**Table 6.4. Histological analysis of tumors after Dox-mediated IFN- $\gamma$  induction.** *J558L-IFN- $\gamma$ <sup>IND</sup> tumors were established in BALB/c mice and Dox was administered for 24, 48, 72 h or intermittently (every 48–72 h). Untreated tumors served as controls. Tumor tissue was excised and sections were stained for CD146<sup>+</sup> endothelial cells. Necrosis was evaluated in H&E stained sections. Analysis was performed by a person blindfolded to the setup of the experiment. Analyzed tumors had a minimum size of 500 mm<sup>3</sup>. Evaluation was performed as follows: 0 no blood vessel destruction or necrosis, + blood vessel destruction or necrosis visible in some parts of the section, ++ blood vessel destruction or necrosis are widely distributed and +++ almost no blood vessels left or for necrosis almost no living tumor cells left.*

Duration of Dox treatment [h]	Day of induction	Blood vessel destruction	Necrosis
0	w/o	0	++
0	w/o	0	0
0	w/o	0	0
0	w/o	0	0
0	w/o	0	+
0	w/o	0	++
0	w/o	0	++
0	w/o	0	0
24	10	+	+
24	13	++	++
24	13	+	+/0
24	13	+	+/0
48	9	0	++
48	12	+++	++
48	12	+	+
48	12	+++	+
48	12	+++	++
72	11	++	+
72	11	+++	+
72	11	+++	+++
interval	11	+	0
interval	11	+++	+++
interval	11	+	+++
interval	11	++	+++

### 6.1.10 IFN- $\gamma$ induction in established J558L-IFN- $\gamma$ <sup>IND</sup> tumors leads to macroscopically visible tumor necrosis

Necrosis was not only visible in immunohistochemistry but also appeared macroscopically four to seven days after IFN- $\gamma$  induction. In those mice that completely rejected the tumor, necrosis persisted throughout the rejection process (Fig. 6.11 A and B). Even tumors that were not fully rejected but stayed stable (Fig. 6.5 E and F) in size for some weeks did not consist of viable tumor tissue but necrotic masses. After IFN- $\gamma$  induction at day 9 one tumor stayed stable in size (52 mm<sup>3</sup>) for approximately 50 days (Fig. 6.5 E). As macroscopically observed, there was no living tumor tissue left but a necrotic mass. One of the tumors induced at day 12 (Fig. 6.5 F) which was not rejected had a size of 157 mm<sup>3</sup>, but the tumor did not grow after a period of 24 days without Dox and was merely made up of necrotic tissue after excision.

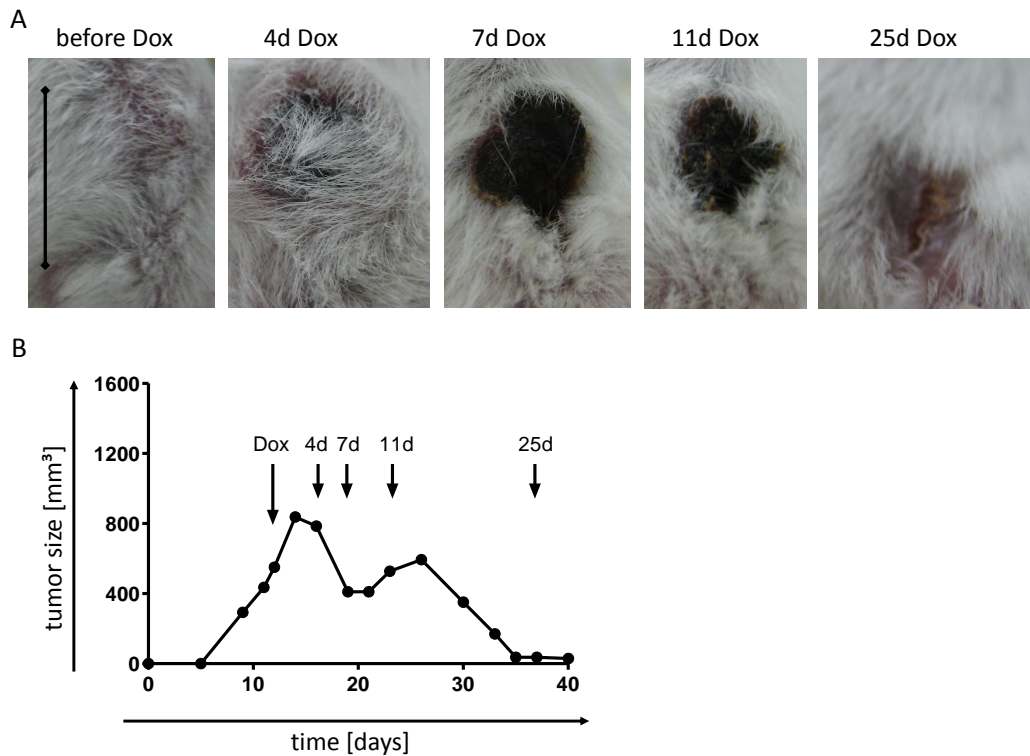


**Figure 6.11. Local IFN- $\gamma$  induction in J558L-IFN- $\gamma$ <sup>IND</sup> tumors leads to macroscopically visible tumor necrosis.** Rejection kinetics of a large J558L-IFN- $\gamma$ <sup>IND</sup> tumor treated with Dox at day 12 after tumor cell injection. (A) Photos of the tumor at different time points during rejection, scale bar 1 cm. (B) Growth curve of the tumor. Arrows indicate the days at which pictures were taken.

### 6.1.11 Summary J558L–IFN– $\gamma$ <sup>IND</sup>

To address the question whether IFN– $\gamma$  has an effect on established tumors, the plasmacytoma cell line J558L was transduced with a vector allowing doxycycline–inducible IFN– $\gamma$  gene expression. In vitro testing of transduced J558L cells showed inducible and titratable expression of IFN– $\gamma$ . After the injection of the tumor cells into mice, IFN– $\gamma$  was induced at different time points. High amounts of IFN– $\gamma$  were detected in the serum of Dox–treated mice confirming the in vitro data. The amount of IFN– $\gamma$  detected in the serum depended on the tumor size.

Tumors did not grow when inducing IFN– $\gamma$  concomitantly with tumor cell inoculation. IFN– $\gamma$  induction in established tumors of wild type BALB/c mice resulted in tumor rejection in half of the cases. Induction of IFN– $\gamma$  2–3 weeks after tumor cell inoculation was less efficient (0–17 % rejection). Collectively, IFN– $\gamma$  efficacy depended on the day of IFN– $\gamma$  induction and the tumor size. Importantly, IFN– $\gamma$  expression by large, established tumors was associated with toxic side effects such as weight loss and increase in liver enzymes. Application of Dox in intervals led to improved survival and a better rejection efficacy. Experiments in NOD/SCID mice showed the effect of IFN– $\gamma$  on tumor cell suspensions and the importance of T cells in tumor rejection. IFN– $\gamma$  induction in established tumors led to a reduction of CD31<sup>+</sup> or CD146<sup>+</sup> endothelial cells and massive necrosis.

## 6.2 The fibrosarcoma MCA313 model

### 6.2.1 Generation and *in vitro* characterization of MCA313-IFN- $\gamma$ <sup>IND</sup> cells

In section 6.1 it was shown for J558L-IFN- $\gamma$ <sup>IND</sup> that tumor rejection depended on the size of the tumor and the day of induction. In order to see if that finding is more generally applicable, we performed the same experiments with an IFN- $\gamma$ R deficient tumor model. The MCA313 tumor cell line is derived from a MCA treated IFN- $\gamma$ R KO mouse on a C57BL/6 genetic background. The same retroviral vector was used to transduce the cells. Because transduction with the ecotropic envelope was not successful, an amphotropic envelope was used. The transduced MCA313 cells were subcloned and IFN- $\gamma$  expression was determined by ELISA using cell culture supernatant. A cell line with inducible IFN- $\gamma$  expression (designated MCA313-IFN- $\gamma$ <sup>IND</sup>) was established from the clones. Figure 6.12 shows that IFN- $\gamma$  expression was inducible with a maximum concentration of 450 ng/ml and correlated with the amount of Dox administered to the cell culture. No IFN- $\gamma$  was detectable without Dox application. Because they lack the IFN- $\gamma$ R, IFN- $\gamma$  cannot have any autocrine functions on the MCA313 tumor cells. Therefore, no further *in vitro* tests were necessary.

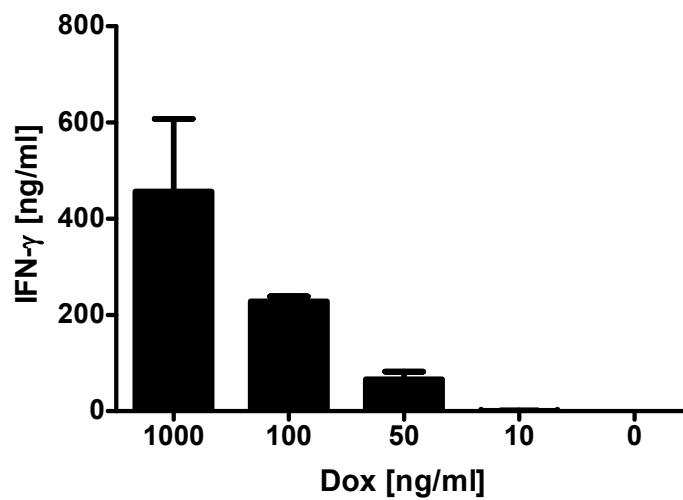


**Figure 6.12.** MCA313IFN- $\gamma$ <sup>IND</sup> cells produce high amounts of IFN- $\gamma$  *in vitro* after Dox application *in vitro*.  $1 \times 10^6$  MCA313-IFN- $\gamma$ <sup>IND</sup> cells were seeded and different concentrations of Dox were added. After 48 h cell culture supernatant was taken and IFN- $\gamma$  concentrations were determined by ELISA. Shown are the mean values and SD from 2 experiments.

## 6.2.2 MCA313-IFN- $\gamma^{\text{IND}}$ tumors express high amounts of IFN- $\gamma$ in vivo

To analyze cytokine serum levels of IFN- $\gamma$  in the mice after IFN- $\gamma$  induction we took blood samples from tumor bearing mice at different time points after Dox application. Cytokine levels were determined using a cytometric bead array (examples for C57BL/6 mice are shown in Figure 6.14).

Injection of MCA313-IFN- $\gamma^{\text{IND}}$  cells into C57BL/6 mice and concomitant application of Dox did not lead to detectable IFN- $\gamma$  expression in the serum at day 19 and 56 after tumor cell injection (Fig. 6.13 A). The most likely explanation for this finding is that IFN- $\gamma$  expressing tumor cells are rejected in wild type mice. Therefore, no IFN- $\gamma$  expressing cells were left. Additionally, we did not detect any IFN- $\gamma$  in the serum without Dox application (Figures 6.14 and Fig. 6.13 A). However, when applying Dox to C57BL/6 mice bearing large tumors (day 14, 340 mm<sup>3</sup>; day 16, 504 mm<sup>3</sup>), we did not detect any IFN- $\gamma$  before Dox application but as soon as three days after Dox application, we detected up to 65 ng/ml. The IFN- $\gamma$  concentration peaked at day 11–13, reaching approximately 150 ng/ml (Fig. 6.13 A). The decrease of IFN- $\gamma$  levels afterwards could be explained by the shrinking tumor size, causing a decrease in the number of IFN- $\gamma$ -producing cells.

To exclude endogenous produced IFN- $\gamma$ , we injected MCA313-IFN- $\gamma^{\text{IND}}$  cells into IFN- $\gamma^{-/-}$  mice. We could not detect any IFN- $\gamma$  in the serum of IFN- $\gamma^{-/-}$  mice when inducing IFN- $\gamma$  expression concomitantly to tumor cell injection or without IFN- $\gamma$  induction. Dox application to mice bearing established tumors (day 14, 619 mm<sup>3</sup>) led to very high levels of IFN- $\gamma$  in the serum, nearly reaching the levels of IFN- $\gamma$  in wild type mice (Fig. 6.13 A and B). Importantly, four of the five mice died shortly afterwards suggesting a stronger toxic effect of IFN- $\gamma$  in the IFN- $\gamma^{-/-}$  mice. Only one IFN- $\gamma^{-/-}$  mouse survived and rejected the tumor, which was associated with undetectable IFN- $\gamma$  in the serum (Fig. 6.13 B).

Due to the lack of the IFN- $\gamma$ R on MCA313-IFN- $\gamma^{\text{IND}}$  cells and in IFN- $\gamma$ R<sup>-/-</sup> mice, we expected higher amounts of IFN- $\gamma$  in the serum of IFN- $\gamma$ R<sup>-/-</sup> mice compared to C57BL/6 and IFN- $\gamma^{-/-}$  mice. As predicted, we detected up to 600 ng/ml of IFN- $\gamma$  in the serum of mice when IFN- $\gamma$  was induced on the day of tumor cell injection (measured at day 19, mean size 1429 mm<sup>3</sup>). There was no IFN- $\gamma$  detectable without IFN- $\gamma$  induction and before IFN- $\gamma$  induction in large tumors. IFN- $\gamma$  induction in large tumors (day 14, 763 mm<sup>3</sup>) led to IFN- $\gamma$  amounts of up to 800 ng/ml (Fig. 6.13 C). As expected, despite the enormous amounts of IFN- $\gamma$  in the serum the IFN- $\gamma$ R<sup>-/-</sup> mice did not die because cells could not react to IFN- $\gamma$ .

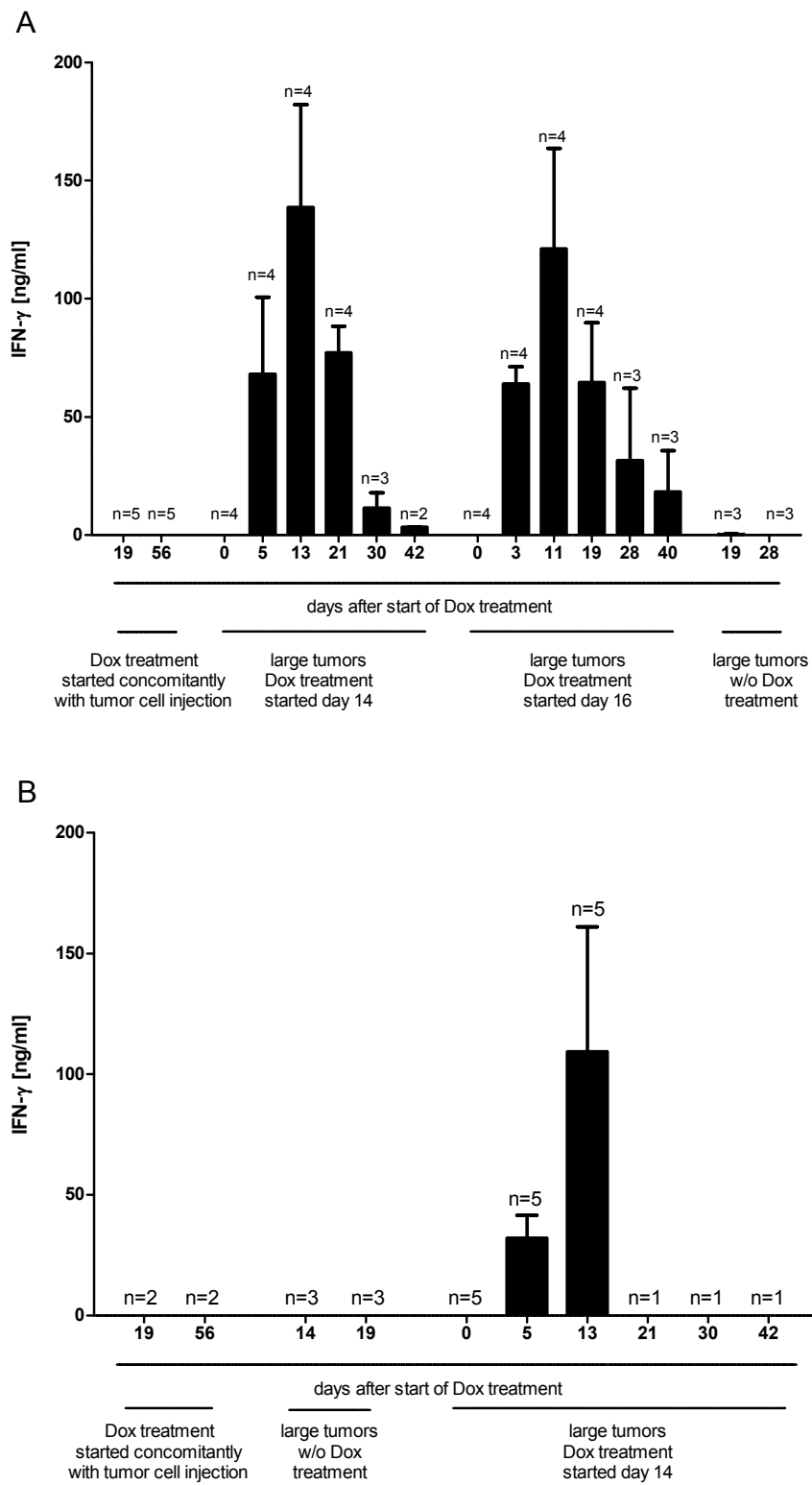
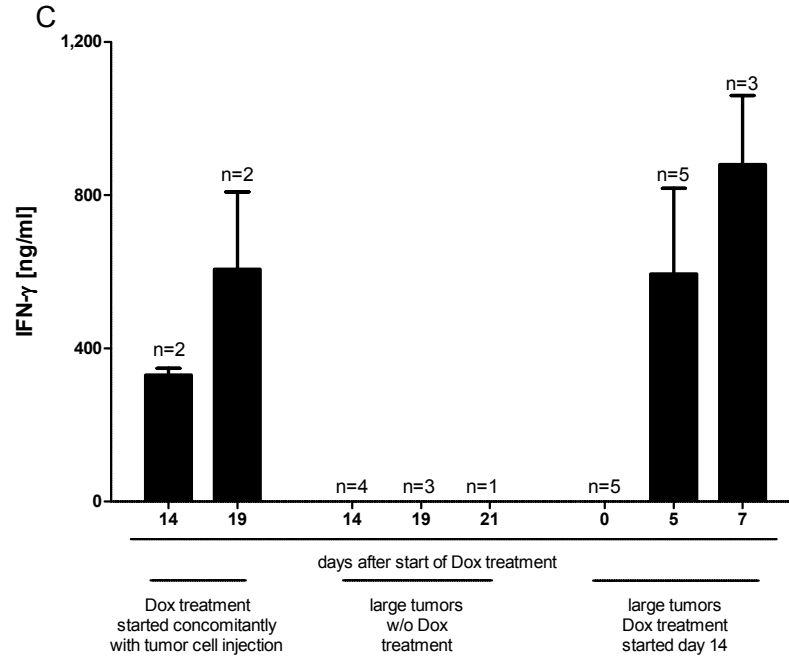
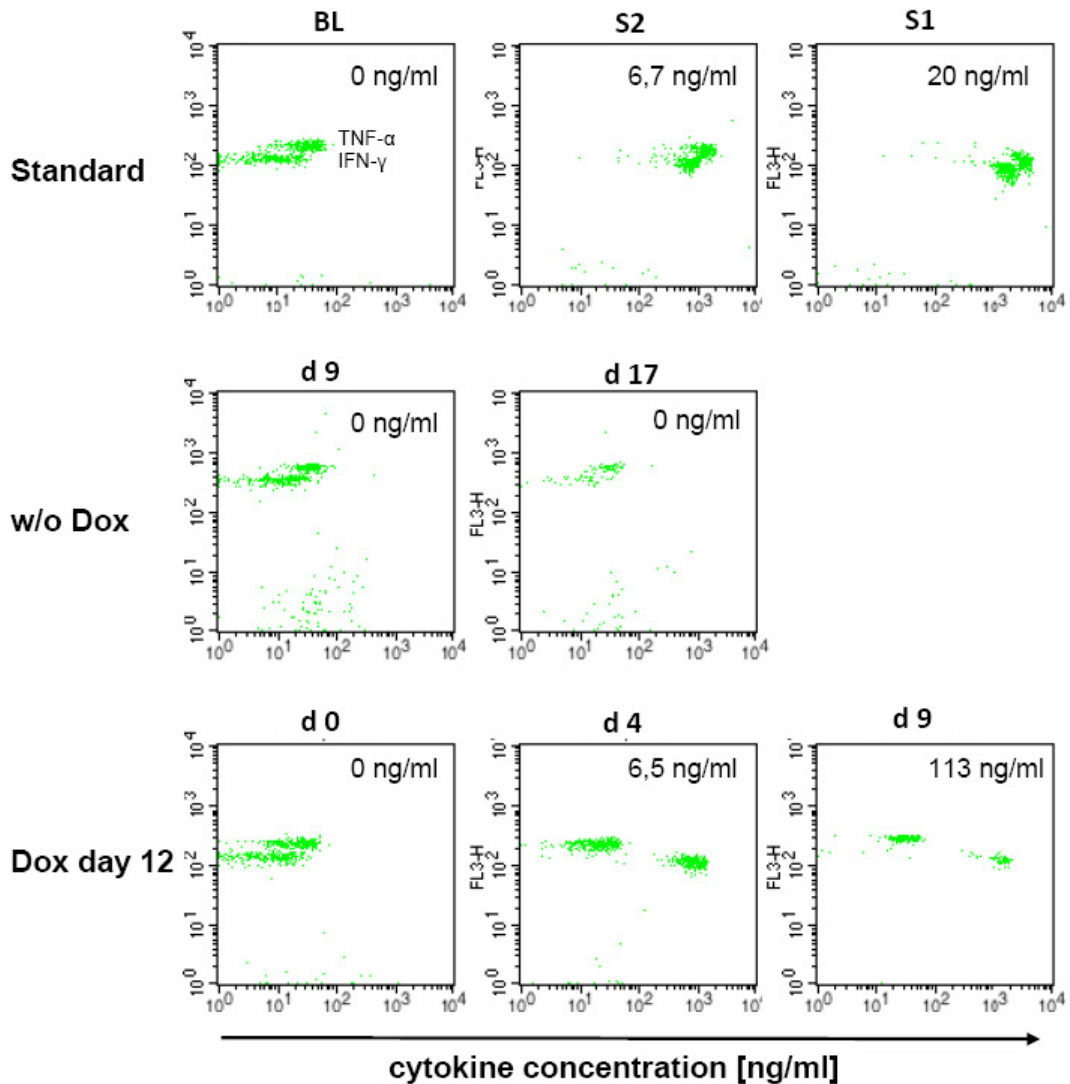


Figure 6.13



**Figure 6.13. (C) High amounts of IFN- $\gamma$  in the serum after IFN- $\gamma$  induction in MCA313-IFN- $\gamma^{IND}$  cells.**  $1 \times 10^6$  MCA313-IFN- $\gamma^{IND}$  cells were injected *s.c.* into C57BL/6, IFN- $\gamma^{-/-}$  and IFN- $\gamma R^{-/-}$  mice and serum was taken at different time points after Dox induction. (A) Serum from C57BL/6 mice induced at the day of tumor cell injection, at day 14,  $340 \pm 102$  ng/ml; day 16,  $504 \pm 77$  ng/ml, and without induction was analyzed for IFN- $\gamma$ . (B) Serum from IFN- $\gamma^{-/-}$  mice bearing tumors induced concomitantly with tumor cell injection, bearing large tumors at day 14,  $619 \pm 84$  ng/ml or tumors without induction was analyzed using a cytometric bead array. (C) Serum of IFN- $\gamma R^{-/-}$  mice induced at the day of tumor cell injection, in large tumors at day 14,  $763 \pm 164$  ng/ml or without induction were analyzed for IFN- $\gamma$ . The mean values and SD of 1–5 mice are shown (n for each time point indicated above the individual bars).





**Figure 6.14.** Cytometric bead array allows the detection of IFN- $\gamma$  produced by MCA313-IFN- $\gamma^{IND}$  cells *in vivo*. Serum samples of differently treated groups were taken and measured via cytometric bead array. Shown are individual examples of C57BL/6 mice bearing MCA313L-IFN- $\gamma^{IND}$  tumors induced concomitantly to tumor cell injection (day 0) and at day 14 after tumor cell injection (mean values shown in Fig. 6.13 A). The cytokines IL-17, IL-4, GM-CSF, TNF- $\alpha$  and IFN- $\gamma$  were measured in this bead array. Blank value and two standards are shown in the first row, cytokine levels of a mouse in which IFN- $\gamma$  was induced at day 0 and analysed for cytokines at day 9 and 17 after Dox administration are shown in the second row. The third row shows cytokine levels of a mouse in which IFN- $\gamma$  was induced at day 14, analysed at day 0, 5 and 21 after Dox administration. Corresponding IFN- $\gamma$  concentrations are depicted in the graphs.

### 6.2.3 Induction of IFN- $\gamma$ in established MCA313-IFN- $\gamma^{\text{IND}}$ tumors can lead to tumor cell rejection

$1 \times 10^6$  MCA313-IFN- $\gamma^{\text{IND}}$  cells were injected subcutaneously into the right flank of C57BL/6 mice. When Dox was administered alongside with the tumor cell injection, the cells did not form tumors. Without Dox administration the tumors reached a size of  $1700 \text{ mm}^3$  within 28 days.

To address the question whether locally produced IFN- $\gamma$  is sufficient to reject established tumors in this model, IFN- $\gamma$  expression was induced at later time points, when tumors were established. When inducing IFN- $\gamma$  expression in established tumors, we show similar to the J558L-IFN- $\gamma^{\text{IND}}$  model IFN- $\gamma$ -dependent tumor rejection.

Upon IFN- $\gamma$  induction at day 14 20 % (1/5) of the mice rejected the tumor (Figure 6.15 B,  $340 \text{ mm}^3$ ). Two days later, IFN- $\gamma$  induction in larger tumors led to tumor rejection in 17 % (1/6) of the mice (Fig. 6.15 C,  $504 \text{ mm}^3$ ) showing similar kinetics as the J558L-IFN- $\gamma^{\text{IND}}$  tumors induced at day 14 (Fig. 6.5 D). The results of Fig. 6.15 B, C and 6.5 showed that tumor rejection depended on the day of IFN- $\gamma$  induction.

MCA313-IFN- $\gamma^{\text{IND}}$  tumors show similar growth kinetics and outcome as did the J558L-IFN- $\gamma^{\text{IND}}$  tumors (Fig. 6.5 A–D) indicating that there is a lower chance for IFN- $\gamma$ -mediated tumor rejection after day 12.

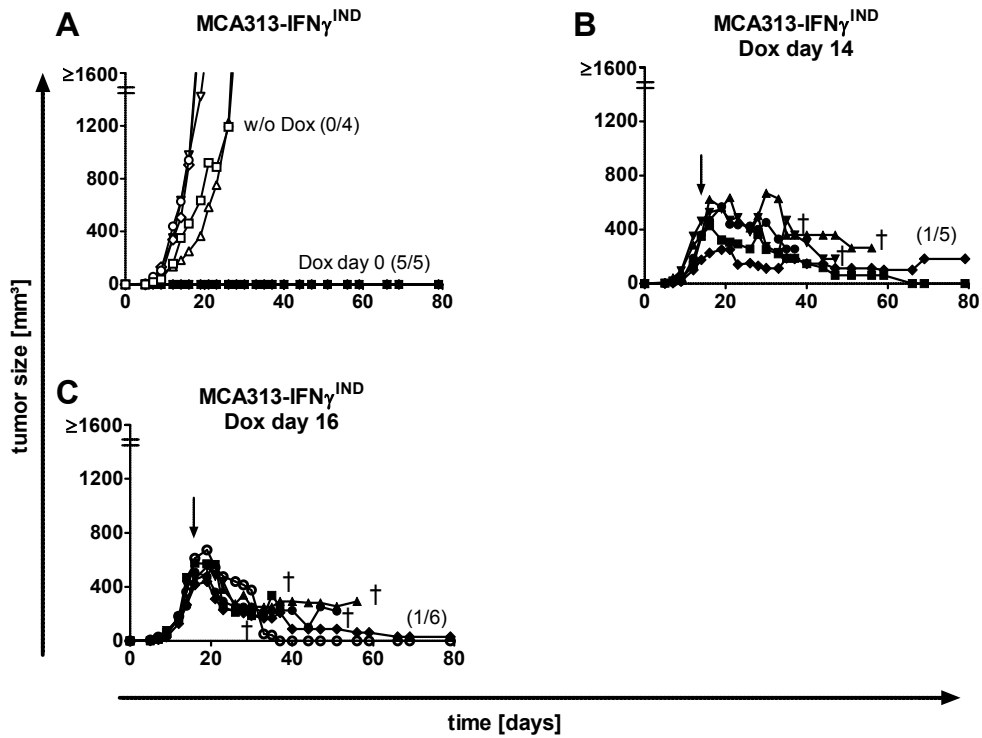


**Figure 6.15.** IFN- $\gamma$  induction in established MCA313-IFN- $\gamma$ <sup>IND</sup> tumors leads to occasional tumor rejection and systemic toxicity.  $1 \times 10^6$  MCA313-IFN- $\gamma$ <sup>IND</sup> cells were injected into C57BL/6 mice. Tumor growth kinetics after induction of local IFN- $\gamma$  expression in MCA313-IFN- $\gamma$ <sup>IND</sup> tumors are shown. (A) Tumor bearing mice without administering Dox (open symbols) and mice receiving Dox from the day of tumor cell injection (closed symbols). (B) Mice injected with MCA313-IFN- $\gamma$ <sup>IND</sup> cells and treated with Dox at day 14 or (C) at day 16. Numbers in parentheses show rejected tumors/total number of mice in the experimental group. A cross indicates that the animal died or had to be sacrificed due to systemic toxicity. Each line represents tumor growth in one animal. IFN- $\gamma$  was induced by administering Dox (1 mg/ml) via the drinking water and arrows indicate the time point of Dox application.

### 6.2.4 IFN- $\gamma$ induction in IFN- $\gamma^{-/-}$ mice can lead to tumor rejection and has no effect in IFN- $\gamma R^{-/-}$ mice

To find out whether endogenous IFN- $\gamma$  contributes to the IFN- $\gamma$  expressed by the tumor cells, we injected the MCA313-IFN- $\gamma^{IND}$  cells into IFN- $\gamma^{-/-}$  mice. IFN- $\gamma^{-/-}$  mice injected with  $1 \times 10^6$  MCA313-IFN- $\gamma^{IND}$  cells did not form tumors when Dox was administered from the day of tumor cell injection. Tumors grew out within 20 days when left untreated (Fig. 6.16 A). Importantly, after IFN- $\gamma$  induction in large tumors at day 14 ( $618 \text{ mm}^3$ ), one mouse rejected the tumor (1/5, 20%) but similar to wild type mice, the majority died (Fig. 6.16 B and Table 6.5).

MCA313-IFN- $\gamma^{IND}$  cells lacking IFN- $\gamma R$  were injected into IFN- $\gamma R^{-/-}$  mice to ascertain whether host cells have to respond to IFN- $\gamma$  to mediate tumor rejection.  $1 \times 10^6$  MCA313-IFN- $\gamma^{IND}$  cells were injected into IFN- $\gamma R^{-/-}$  mice and Dox treatment was started immediately after tumor cell injection or in large tumors at day 14. Dox treated tumors grew with similar kinetics as untreated tumors (Fig. 6.16 C–D, table 6.5), suggesting that IFN- $\gamma$  acts on the host cells, probably within the tumor tissue.

**Table 6.5. The efficiency of tumor rejection by locally produced IFN- $\gamma$  depends on the time tumors have grown in the mice.**  $1 \times 10^6$  MCA313-IFN- $\gamma^{IND}$  cells were injected s.c. into C57BL/6, IFN- $\gamma^{-/-}$  and IFN- $\gamma R^{-/-}$  mice. Mice with similar tumor size were divided into groups and Dox was applied at the day indicated in the table. Shown are individual experiments with MCA313-IFN- $\gamma^{IND}$  tumors. Asterisks indicate tumor relapse after terminating Dox application at day 79.

Mouse strain	Day of IFN- $\gamma$ induction	Tumor vol ( $\text{mm}^3$ )	No. of mice with rejected tumor/injected mice (%)	No. of mice with therapy-induced death
C57BL/6	0	0	10/10 (100 %)	0
	14	$340 \pm 103$	1/5 (20 %)*	3
	16	$504 \pm 77$	1/6 (17 %)*	4
	17	$477 \pm 54$	0/3 (0 %)	3
IFN- $\gamma^{-/-}$	0	0	8/8 (100 %)	0
	13	$473 \pm 5$	0/2 (0 %)	2
	14	$619 \pm 84$	1/5 (20 %)	4
	15	$462 \pm 0$	0/1 (0 %)	1
	w/o		0/7 (0 %)	0
IFN- $\gamma R^{-/-}$	0	0	0/8 (0 %)	0
	14	$763 \pm 164$	0/5 (0 %)	0
	17	$653 \pm 83$	0/3 (0 %)	0
	w/o		0/4 (0 %)	0

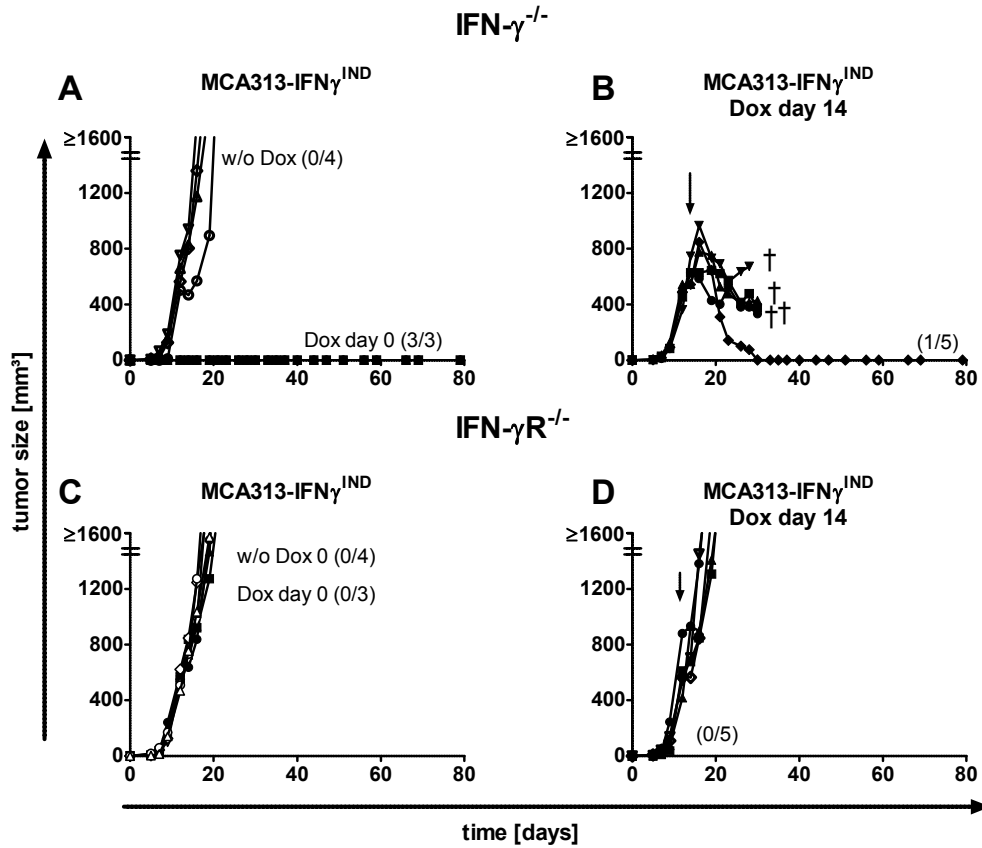


**Figure 6.16.**  $IFN-\gamma R$  expression on host cells is necessary for  $IFN-\gamma$  mediated tumor rejection.  $1 \times 10^6$  MCA313- $IFN-\gamma^{IND}$  cells were injected into (A) and (B)  $IFN-\gamma^{-/-}$  or (C) and (D)  $IFN-\gamma R^{-/-}$  mice. Tumor growth kinetics after induction of local  $IFN-\gamma$  expression in MCA313- $IFN-\gamma^{IND}$  tumors are shown. (A) Tumor bearing mice without administering Dox (open symbols) and mice receiving Dox from the day of tumor cell injection (closed symbols). (B) Mice injected with MCA313- $IFN-\gamma^{IND}$  cells treated with Dox at day 14. (C) Tumor bearing mice  $IFN-\gamma R^{-/-}$  mice without administering Dox (open symbols) and mice receiving Dox from the day of tumor cell injection (closed symbols). (D)  $IFN-\gamma$  induction at day 14 in  $IFN-\gamma R^{-/-}$  mice injected with MCA313- $IFN-\gamma^{IND}$  cells. Numbers in parentheses show rejected tumors/total number of mice in the experimental group. A cross indicates that the animal died or had to be sacrificed due systemic toxicity. Each line represents tumor growth in one animal.  $IFN-\gamma$  was induced by administering Dox (1 mg/ml) via the drinking water and arrows indicate the time point of Dox application.

### 6.2.5 IFN- $\gamma$ induction in MCA313-IFN- $\gamma^{\text{IND}}$ cells leads to weight loss in IFN- $\gamma$ R-competent mice

Similar to the J558L-IFN- $\gamma^{\text{IND}}$  model, induction of IFN- $\gamma$  in wild type C57BL/6 mice bearing MCA313-IFN- $\gamma^{\text{IND}}$  tumors was associated with toxic side effects which became apparent by weight loss. As shown in Fig. 6.17, mice in which IFN- $\gamma$  was induced in established tumors (day 14 and 16) showed weight loss, whereas untreated mice and mice treated with Dox from day 0 did not. Only those mice which were able to reject the tumor gained in weight after preceding weight loss (Fig. 6.17 B and C).

Induction of IFN- $\gamma$  in IFN- $\gamma^{-/-}$  mice bearing large, established tumors led to massive weight loss followed by death in the majority of mice. Only one mouse rejected the tumor and regained weight (Fig. 6.18 B). Again, untreated mice and mice treated with Dox at the day of tumor cell injection did not show any signs of toxicity (Fig. 6.18 A).

To prove that IFN- $\gamma$  is responsible for the toxic effects, we injected MCA313-IFN- $\gamma^{\text{IND}}$  cell into IFN- $\gamma$ R $^{-/-}$  mice which cannot react to IFN- $\gamma$ . As expected, IFN- $\gamma$  induction in mice bearing established tumors had no influence on tumor growth and weight loss. Similar to untreated mice, treated mice gained weight due to tumor burden (Fig. 6.18 C and D). In summary, IFN- $\gamma$  induction in established tumors led to weight loss of mice expressing the IFN- $\gamma$ R, whereas there were no toxic side effects observed when the mice did not express the IFN- $\gamma$ R, thus arguing for a direct toxic effect of IFN- $\gamma$  on host cells and not cancer cells.

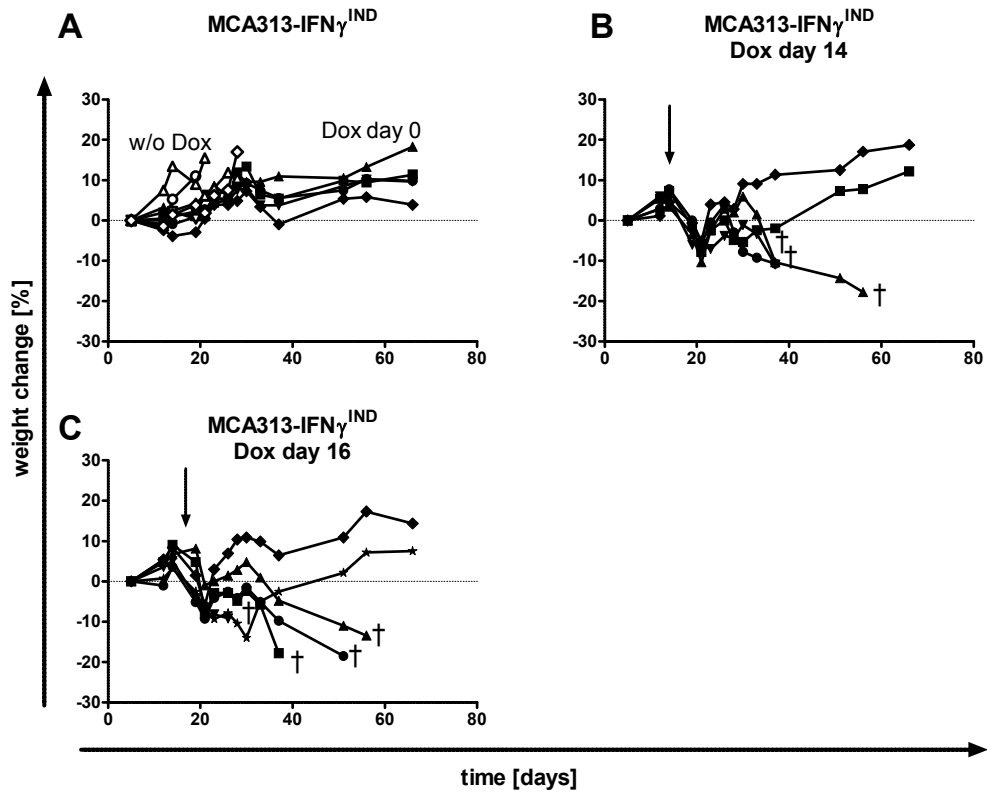


**Figure 6.17.** IFN- $\gamma$  induction can lead to weight loss of MCA313-IFN- $\gamma^{IND}$  bearing mice.  $1 \times 10^6$  MCA313-IFN- $\gamma^{IND}$  cells were injected s.c. into C57BL/6 mice. Weight change after induction of local IFN- $\gamma$  expression in MCA313-IFN- $\gamma^{IND}$  tumors is shown. (A) Tumor bearing mice without administering Dox (open symbols) and mice receiving Dox from the day of tumor cell injection (closed symbols). (B) Mice injected with MCA313-IFN- $\gamma^{IND}$  cells treated with Dox at day 14 or (C) at day 16. IFN- $\gamma$  was induced by administering Dox (1 mg/ml) via the drinking water and arrows indicate the time point of Dox application. Weight loss of mice depicted in Fig. 6.15 are shown.

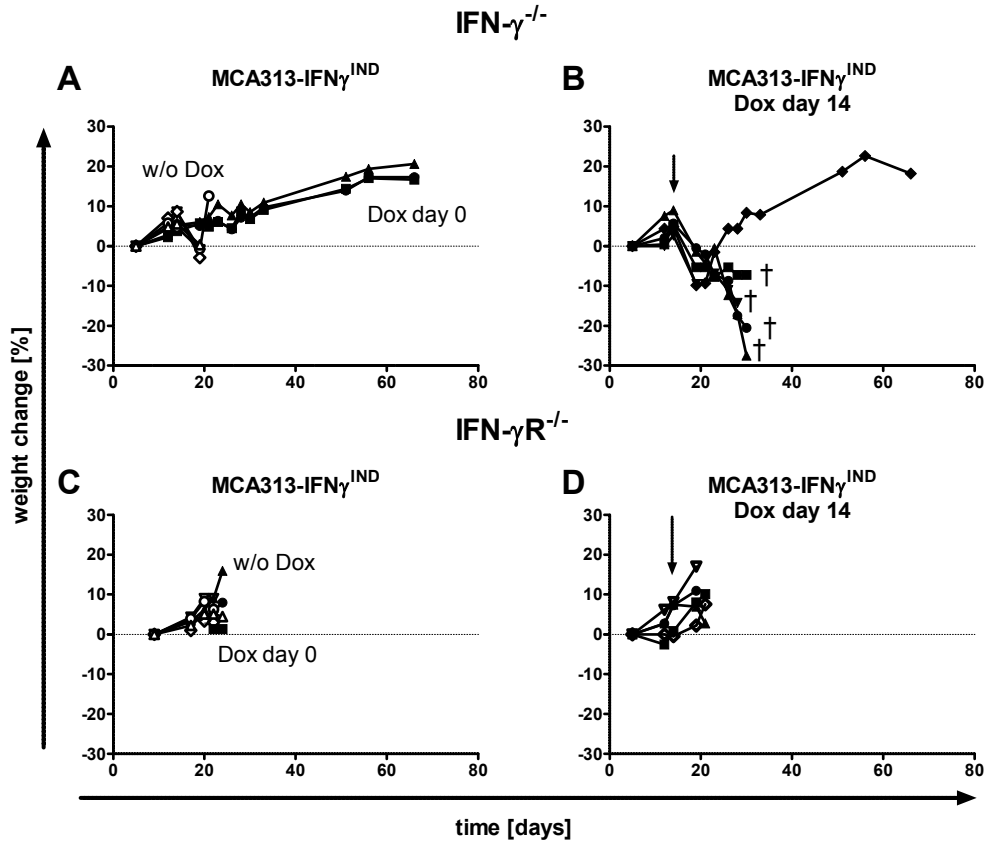


**Figure 6.18.** IFN- $\gamma$  induction in MCA313-IFN- $\gamma^{IND}$  tumors leads to weight loss of IFN- $\gamma^{-/-}$  but not IFN- $\gamma R^{-/-}$  mice.  $1 \times 10^6$  MCA313-IFN- $\gamma^{IND}$  cells were injected s.c. into IFN- $\gamma^{-/-}$  mice (A and B) and IFN- $\gamma R^{-/-}$  mice (C and D). Weight change after induction of local IFN- $\gamma$  expression in MCA313-IFN- $\gamma^{IND}$  tumors are shown. (A) Tumor bearing IFN- $\gamma^{-/-}$  and (C) IFN- $\gamma R^{-/-}$  mice without administering Dox (open symbols) and mice receiving Dox from the day of tumor cell injection (closed symbols). (B) IFN- $\gamma^{-/-}$  and (D) IFN- $\gamma R^{-/-}$  mice injected with MCA313-IFN- $\gamma^{IND}$  cells treated with Dox at day 14. Each line represents weight change of one animal. IFN- $\gamma$  was induced by administering Dox (1 mg/ml) via the drinking water and arrows indicate the time point of Dox application. Weight loss of mice depicted in Fig. 6.16 are shown.



### 6.2.6 Summary MCA313-IFN- $\gamma$ <sup>IND</sup>

To draw a more general applicable conclusion about the effect of IFN- $\gamma$  on established tumors, we performed experiments in second tumor model. MCA313 cells were transduced with the same tet-IFN- $\gamma$  vector and first tested in vitro. As demonstrated for the J558L-IFN- $\gamma$ <sup>IND</sup> cells, IFN- $\gamma$  expression by MCA313-IFN- $\gamma$ <sup>IND</sup> cells was inducible and titratable. Yet they produced higher amounts of IFN- $\gamma$  in vitro and in vivo. High IFN- $\gamma$  serum levels were detected in C57BL/6 and IFN- $\gamma$ <sup>-/-</sup> mice after IFN- $\gamma$  induction in established tumors. Immense IFN- $\gamma$  serum levels (800 ng/ml) were detected in IFN- $\gamma$ R<sup>-/-</sup> mice which cannot respond to IFN- $\gamma$ . IFN- $\gamma$  induction concomitantly to tumor cell injection prevented tumor formation in wild type C57BL/6 mice and IFN- $\gamma$ <sup>-/-</sup> mice. IFN- $\gamma$  induction in established tumors in those mice led to tumor rejection in 20 % of the mice if induced at day 14.

As with the previous tumor model, later induction was less efficient. Probably due to the very high IFN- $\gamma$  serum levels the majority of mice, in which IFN- $\gamma$  was induced in established tumors, died. Importantly, MCA313-IFN- $\gamma$ <sup>IND</sup> cells injected into IFN- $\gamma$ R<sup>-/-</sup> mice grew with the same kinetics as untreated cells in wild type mice irrespective of Dox application.

## 7 Discussion

T cells may utilize a number of different effector molecules - such as TNF- $\alpha$ , perforin, IFN- $\gamma$  and Fas-ligand - to attack blood vessel. In this study, we used ectopic inducible expression of IFN- $\gamma$  to exclude all other effector molecules and to investigate the role of this cytokine alone.

Using the tetracycline system to induce local expression of IFN- $\gamma$  in tumors, we have shown that a suspension of tumor cells is completely rejected, while approximately only 17 to 50 % of the vascularized tumors were rejected. Furthermore, we observed that rejection of vascularized tumors have to better mimic the clinical situation – that is, established tumors.

In patients, tumors are usually detected when they have grown to a size of  $10^9$  cells, which equates a tumor size of approximately 1 cm [78]. In the mouse model, Schreiber et al. define an established tumor as having a minimum size of 1 cm in diameter and being approximately 14 days old [37]. In our model, the tumors had a approximate size of 1 cm and were 12-14 days old and because tumors at day 12 and 14 after injection were well vascularized when analyzed, our data support the observations described by Schreiber et al [37]. However, IFN- $\gamma$  induction at later time points in large tumors resulted in a lower rejection frequency. This might indicate, that these tumors are more established than those induced at earlier time points.

In our model, IFN- $\gamma$  mediated tumor rejection was associated with blood vessel destruction and necrosis. We observed blood vessel destruction in all histological samples that were analyzed after IFN- $\gamma$  induction (Table 6.4). Macroscopically hemorrhagic tumor necrosis was apparent on the surface of almost all tumors. Nevertheless, only a proportion was rejected despite the fact that all tumors showed necrosis macroscopically as well as in histological analysis.

Even though IFN- $\gamma$  release in tumors resulted in rapid destruction of the tumor vasculature, it is not clear whether IFN- $\gamma$  directly affects the endothelial cells in the blood vessels. Endothelial cells depend on V3-integrin-binding [64] and paracrine signals by other stromal cells such as pericytes or smooth muscle cells. Therefore,

killing of surrounding stroma cells by IFN- $\gamma$  might induce anoikis of the endothelial cells. IFN- $\gamma$  from tumor-specific T cells has also been shown to be associated with blood vessel destruction [63].

Our data suggests that IFN- $\gamma$  alone is sufficient to induce blood vessel destruction and to initiate rejection of established tumors. Even though we did not detect elevated TNF- $\alpha$  levels in the serum after IFN- $\gamma$  induction, we cannot exclude that locally, other factors such as TNF- $\alpha$  were induced that contributed to blood vessel destruction. Nevertheless, the observation that local expression of IFN- $\gamma$  alone can induce substantial regression of large tumors is compatible with the observation that T cells lacking several effector molecules (such as TNF- $\alpha$ , lymphotoxin- $\beta$ , perforin or Fas) but not IFN- $\gamma$  were as effective in suppressing tumor growth as wild type T cells [79].

## 7.1 J558L-IFN- $\gamma$ <sup>IND</sup>

IFN- $\gamma$  induction in large J558L-IFN- $\gamma$ <sup>IND</sup> tumors was associated with toxicity. Attempts to reduce toxicity showed that titration of IFN- $\gamma$  had no effect, whereas treatment in intervals successfully reduced toxicity and thus enhanced the efficacy of tumor rejection. Further studies will be needed to define the therapeutic window of local IFN- $\gamma$  treatment. Toxicity was more pronounced if tumors had grown for longer periods in the mice. For example, when IFN- $\gamma$  was induced on day 21 after tumor cell injection, all mice died of toxic side effects. Larger tumors probably induced toxicity because they contained more IFN- $\gamma$  secreting tumor cells that caused systemic in addition to local effects.

Toxicity was also observed when renal cell carcinoma patients were treated with systemic IFN- $\gamma$  [80]; here, the toxicity profile (including weight loss and liver damage) was similar to the one observed in our study [81].

How local IFN- $\gamma$  causes tumor rejection is unclear, but it seems unlikely that IFN- $\gamma$  secreted by the tumor cells acts on the tumor cells themselves, since we observed neither a growth delay in vitro nor a growth delay in Rag1<sup>-/-</sup> x IFN- $\gamma$ R<sup>-/-</sup> mice in vivo after induction of IFN- $\gamma$ . However, because we performed the experiments in Rag1<sup>-/-</sup> and Rag1<sup>-/-</sup> x IFN- $\gamma$ R<sup>-/-</sup> mice, our findings may be confounded by genetic background of the mice used.

Rejection of large tumors is T cell dependent as shown by our experiments in NOD/SCID mice. However, blood vessel destruction is T cell independent, since IFN- $\gamma$  induction in NOD/SCID mice led to blood vessels destruction. Even though

T cells are required for tumor rejection of large tumors, we think that T cells were not directly induced by IFN- $\gamma$ , but rather that IFN- $\gamma$  induced necrosis and bystander elimination of tumor cells. This in turn could allow T cells a more efficient eradication of tumor cells that survive IFN- $\gamma$  treatment and that are usually found at the rim of the tumor [82].

Tumor cells re-isolated from tumors induced at later time points (day 8–14, Fig. 6.9) produced IFN- $\gamma$  after induction *in vitro*. Tumors that grew despite IFN- $\gamma$  induction at the day of tumor cell injection were re-isolated from NOD/SCID and Rag1<sup>-/-</sup> x IFN- $\gamma$ R<sup>-/-</sup> mice. In contrast to tumors isolated from Rag1<sup>-/-</sup> x IFN- $\gamma$ R<sup>-/-</sup> mice, tumors from NOD/SCID mice lost the ability to produce IFN- $\gamma$ , suggesting a selection process. The growth of IFN- $\gamma$ -secreting tumor cells possibly was prevented in NOD/SCID mice, but the T cell-deficiency allowed outgrowth of loss-variants. Because tumors re-isolated from Rag1 x IFN- $\gamma$ R<sup>-/-</sup> mice produced IFN- $\gamma$ , tumor elimination here appeared to be T cell and not IFN- $\gamma$  dependent.

The rejection process induced by locally produced IFN- $\gamma$  is reminiscent of what has been described for low dose cyclophosphamide (CY) mediated rejection of large MOPC315 or J558L tumors [58, 83]. Low dose CY treatment was successful only within a certain time window (4–12 days of tumor growth) [83]. In the CY model, tumor rejection is mediated primarily by immune effector mechanisms and, in particular, involves IFN- $\gamma$  [58]. Similar to the J558L-IFN- $\gamma$ <sup>IND</sup> model of local IFN- $\gamma$  mediated rejection, separate phases of tumor destruction have been observed during low dose CY mediated tumor rejection. In the initial phase (within the first days after CY application) blood vessels were destroyed in an IFN- $\gamma$  dependent fashion and massive necrosis ensued. In the second phase, the late rejection phase, residual tumor cells were eliminated by T cells [58].

## 7.2 MCA313-IFN- $\gamma$ <sup>IND</sup>

Using MCA313-IFN- $\gamma$ <sup>IND</sup> tumor cells which do not express the IFN- $\gamma$ R, we show that IFN- $\gamma$  produced by the tumor cells does not act in an autocrine way. In IFN- $\gamma$ R<sup>-/-</sup> mice in which host cells cannot respond to IFN- $\gamma$ , IFN- $\gamma$  producing tumor cells grew with the same kinetics as untreated tumor cells. Evidently, the delay of tumor growth or rejection was caused by the effect of IFN- $\gamma$  on stroma cells. Moreover, the results of this second tumor model confirm the data gained from the J558L-IFN- $\gamma$ <sup>IND</sup> experiments. IFN- $\gamma$  is able to prevent tumor formation if induced concomitantly to tumor cell injection.

Even though less animals were tested in the MCA313 model, it seems that the later IFN- $\gamma$  is induced after tumor cell injection the less effective it is. Induction at day 14 led to tumor rejection in 20 % of C57BL/6 and IFN- $\gamma^{-/-}$  mice, whereas induction at later time points was less efficient (Figure 6.5).

If IFN- $\gamma$  expression was started concomitantly to tumor cell injection, tumor formation was prevented in IFN- $\gamma^{-/-}$  mice. Importantly, IFN- $\gamma$  induction led to lower detectable levels of IFN- $\gamma$  in the serum of IFN- $\gamma^{-/-}$  mice compared to wild type mice (Fig. 6.13). In mice in which IFN- $\gamma$  was induced on the same day (day 14, Fig. 6.5) we found that one wild type and one IFN- $\gamma^{-/-}$  mouse rejected the tumor, respectively. These data imply that endogenous IFN- $\gamma$  plays a minor role in our model.

Induction of IFN- $\gamma$  in IFN- $\gamma^R^{-/-}$  mice did not affect tumor growth regardless if induced concomitant to tumor cell injection or in established tumors. Here, host cells were not able to react to IFN- $\gamma$  suggesting that IFN- $\gamma$  acts on stroma and not tumor cells.

As in the J558LIFN- $\gamma^{\text{IND}}$  model IFN- $\gamma$  induction in established MCA313IFN- $\gamma^{\text{IND}}$  tumors was associated with toxicity. Of note, even though serum levels were approximately 3.5 fold higher (see 6.2 and 6.13 for comparison), toxicity in this C57BL/6 model was not increased.

## 7.3 Conclusion

Taken together, we show that vascularized tumors can be rejected by IFN- $\gamma$ . However, IFN- $\gamma$ -mediated rejection of established tumors is less efficient with time, suggesting that transplanted tumors become less susceptible to local IFN- $\gamma$  treatment the better they are established. Finally, we show that IFN- $\gamma$  induction in established tumors is first followed by a reduction of CD31<sup>+</sup> or CD146<sup>+</sup> endothelial cells, which in turn is followed by massive necrosis.

Because IFN- $\gamma^{-/-}$  mice were able to reject IFN- $\gamma$  producing tumor cell suspensions and established tumors, we think that endogenous IFN- $\gamma$  plays a minor role in tumor cell rejection. The main effect apparently results from the IFN- $\gamma$  produced by the tumor cells. However, we cannot exclude a synergic effect of endogenous IFN- $\gamma$  because in contrast to the MCA313-IFN- $\gamma^{\text{IND}}$  model, IFN- $\gamma$  induction in J558L-IFN- $\gamma^{\text{IND}}$  tumors in wild type BALB/c mice shows a higher rejection rate compared to the IFN- $\gamma^{-/-}$  mice on the same background (Fig. 6.1). Though endogenous IFN- $\gamma$  does not play a crucial role in tumor rejection, T cells do. Experiments per-

formed in NOD/SCID mice showed a delay in tumor growth after IFN- $\gamma$  induction but no rejection. This suggests an effect of IFN- $\gamma$  in early destruction of the tumor stroma and the resulting death of tumor cells. Nevertheless, T cells are necessary to destroy the remaining tumor cells and are crucial to prevent relapse.

It is difficult to define, when after injection of a tumor cell suspension a tumor can be considered "established". While there is no commonly accepted definition of what comprises an established tumor, our definition for an established tumor is based on data by Schreiber et al. [37] showing that injection of tumor cell suspensions causes artifacts, such as necrosis and inflammation, during the first days after injection. Thus, we define an established tumor as a tumor growing for a minimum of 10–14 days in the mouse and having a size of approximately 10 mm in each diameter. However, what can be considered as an established tumor may vary for different tumor models with different abilities to recruit stromal cells.

In principle, we have established a tool that would not only allow the investigation of the anti-angiogenic effect of IFN- $\gamma$ , but also of other cytokines such as IL-4, IL-10 and TNF- $\alpha$  in more detail. Additionally, using the inducible IFN- $\gamma$  model, one can now scrutinize the exact mechanisms of rejection, using for example confocal microscopy or 2-photon imaging.

Furthermore, with the help of our model and tissue specific IFN- $\gamma$ R deficient mice, one can determine if IFN- $\gamma$  acts directly on endothelial cells or whether blood vessel destruction is mediated indirectly via anti-angiogenic chemokines such as IP-10 or MIG [66, 67]. Collectively, this study shows that IFN- $\gamma$  can mediate the rejection of established tumors by acting on stroma cells, namely endothelial cells. Thus, after elimination of the toxic side effects e.g. via interval treatment, IFN- $\gamma$  may be a valuable tool to be used in immunotherapy to treat cancer.

# Bibliography

- [1] *Website of the German Cancer Research Center (DKFZ)*, <http://www.dkfz.de/en/krebsatlas/index.html>. 12 2010
- [2] HANAHAN, D. ; WEINBERG, R. A.: The hallmarks of cancer. In: *Cell* 100 (2000), Jan, Nr. 1, S. 57–70
- [3] NAGY, R. ; SWEET, K. ; ENG, C.: Highly penetrant hereditary cancer syndromes. In: *Oncogene* 23 (2004), Aug, Nr. 38, S. 6445–6470
- [4] RENDU, F. ; PEOC'H, K. ; BERLIN, I. ; THOMAS, D. ; LAUNAY, J.-M.: Smoking related diseases: the central role of monoamine oxidase. In: *Int J Environ Res Public Health* 8 (2011), Jan, Nr. 1, S. 136–147
- [5] WU, M. ; ZHAO, J.-K. ; ZHANG, Z.-F. ; HAN, R.-Q. ; YANG, J. ; ZHOU, J.-Y. ; WANG, X.-S. ; ZHANG, X.-F. ; LIU, A.-M. ; VEER, P. Van' T. ; KOK, F.J. ; KAMPMAN, E.: Smoking and alcohol drinking increased the risk of esophageal cancer among Chinese men but not women in a high-risk population. In: *Cancer Causes Control* (2011), Feb
- [6] JOSHU, C.E. ; MONDUL, A.M. ; MENKE, A. ; MEINHOLD, C.L. ; HAN, M. ; HUMPHREYS, E. ; FREEDLAND, S.J. ; WALSH, P.C. ; PLATZ, E.A.: Weight gain is associated with an increased risk of prostate cancer recurrence after prostatectomy in the PSA era. In: *Cancer Prev Res (Phila)* (2011), Feb
- [7] REEVES, K.W. ; CARTER, G.C. ; RODABOUGH, R.J. ; LANE, D. ; MCNEELEY, S.G. ; STEFANICK, M.L. ; PASKETT, E. D.: Obesity in relation to endometrial cancer risk and disease characteristics in the Women's Health Initiative. In: *Gynecol Oncol* (2011), Feb
- [8] LONG, H.M. ; TAYLOR, G.S. ; RICKINSON, A.B.: Immune defence against EBV and EBV-associated disease. In: *Curr Opin Immunol* (2011), Jan
- [9] GALLAGHER, R.P. ; LEE, T.K. ; BAJDIK, C.D. ; BORUGIAN, M.: Ultraviolet radiation. In: *Chronic Dis Can* 29 Suppl 1 (2010), S. 51–68

- [10] COUSSENS, L. M. ; WERB, Z.: Inflammatory cells and cancer: think different! In: *J Exp Med* 193 (2001), Mar, Nr. 6, S. F23–F26
- [11] WEINBERG, R. A.: Oncogenes, antioncogenes, and the molecular bases of multistep carcinogenesis. In: *Cancer Res* 49 (1989), Jul, Nr. 14, S. 3713–3721
- [12] LAND, H. ; PARADA, L. F. ; WEINBERG, R. A.: Tumorigenic conversion of primary embryo fibroblasts requires at least two cooperating oncogenes. In: *Nature* 304 (1983), Nr. 5927, S. 596–602
- [13] HAHN, W. C. ; WEINBERG, R. A.: Rules for making human tumor cells. In: *N Engl J Med* 347 (2002), Nov, Nr. 20, S. 1593–1603
- [14] CRINO, L. ; DANSIN, E. ; GARRIDO, P. ; GRIESINGER, F. ; LASKIN, J. ; PAVLAKIS, N. ; STROIKOVSKI, D. ; THATCHER, N. ; TSAI, CM ; WU, YI ; ZHOU, Caicun: Safety and efficacy of first-line bevacizumab-based therapy in advanced non-squamous non-small-cell lung cancer (SAiL, MO19390): a phase 4 study. In: *Lancet Oncol* 11 (2010), Aug, Nr. 8, S. 733–740
- [15] BERGERS, G. ; JAVAHERIAN, K. ; LO, K. M. ; FOLKMAN, J. ; HANAHAN, D.: Effects of angiogenesis inhibitors on multistage carcinogenesis in mice. In: *Science* 284 (1999), Apr, Nr. 5415, S. 808–812
- [16] SIMONDS, H.M. ; MILES, D.: Adjuvant treatment of breast cancer: impact of monoclonal antibody therapy directed against the HER2 receptor. In: *Expert Opin Biol Ther* 7 (2007), Apr, Nr. 4, S. 487–491
- [17] HEGE, K. M. ; JOOSS, K. ; PARDOLL, D.: GM-CSF gene-modified cancer cell immunotherapies: of mice and men. In: *Int Rev Immunol* 25 (2006), Nr. 5-6, S. 321–352
- [18] HOCK, H. ; DORSCH, M. ; KUNZENDORF, U. ; UBERLA, K. ; QIN, Z. ; DIAMANTSTEIN, T. ; BLANKENSTEIN, T.: Vaccinations with tumor cells genetically engineered to produce different cytokines: effectivity not superior to a classical adjuvant. In: *Cancer Res* 53 (1993), Feb, Nr. 4, S. 714–716
- [19] HOCK, H. ; DORSCH, M. ; KUNZENDORF, U. ; QIN, Z. ; DIAMANTSTEIN, T. ; BLANKENSTEIN, T.: Mechanisms of rejection induced by tumor cell-targeted gene transfer of interleukin 2, interleukin 4, interleukin 7, tumor necrosis factor, or interferon gamma. In: *Proc Natl Acad Sci U S A* 90 (1993), Apr, Nr. 7, S. 2774–2778



- [20] WYSOCKI, P.J. ; KARCZEWSKA-DZIONK, A. ; MACKIEWICZ-WYSOCKA, M. ; MACKIEWICZ, A.: Human cancer gene therapy with cytokine gene-modified cells. In: *Expert Opin Biol Ther* 4 (2004), Oct, Nr. 10, S. 1595–1607
- [21] KAMMERTOENS, T. ; BLANKENSTEIN, T.: Making and circumventing tolerance to cancer. In: *Eur J Immunol* 39 (2009), Sep, Nr. 9, S. 2345–2353
- [22] JURGENS, L.A. ; KHANNA, R. ; WEBER, J. ; ORENTAS, R.J.: Transduction of primary lymphocytes with Epstein-Barr virus (EBV) latent membrane protein-specific T-cell receptor induces lysis of virus-infected cells: A novel strategy for the treatment of Hodgkin's disease and nasopharyngeal carcinoma. In: *J Clin Immunol* 26 (2006), Jan, Nr. 1, S. 22–32
- [23] MOOSMANN, A. ; BIGALKE, I. ; TISCHER, J. ; SCHIRRMANN, L. ; KASTEN, J. ; S.TIPPMER ; LEEPING, M. ; PREVALSEK, D. ; JAEGER, G. ; LEDDEROSE, G. ; MAUTNER, J. ; HAMMERSCHMIDT, W. ; SCHENDEL, D.J. ; KOLB, H.-J.: Effective and long-term control of EBV PTLTD after transfer of peptide-selected T cells. In: *Blood* 115 (2010), Apr, Nr. 14, S. 2960–2970
- [24] MORGAN, R.A. ; DUDLEY, M.E. ; WUNDERLICH, J.R. ; HUGHES, M.S. ; YANG, J.C. ; SHERRY, R.M. ; ROYAL, R.E. ; TOPALIAN, S.L. ; KAMMULA, U.S. ; RESTIFO, N.P. ; ZHENG, Z. ; NAHVI, A. ; VRIES, C.R. de ; ROGERS-FREEZER, L.J. ; MAVROUKAKIS, S.A. ; ROSENBERG, S.A.: Cancer regression in patients after transfer of genetically engineered lymphocytes. In: *Science* 314 (2006), Oct, Nr. 5796, S. 126–129
- [25] ZHANG, B. ; KARRISON, T. ; ROWLEY, D.A. ; SCHREIBER, H.: IFN-gamma- and TNF-dependent bystander eradication of antigen-loss variants in established mouse cancers. In: *J Clin Invest* 118 (2008), Apr, Nr. 4, S. 1398–1404
- [26] M.E.DUDLEY, S.A.Rosenberg: Adoptive cell therapy for the treatment of patients with metastatic melanoma. In: *Curr Opin Immunol* 21 (2009), Apr, Nr. 2, S. 233–240
- [27] DUDLEY, M.E. ; WUNDERLICH, J.R. ; ROBBINS, P.F. ; YANG, J.C. ; HWU, P. ; SCHWARTZENTRUBER, D.J. ; TOPALIAN, S.L. ; SHERRY, R. ; RESTIFO, N.P. ; HUBICKI, A.M. ; ROBINSON, M.R. ; RAFFELD, M. ; DURAY, P. ; SEIPP, C.A. ; ROGERS-FREEZER, L. ; MORTON, K.E. ; MAVROUKAKIS, S.A. ; WHITE, D.E. ; ROSENBERG, S.A.: Cancer regression and autoimmunity in patients after

- clonal repopulation with antitumor lymphocytes. In: *Science* 298 (2002), Oct, Nr. 5594, S. 850–854
- [28] BESSER, M.J. ; SHAPIRA-FROMMER, R. ; TREVES, A.J. ; ZIPPEL, D. ; O.ITZHAKI ; HERSHKOVITZ, L. ; LEVY, D. ; KUBI, A. ; HOVAV, E. ; CHERMOSHNIUK, N. ; SHALMON, B. ; HARDAN, I. ; CATANE, R. ; MARKEL, G. ; APTER, S. ; BEN-NUN, A. ; KUCHUK, I. ; SHIMONI, A. ; NAGLER, A. ; J.SCHACHTER: Clinical responses in a phase II study using adoptive transfer of short-term cultured tumor infiltration lymphocytes in metastatic melanoma patients. In: *Clin Cancer Res* 16 (2010), May, Nr. 9, S. 2646–2655
- [29] DUDLEY, M. E. ; ROSENBERG, S.A.: Adoptive-cell-transfer therapy for the treatment of patients with cancer. In: *Nat Rev Cancer* 3 (2003), Sep, Nr. 9, S. 666–675
- [30] DUDLEY, M.E. ; GROSS, C.A. ; LANGHAN, M.M. ; GARCIA, M.R. ; SHERRY, R.M. ; YANG, J.C. ; PHAN, G.Q. ; KAMMULA, U.S. ; HUGHES, M.S. ; CITRIN, D.E. ; RESTIFO, N.P. ; WUNDERLICH, J.R. ; PRIETO, P.A. ; HONG, J.J. ; LANGAN, R.C. ; ZLOTT, D.A. ; MORTON, K.E. ; WHITE, D.E. ; LAURENCOT, C.M. ; ROSENBERG, S. A.: CD8+ enriched "young" tumor infiltrating lymphocytes can mediate regression of metastatic melanoma. In: *Clin Cancer Res* 16 (2010), Dec, Nr. 24, S. 6122–6131
- [31] DUDLEY, M.E. ; WUNDERLICH, J.R. ; YANG, J.C. ; SHERRY, R.M. ; TOPALIAN, S.L. ; RESTIFO, N.P. ; ROYAL, R.E. ; KAMMULA, U. ; WHITE, D.E. ; ROSENBERG, S.A. ; MAVROUKAKIS, S.A. ; ROGERS, L.J. ; GRACIA, G.J. ; JONES, S.A. ; MANGIAMELI, D.P. ; PELLETIER, M.M. ; GEA-BANACLOCHE, J. ; ROBINSON, M.R. ; BERMAN, D.M. ; FILIE, A.C. ; ABATI, A. ; ROSENBERG, S.A.: Adoptive cell transfer therapy following non-myeloablative but lymphodepleting chemotherapy for the treatment of patients with refractory metastatic melanoma. In: *J Clin Oncol* 23 (2005), Apr, Nr. 10, S. 2346–2357
- [32] QUEZADA, S.A. ; SIMPSON, T.R. ; PEGGS, K.S. ; MERGHOUB, T. ; VIDER, J. ; FAN, X. ; BLASBERG, R. ; YAGITA, H. ; ANTONY, P. Muranski P. ; RESTIFO, N.P. ; ALLISON, J.P.: Tumor-reactive CD4(+) T cells develop cytotoxic activity and eradicate large established melanoma after transfer into lymphopenic hosts. In: *J Exp Med* 207 (2010), Mar, Nr. 3, S. 637–650
- [33] SPAAPEN, R.M. ; R.W.J.GROEN ; OUDENALDER, K.van den ; GUICHELAAR, T. ; ELK, M. van ; AARTS-RIEMENS, T. ; BLOEM, A.C. ; G.STORM ; MARTENS,

- A.C. ; LOKHORST, H.M. ; MUTIS, T.: Eradication of Medullary Multiple Myeloma by CD4+ Cytotoxic Human T Lymphocytes Directed at a Single Minor Histocompatibility Antigen. In: *Clin Cancer Res* 16 (2010), Nov, Nr. 22, S. 5481–5488
- [34] KAMMERTOENS, T. ; SCHUELER, T. ; BLANKENSTEIN, T.: Immunotherapy: target the stroma to hit the tumor. In: *Trends Mol Med* 11 (2005), May, Nr. 5, S. 225–231
- [35] MUMBERG, D. ; MONACH, P. A. ; WANDERLING, S. ; PHILIP, M. ; TOLEDANO, A. Y. ; SCHREIBER, R. D. ; SCHREIBER, H.: CD4(+) T cells eliminate MHC class II-negative cancer cells in vivo by indirect effects of IFN-gamma. In: *Proc Natl Acad Sci U S A* 96 (1999), Jul, Nr. 15, S. 8633–8638
- [36] DVORAK, H. F.: Tumors: wounds that do not heal. Similarities between tumor stroma generation and wound healing. In: *N Engl J Med* 315 (1986), Dec, Nr. 26, S. 1650–1659
- [37] SCHREIBER, K. ; ROWLEY, D.A. ; RIETHMUELLER, G. ; SCHREIBER, H.: Cancer immunotherapy and preclinical studies: why we are not wasting our time with animal experiments. In: *Hematol Oncol Clin North Am* 20 (2006), Jun, Nr. 3, S. 567–584
- [38] SPIOTTO, M.T. ; ROWLEY, D.A. ; SCHREIBER, H.: Bystander elimination of antigen loss variants in established tumors. In: *Nat Med* 10 (2004), Mar, Nr. 3, S. 294–298
- [39] SPIOTTO, M.T. ; SCHREIBER, H.: Rapid destruction of the tumor microenvironment by CTLs recognizing cancer-specific antigens cross-presented by stromal cells. In: *Cancer Immun* 5 (2005), S. 8
- [40] SCHIETINGER, A. ; M.PHILIP ; LIU, R.B. ; SCHREIBER, K. ; SCHREIBER, H.: Bystander killing of cancer requires the cooperation of CD4(+) and CD8(+) T cells during the effector phase. In: *J Exp Med* 207 (2010), Oct, Nr. 11, S. 2469–2477
- [41] ALLIONE, A. ; CONSALVO, M. ; NANNI, P. ; LOLLINI, P. L. ; CAVALLO, F. ; GIOVARELLI, M. ; FORNI, M. ; GULINO, A. ; COLOMBO, M. P. ; DELLABONA, P.: Immunizing and curative potential of replicating and nonreplicating murine

- mammary adenocarcinoma cells engineered with interleukin (IL)-2, IL-4, IL-6, IL-7, IL-10, tumor necrosis factor alpha, granulocyte-macrophage colony-stimulating factor, and gamma-interferon gene or admixed with conventional adjuvants. In: *Cancer Res* 54 (1994), Dec, Nr. 23, S. 6022–6026
- [42] RICHTER, G. ; KRUEGER-KRASAGAKES, S. ; HEIN, G. ; HUELS, C. ; SCHMITT, E. ; DIAMANTSTEIN, T. ; BLANKENSTEIN, T.: Interleukin 10 transfected into Chinese hamster ovary cells prevents tumor growth and macrophage infiltration. In: *Cancer Res* 53 (1993), Sep, Nr. 18, S. 4134–4137
- [43] Z.QIN ; SCHWARTZKOPFF, J. ; PRADERA, F. ; KAMMERTOENS, T. ; SELIGER, B. ; PIRCHER, H. ; BLANKENSTEIN, T.: A critical requirement of interferon gamma-mediated angiostasis for tumor rejection by CD8+ T cells. In: *Cancer Res* 63 (2003), Jul, Nr. 14, S. 4095–4100
- [44] SCHUELER, T. ; KOERNIG, S. ; BLANKENSTEIN, T.: Tumor rejection by modulation of tumor stromal fibroblasts. In: *J Exp Med* 198 (2003), Nov, Nr. 10, S. 1487–1493
- [45] QIN, Z. ; BLANKENSTEIN, T.: CD4+ T cell-mediated tumor rejection involves inhibition of angiogenesis that is dependent on IFN gamma receptor expression by nonhematopoietic cells. In: *Immunity* 12 (2000), Jun, Nr. 6, S. 677–686
- [46] SINGH, S. ; ROSS, S. R. ; ACENA, M. ; ROWLEY, D. A. ; SCHREIBER, H.: Stroma is critical for preventing or permitting immunological destruction of antigenic cancer cells. In: *J Exp Med* 175 (1992), Jan, Nr. 1, S. 139–146
- [47] YU, P. ; ROWLEY, D.A. ; FU, Y.-X. ; SCHREIBER, H.: The role of stroma in immune recognition and destruction of well-established solid tumors. In: *Curr Opin Immunol* 18 (2006), Apr, Nr. 2, S. 226–231
- [48] KAUFMANN, S. H.: [Lymphokines, interleukins, cytokines: function and action]. In: *Immun Infekt* 15 (1987), Jul, Nr. 4, S. 127–134
- [49] NANNI, P. ; FORNI, G. ; LOLLINI, P. L.: Cytokine gene therapy: hopes and pitfalls. In: *Ann Oncol* 10 (1999), Mar, Nr. 3, S. 261–266
- [50] BILLIAU, A.: Interferon-gamma: biology and role in pathogenesis. In: *Adv Immunol* 62 (1996), S. 61–130

- [51] BACH, E. A. ; AGUET, M. ; SCHREIBER, R. D.: The IFN gamma receptor: a paradigm for cytokine receptor signaling. In: *Annu Rev Immunol* 15 (1997), S. 563–591
- [52] BOEHM, U. ; KLAMP, T. ; GROOT, M. ; HOWARD, J. C.: Cellular responses to interferon-gamma. In: *Annu Rev Immunol* 15 (1997), S. 749–795
- [53] NEVILLE, L. F. ; MATHIAK, G. ; BAGASRA, O.: The immunobiology of interferon-gamma inducible protein 10 kD (IP-10): a novel, pleiotropic member of the C-X-C chemokine superfamily. In: *Cytokine Growth Factor Rev* 8 (1997), Sep, Nr. 3, S. 207–219
- [54] GREENLUND, A. C. ; FARRAR, M. A. ; VIVIANO, B. L. ; SCHREIBER, R. D.: Ligand-induced IFN gamma receptor tyrosine phosphorylation couples the receptor to its signal transduction system (p91). In: *EMBO J* 13 (1994), Apr, Nr. 7, S. 1591–1600
- [55] GANSBACHER, B. ; BANNERJI, R. ; DANIELS, B. ; ZIER, K. ; CRONIN, K. ; GILBOA, E.: Retroviral vector-mediated gamma-interferon gene transfer into tumor cells generates potent and long lasting antitumor immunity. In: *Cancer Res* 50 (1990), Dec, Nr. 24, S. 7820–7825
- [56] PREVOST-BLONDEL, A. ; NEUENHAHN, M. ; RAWIEL, M. ; PIRCHER, H.: Differential requirement of perforin and IFN-gamma in CD8 T cell-mediated immune responses against B16.F10 melanoma cells expressing a viral antigen. In: *Eur J Immunol* 30 (2000), Sep, Nr. 9, S. 2507–2515
- [57] DIGHE, A. S. ; RICHARDS, E. ; OLD, L. J. ; SCHREIBER, R. D.: Enhanced in vivo growth and resistance to rejection of tumor cells expressing dominant negative IFN gamma receptors. In: *Immunity* 1 (1994), Sep, Nr. 6, S. 447–456
- [58] IBE, S. ; QIN, Z. ; SCHUELER, T. ; PREISS, S. ; BLANKENSTEIN, T.: Tumor rejection by disturbing tumor stroma cell interactions. In: *J Exp Med* 194 (2001), Dec, Nr. 11, S. 1549–1559
- [59] BLANKENSTEIN, T.: The role of tumor stroma in the interaction between tumor and immune system. In: *Curr Opin Immunol* 17 (2005), Apr, Nr. 2, S. 180–186
- [60] PLATZER, C. ; RICHTER, G. ; UBERLA, K. ; HOCK, H. ; DIAMANTSTEIN, T. ; BLANKENSTEIN, T.: Interleukin-4-mediated tumor suppression in nude

- mice involves interferon-gamma. In: *Eur J Immunol* 22 (1992), Jul, Nr. 7, S. 1729–1733
- [61] SCHUELER, T. ; BLANKENSTEIN, T.: Cutting edge: CD8<sup>+</sup> effector T cells reject tumors by direct antigen recognition but indirect action on host cells. In: *J Immunol* 170 (2003), May, Nr. 9, S. 4427–4431
- [62] GIRARDI, M. ; OPPENHEIM, D. ; GLUSAC, E.J. ; FILLER, R. ; BALMAIN, A. ; TIGELAAR, R.E. ; A.C.HAYDAY: Characterizing the protective component of the alphabeta T cell response to transplantable squamous cell carcinoma. In: *J Invest Dermatol* 122 (2004), Mar, Nr. 3, S. 699–706
- [63] BLOHM, U. ; POTTHOFF, D. ; KOGEL, A. J. d. ; PIRCHER, H.: Solid tumors "melt" from the inside after successful CD8 T cell attack. In: *Eur J Immunol* 36 (2006), Feb, Nr. 2, S. 468–477
- [64] RUEGG, C. ; YILMAZ, A. ; BIELER, G. ; BAMAT, J. ; CHAUBERT, P. ; LEJEUNE, F. J.: Evidence for the involvement of endothelial cell integrin alphaVbeta3 in the disruption of the tumor vasculature induced by TNF and IFN-gamma. In: *Nat Med* 4 (1998), Apr, Nr. 4, S. 408–414
- [65] MUELLER-HERMELINK, N. ; BRAUMUELLER, H. ; PICHLER, B. ; WIEDER, T. ; MAILHAMMER, R. ; SCHAAK, K. ; GHORESCHI, K. ; YAZDI, A. ; HAUBNER, R. ; SANDER, C.A. .. ; MOCIKAT, R. ; SCHWAIGER, M. ; FOERSTER, I. ; HUSS, R. ; WEBER, W.A. ; KNEILLING, M. ; ROECKEN, M.: TNFR1 signaling and IFN-gamma signaling determine whether T cells induce tumor dormancy or promote multistage carcinogenesis. In: *Cancer Cell* 13 (2008), Jun, Nr. 6, S. 507–518
- [66] SGADARI, C. ; ANGIOLILLO, A. L. ; TOSATO, G.: Inhibition of angiogenesis by interleukin-12 is mediated by the interferon-inducible protein 10. In: *Blood* 87 (1996), May, Nr. 9, S. 3877–3882
- [67] SGADARI, C. ; FARBER, J. M. ; ANGIOLILLO, A. L. ; LIAO, F. ; TERUYA-FELDSTEIN, J. ; BURD, P. R. ; YAO, L. ; GUPTA, G. ; KANEGANE, C. ; TOSATO, G.: Mig, the monokine induced by interferon-gamma, promotes tumor necrosis in vivo. In: *Blood* 89 (1997), Apr, Nr. 8, S. 2635–2643
- [68] GOSSEN, M. ; BUJARD, H.: Tight control of gene expression in mammalian cells by tetracycline-responsive promoters. In: *Proc Natl Acad Sci U S A* 89 (1992), Jun, Nr. 12, S. 5547–5551

- [69] GOSSEN, M. ; BONIN, A. L. ; BUJARD, H.: Control of gene activity in higher eukaryotic cells by prokaryotic regulatory elements. In: *Trends Biochem Sci* 18 (1993), Dec, Nr. 12, S. 471–475
- [70] GOSSEN, M. ; BUJARD, H.: Anhydrotetracycline, a novel effector for tetracycline controlled gene expression systems in eukaryotic cells. In: *Nucleic Acids Res* 21 (1993), Sep, Nr. 18, S. 4411–4412
- [71] URLINGER, S. ; BARON, U. ; THELLMANN, M. ; HASAN, M. T. ; BUJARD, H. ; HILLEN, W.: Exploring the sequence space for tetracycline-dependent transcriptional activators: novel mutations yield expanded range and sensitivity. In: *Proc Natl Acad Sci U S A* 97 (2000), Jul, Nr. 14, S. 7963–7968
- [72] PERICLE, F. ; GIOVARELLI, M. ; COLOMBO, M. P. ; FERRARI, G. ; MUSIANI, P. ; MODESTI, A. ; CAVALLO, F. ; PIERRO, F. D. ; NOVELLI, F. ; FORNI, G.: An efficient Th2-type memory follows CD8+ lymphocyte-driven and eosinophil-mediated rejection of a spontaneous mouse mammary adenocarcinoma engineered to release IL-4. In: *J Immunol* 153 (1994), Dec, Nr. 12, S. 5659–5673
- [73] OI, V. T. ; MORRISON, S. L. ; HERZENBERG, L. A. ; BERG, P.: Immunoglobulin gene expression in transformed lymphoid cells. In: *Proc Natl Acad Sci U S A* 80 (1983), Feb, Nr. 3, S. 825–829
- [74] MORITA, S. ; KOJIMA, T. ; KITAMURA, T.: Plat-E: an efficient and stable system for transient packaging of retroviruses. In: *Gene Ther* 7 (2000), Jun, Nr. 12, S. 1063–1066
- [75] LOEW, R. ; MEYER, Y. ; KUEHLCKE, K. ; GAMA-NORTON, L. ; WIRTH, D. ; HAUSER, H. ; STEIN, S. ; GREZ, M. ; THORNHILL, S. ; THRASHER, A. ; BAUM, C. ; SCHAMBACH, A.: A new PG13-based packaging cell line for stable production of clinical-grade self-inactivating gamma-retroviral vectors using targeted integration. In: *Gene Ther* 17 (2010), Feb, Nr. 2, S. 272–280
- [76] HEINZ, N. ; SCHAMBACH, A. ; GALLA, M. ; MAETZIG, T. ; BAUM, C. ; R.LOEW ; SCHIEDLMEIER, B.: Retroviral and transposon-based tet-regulated All-In-One vectors with reduced background expression and improved dynamic range. In: *Hum Gene Ther* (2010), Sep

- [77] SCHRAGE, A. ; LODDENKEMPER, C. ; ERBEN, U. ; LAUER, U. ; HAUSDORF, G. ; JUNGBLUT, P.R. ; JOHNSON, J. ; KNOLLE, P.A. ; ZEITZ, M. ; HAMANN, A. ; KLUGEWITZ, K.: Murine CD146 is widely expressed on endothelial cells and is recognized by the monoclonal antibody ME-9F1. In: *Histochem Cell Biol* 129 (2008), Apr, Nr. 4, S. 441–451
- [78] PECK, K. ; SHER, Y. P. ; SHIH, J. Y. ; ROFFLER, S. R. ; WU, C. W. ; YANG, P. C.: Detection and quantitation of circulating cancer cells in the peripheral blood of lung cancer patients. In: *Cancer Res* 58 (1998), Jul, Nr. 13, S. 2761–2765
- [79] HOLLENBAUGH, J.A. ; REOME, J. ; DOBRZANSKI, M. ; DUTTON, R. W.: The rate of the CD8-dependent initial reduction in tumor volume is not limited by contact-dependent perforin, Fas ligand, or TNF-mediated cytotoxicity. In: *J Immunol* 173 (2004), Aug, Nr. 3, S. 1738–1743
- [80] GLEAVE, M. E. ; ELHILALI, M. ; FRADET, Y. ; DAVIS, I. ; VENNEN, P. ; SAAD, F. ; KLOTZ, L. H. ; MOORE, M. J. ; PATON, V. ; BAJAMONDE, A.: Interferon gamma-1b compared with placebo in metastatic renal-cell carcinoma. Canadian Urologic Oncology Group. In: *N Engl J Med* 338 (1998), Apr, Nr. 18, S. 1265–1271
- [81] BROWN, T. D. ; KOELLER, J. ; BEOUGHER, K. ; GOLANDO, J. ; BONNEM, E. M. ; SPIEGEL, R. J. ; HOFF, D. D. V.: A phase I clinical trial of recombinant DNA gamma interferon. In: *J Clin Oncol* 5 (1987), May, Nr. 5, S. 790–798
- [82] B.ZHANG ; ZHANG, Y. ; BOWERMAN, N.A. ; A.SCHIETINGER ; FU, Y.-X. ; KRANZ, D.M. ; ROWLEY, D. A. ; SCHREIBER, H.: Equilibrium between host and cancer caused by effector T cells killing tumor stroma. In: *Cancer Res* 68 (2008), Mar, Nr. 5, S. 1563–1571
- [83] HENGST, J. C. ; MOKYR, M. B. ; DRAY, S.: Importance of timing in cyclophosphamide therapy of MOPC-315 tumor-bearing mice. In: *Cancer Res* 40 (1980), Jul, Nr. 7, S. 2135–2141



# Nomenclature

$\mu\text{l}$	Microliter
$\mu\text{g}$	Microgram
IFN- $\gamma$	Interferon gamma
ALT	Alanine aminotransferase
AST	Aspartate aminotransferase
ATT	Adoptive T cell transfer
CTA	Cancer testis antigen
CTE	Constitutive transport element
CY	Cyclophosphamide
DNA	Deoxyribonucleic acid
Dox	Doxycycline
EBV	Epstein-Barr virus
ECM	Extracellular matrix
ELISA	Enzyme-linked immunosorbent assay
FDA	U.S. Food and Drug Administration
H&E	Hematoxylin and eosin
hghpA	Human growth hormone polyadenylation signal
hghpA	Human growth hormone polyadenylation
hPGK	Human phosphoglycerate kinase

IP-10	Interferon gamma-induced protein 10 kDa
MART-1	Melanoma antigen recognized by T cells 1
mg	Milligram
MHC	Major Histocompatibility Class
MIG	Monokine induced by gamma interferon
ml	Milliliter
NK cells	Natural Killer cells
P <sub>CMV</sub>	Cytomegalovirus promoter
PBL	Peripheral blood lymphocytes
Plat-E	Platinum-E
polyA	Polyadenylation signal
PRE	Posttranscriptional regulatory element
RAG	Recombination activating gene
s.c.	Subcutaneously
SD	Standard deviation
SIN-LTR	Self-inactivating long terminal repeats
tet	Tetracycline
TetR	Tetracycline repressor
TIL	Tumor infiltrating lymphocytes
TNF	Tumor necrosis factor
TRE	Tet responsive element
tTA	Tet controlled transactivator
VEGF	Vascular endothelial growth factor

# A Vectors

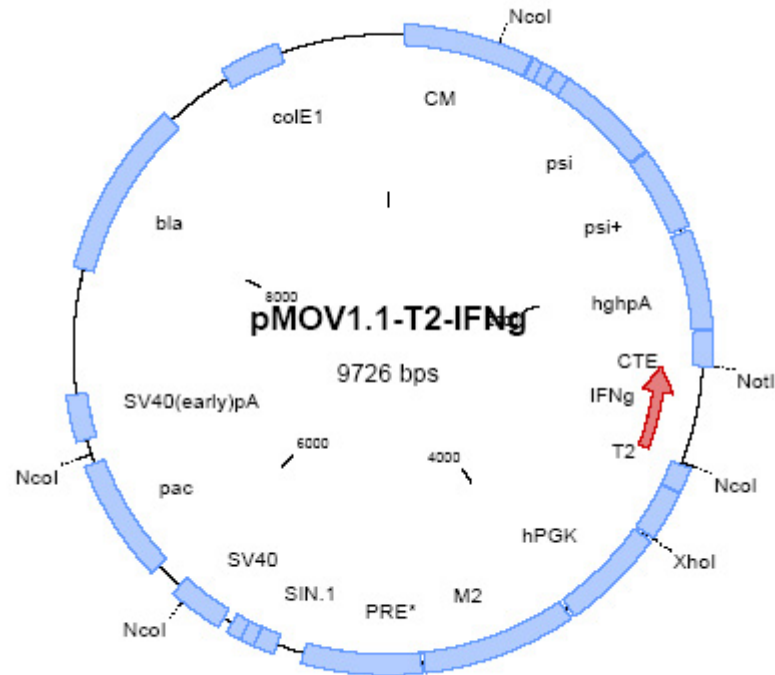


**Figure A.1.** Vector map of pMOV1.1-T2-IFN- $\gamma$ . The retroviral vector consists of SIN-LTRs ( $\Delta$ U3), an extended packing region ( $\psi, \psi^+$ ), splice donor (SD) and acceptor sites (SA). The elements for the tet-regulated transgene expression were inserted as a bidirectional expression cassette. In sense direction the reverse tet-responsive transactivator variant M2 is constitutively expressed by the human phosphoglycerate kinase promoter (hPGK), which is followed by the woodchuck hepatitis virus posttranscriptional regulatory element (PRE). In antisense direction the  $P_{tet}$  promoter variant T2 drives tet-inducible expression of IFN- $\gamma$  which is integrated along with the constitutive transport element (CTE), from Mazon Pfizer Monkey Virus and the human growth hormone (hghpA) polyadenylation signal (polyA). Puromycin (pac) and ampicillin (bla) resistance genes are integrated in the vector along with the simian virus 40 (SV40) polyA and the *E.coli* origin of replication (ColE1).

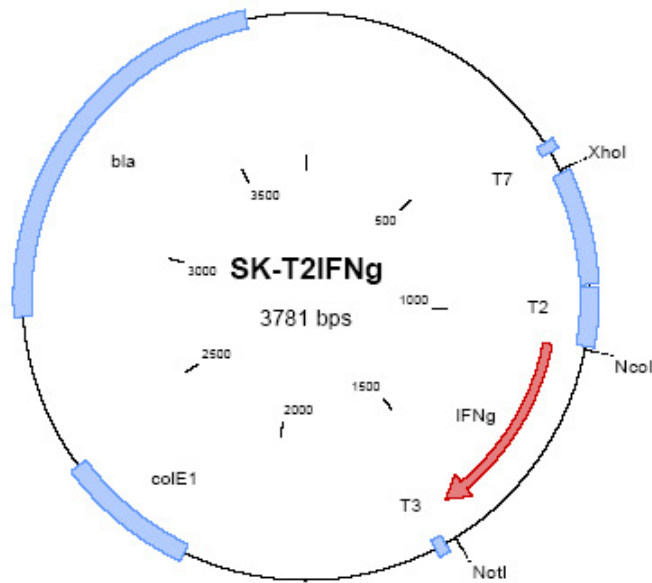


**Figure A.2.** Vector map of SK-T2IFN- $\gamma$ . The IFN- $\gamma$  cDNA could not be cloned directly in to the pMOV1.1-T2 because of an additional NcoI restriction site in this plasmid. Therefore, the PCR product was first integrated into the plasmid SK-T2eGFP replacing the EGFP gene via NcoI and NotI restriction sites. The  $P_{tet}$  promoter variants T2, T3, T7 and the IFN- $\gamma$  gene are integrated into the vector along with an ampicillin resistance gene (*bla*) and *colE1* ori.

# B Sequence Data

## B.1 Primer sequences

Name	Sequence
Primer IFN- $\gamma$ fw	5'-CAGCCATGGCCACCATGAACGCTACACACTGCA-3'
Primer IFN- $\gamma$ rv	5'-GATGCGGCCGCTCAGCAGCGACTCCTTTT-3'

## B.2 DNA-Sequence of tet-IFN- $\gamma$

Sequencing data of the IFN- $\gamma$  gene in the pMOV1.1-T2-IFN- $\gamma$  vector.

### IFN- $\gamma$ coding sequence

```
1 CTGCCTTGGA AAAGGCGCAC CCCAACCCCG TGGAATTATC ACCTCGAGTT
51 TACTCCCTAT CAGTGATAGA GAACGTATGA AGAGTTTACT CCCTATCAGT
101 GATAGAGAAC GTATGCAGAC TTTACTCCCT ATCAGTGATA GAGAACGTAT
151 AAGGAGTTTA CTCCCTATCA GTGATAGAGA ACGTATGACC AGTTTACTCC
201 CTATCAGTGA TAGAGAACGT ATCTACAGTT TACTCCCTAT CAGTGATAGA
251 GAACGTATAT CCAGTTTACT CCCTATCAGT GATAGAGAAC GTATAAGCTT
301 GGTAGGCGTG TACGGTGGGC GCCTATAAAA GCAGAGCTCG TTTAGTGAAC
351 CGTCAGATCG CCTGGAGACG CCATCCACGC TGTTTTGACC TCCATAGAAG
401 ACACCGGGAC CGATCCAGCC TCCGCGGTCG ACACCATGGC CACCATGAAC
451 GCTACACACT GCATCTTGGC TTTGCAGCTC TTCCTCATGG CTGTTTCTGG
501 CTGTTACTGC CACGGCACAG TCATTGAAAG CCTAGAAAAGT CTGAATAACT
551 ATTTTAACTC AAGTGGCATA GATGTGGAAG AAAAGAGTCT CTTCTTGGAT
601 ATCTGGAGGA ACTGGCAAAA GGATGGTGAC ATGAAAATCC TGCAGAGCCA
651 GATTATCTCT TTCTACCTCA GACTCTTTGA AGTCTTGAAA GACAATCAGG
701 CCATCAGCAA CAACATAAGC GTCATTGAAT CACACCTGAT TACTACCTTC
751 TTCAGCAACA GCAAGGCGAA AAAGGATGCA TTCATGAGTA TTGCCAAGTT
```

801 **TGAGGTCAAC** **AACCCACAGG** **TCCAGCGCCA** **AGCATTCAAT** **GAGCTCATCC**  
851 **GAGTGGTCCA** **CCAGCTGTTG** **CCGGAATCCA** **GCCTCAGGAA** **GCGGAAAAGG**  
901 **AGTCGCTGCT** **GACTGCCTTG** GAAAAGGCGC ACCCCAACCC CGTGGAATTA  
951 TCACCTCGAG TTTACTCCCT ATCAGTGATA GAGAACGTAT GAAGAGTTTA  
1001 CTCCTATCA GTGATAGAGA ACGTATGCAG ACTTTACTCC CTATCAGTGA  
1051 TAGAGAACGT ATAAGGAGTT TACTCCCTAT CAGTGATAGA GAACGTATGA  
1101 CCAGTTTACT CCCTATCAGT GATAGAGAAC GTATCTACAG TTTACTCCCT  
1151 ATCAGTGATA GAGAACGTAT ATCCAGTTTA CTCCTATCA GTGATAGAGA  
1201 ACGTATAAGC TTGGTAGGCG TGTACGGTGG GCGCCTATAA AAGCAGAGCT  
1251 CGTTTAGTGA ACCGTCAGAT CGCCTGGAGA CGCCATCCAC GCTGTTTTGA  
1301 CCTCCATAGA AGACACCGGG ACCGATCCAG CCTCCGCGGT CGACACCATG  
1351 GCCACCATGA ACGCTACACA CTGCATCTTG GCTTTGCAGC TCTTCCTCAT  
1401 GGCTGTTTCT GGCTGTTACT GCCACGGCAC AGTCATTGAA AGCCTAGAAA  
1451 GTCTGAATAA CTATTTTAACTCAAGTGGCA TAGATGTGGA AGAAAAGAGT  
1501 CTCTTCTTGG ATATCTGGAG GAACTGGCAA AAGGATGGTG ACATGAAAAT  
1551 CCTGCAGAGC CAGATTATCT CTTTCTACCT CAGACTCTTT GAAGTCTTGA  
1601 AAGACAATCA GGCCATCAGC AACAACATAA GCGTCATTGA ATCACACCTG  
1651 ATTACTACCT TCTTCAGCAA CAGCAAGGCG AAAAAGGATG CATTATGAG  
1701 TATTGCCAAG TTTGAGGTCA ACAACCCACA GGTCCAGCGC CAAGCATTCA  
1751 ATGAGCTCAT CCGAGTGGTC CACCAGCTGT TGCCGGAATC CAGCCTCAGG  
1801 AAGCGGAAAA GGAGTCGCTG CTGAGCGGCC GCTCAGACCA CCTCCCCTGC  
1851 GAGCTAAGCT GGACAGCCAA TGACGGGTAA GAGAGTGACA TTTTTCATA  
1901 ACCTAAGACA GGAGGGCCGT CAGAGCTACT GCCTAATCCA AAGACGGGTA  
1951 AAAGTGATAA AAATGTATCA CTCCAACCTA AGACAGGCGC AGCTTCCGAG  
2001 GGATTTGATA ATTCGATGGT GGCATCCCTG TGACCCCTCC CCAGTGCCTC  
2051 TCCTGGCCCT GGAAGTTGCC ACTCCAGTGC CCACCAGCCT TGTCCTAATA  
2101 AAATTAAGTT GCATCATTTT GTCTGACTAG GTGTCCTTCT ATAATATTAT  
2151 GGGGTGGAGG GGGGGGGT

## C Acknowledgements

I would like to acknowledge the help of many people during my PhD.

First, I want to thank Thomas Blankenstein for the interesting discussions, helpful suggestions and of course for opportunity to work in his group.

I am indebted to Thomas Kammertoens for supervising me and helping me to become a scientist. You told me first about the emotional mountains and valleys of doing science, which sometimes seemed to be valleys only. I am especially grateful for the always beloved internal group meetings.

I wish to thank Daniel Sommermeyer for introducing me to the techniques of molecular biology and helping me with the cloning and the retroviral vector transductions. I am grateful to Wolfgang Uckert for the opportunity to learn and work in his lab. I would also like to thank Simone Spiekermann who helped me with the immunohistology stainings.

Special thanks for the excellent technical assistance and support to Tanja Specowius, Christian Friese and Gabriele Wagner. Big thanks also to Carla Cuartero Isern for being my student and showing me how to teach.

I wish to thank my other colleagues for their help: Christian Schoen, Mathias Friedrich, Michael Rothe, Katrin Deiser, Diana Stoycheva, Kristin Retzlaff and Dirk Femerling. To Sabrina Horn, Dana Hoser and Kathrin Borgwald I am grateful for their support, for cheering me up and the sometimes needed distractions. Maya Schreiber and Mathias Friedrich I thank for the critical reading of my thesis. Mathias I also thank for introducing me to the L<sup>A</sup>T<sub>E</sub>X program and helping me with all the resulting problems.

Special thanks go to the Stefan George circle for never-ending discussions, the exchanged wisdom, the laughs and the coffee.

Most importantly, I wish to thank my family – my parents Wolfgang and Karin and my brother Markus – for being supportive the whole time, especially when everything seemed to go wrong.